

Investigation of Bioanalytical Methodologies for the Detection of Different Analytes

Dissertation

zur Erlangung des Doktorgrades der Naturwissenschaften

(Dr. rer. nat.)

der Fakultät für Chemie und Pharmazie

der Universität Regensburg



vorgelegt von

Thomas Zanni

aus Feltre, Italien

2015

The experimental work was carried out between August 2011 and December 2014 at the University of Regensburg, Institute of Organic Chemistry under the supervision of Prof. Dr. Burkhard König.

Date of submission: 21.05.2015

Date of the colloquium: 10.07.2015

Board of examiners:

Prof. Dr. Olga Garcia Mancheño (Chair)

Prof. Dr. Burkhard König (1st Referee)

Prof. Dr. Joachim Wegener (2nd Referee)

PD Dr. Sabine Amslinger (3rd Examiner)

Table of Contents

Chapter 1. Introduction	1
1.1 BACKGROUND ON VESICULAR CHEMOSENSORS	2
1.2 REFERENCES	4
Chapter 2. A bis (zinc-cyclen)–biotin conjugate probe for detection of phosphoproteins in western blot analysis.....	7
2.1 INTRODUCTION	8
2.2 RESULTS AND DISCUSSION.....	10
2.2.1 Protein detection with BSA as blocking agent	10
2.2.2 pDNA detection	11
2.2.3 α -s1-Casein detection with overnight ovalbumin blocking	12
2.3 CONCLUSION	16
2.4 EXPERIMENTAL SECTION	17
2.5 REFERENCES	19
Chapter 3. SPR and QCM-D investigations of functionalized supported membranes	21
3.1 INTRODUCTION	22
3.1.1 Description of the vesicular systems used	23
3.1.2 Different experimental approaches	24
3.2 RESULTS AND DISCUSSION.....	27
3.2.1 Interaction of analytes with supported membranes monitored by SPR	27
3.2.2 Interaction of functionalized vesicles with surface immobilized analyte	33
3.2.3 Interaction of gold nanoparticles with supported membranes monitored by SPR	40
3.2.4 Affinity of selected peptides to supported functionalized membrane monitored by quartz crystal microbalance	42
3.3 CONCLUSION	44

3.4 EXPERIMENTAL SECTION	46
3.5 REFERENCES	49
Chapter 4. Fluorescence microscopy characterization of vesicular chemosensors.....	51
4.1 INTRODUCTION	52
4.2 RESULTS AND DISCUSSION	55
4.2.1 MC540 as reporting dye in vesicular chemosensors.....	55
4.2.2 STORM and TIRFM characterization of vesicular chemosensors	58
4.3 CONCLUSION	61
4.4 EXPERIMENTAL SECTION	62
4.5 REFERENCES	64
Chapter 5. Investigations of functionalized vesicular systems for monitoring of β-lactamases	67
5.1 INTRODUCTION	68
5.2 RESULTS AND DISCUSSION	71
5.2.1 Synthesis of the amphiphilic ampicillin (Amp-C ₁₈) derivative	71
5.2.2 First approach: dye-encapsulating vesicles.....	71
5.2.3 Second approach: amphiphilic dye and Amp-C ₁₈ doped vesicular systems.....	75
5.2.4 Third approach: fluorophore embedded in membrane, ampicillin in solution	78
5.3 CONCLUSION	86
5.4 EXPERIMENTAL SECTION	87
5.4.1 General	87
5.4.2 Synthesis.....	89
5.4.3 Dye-encapsulating vesicles.....	90
5.4.4 Amphiphilic dye and Amp-C ₁₈ doped vesicular systems	90
5.4.5 Fluorophore embedded in membrane, ampicillin in solution	90
5.5 REFERENCES	93

SUMMARY.....	95
ZUSAMMENFASSUNG.....	97
LIST OF ABBREVIATIONS.....	99
CURRICULUM VITAE	103
ACKNOWLEDGEMENTS.....	105

Chapter 1

Introduction

1.1 BACKGROUND ON VESICULAR CHEMOSENSORS

Over the past ten years, a part of the work in the König group focused on the development of new tools in molecular recognition. Firstly, a number of chemosensors was developed being able to reveal the presence of specific analytes in homogenous solution. The target molecules included biologically relevant peptides [1-3] as well as nucleotides [4]. The general approach to design such sensors involves the combination of one or more recognition moieties with a reporting one in the same molecule.

A further development in the field of chemosensors which partly reduces the often demanding synthesis of the sensors was achieved in the group by combining the recognition and the reporting elements in supramolecular structures such as liposomes.

Functionalized liposomes find countless applications ranging from bioanalysis [5] to medicinal chemistry [6] to model systems for cellular membranes [7, 8]. One of the main advantages of using liposomes is their relatively easy preparation and functionalization: molecules which possess a long alkyl chain can be embedded in the liposomes simply by self-assembly.

In the case of vesicular chemosensors, amphiphilic artificial receptors and amphiphilic dyes can be incorporated in phospholipid vesicles and be used to reveal the presence of analytes which are able to bind to the receptor. The sensing mechanism involves a reorganization of the embedded molecules upon binding of the analyte which provokes a change of the fluorescence emission intensity of the dye [9, 10]. The concept is shown in Figure 1.1.

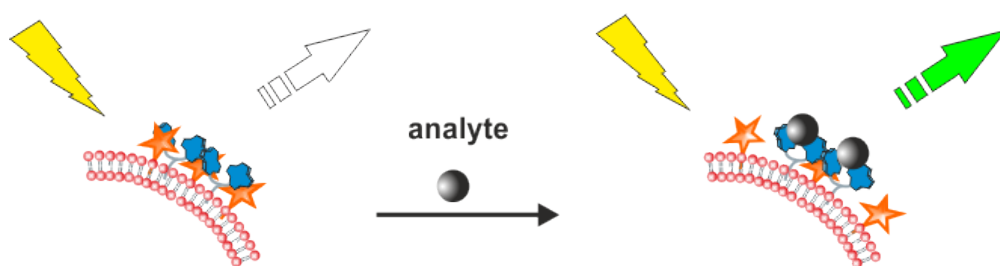


Figure 1.1: Schematic representation of the vesicular chemosensors working principle. Embedded dyes and receptors are organized in patches on the surface of the vesicles. The binding of the analyte molecules to the receptors provokes the reorganization of such patches which induces a change in the fluorescence.

Thanks to the relatively easy preparation method, it is possible to embed different types of amphiphilic receptors and to induce cooperative effects between the embedded receptors resulting in better performances. Moreover, one of the advantages of having recognition elements embedded in the membrane is given by the fluidity of the membrane, which allows lateral diffusion of the molecules. Such lateral diffusion might be exploited to spatially arrange the embedded receptors [11] and to develop sensors with higher affinities towards the target analytes, for example via imprinting techniques [12, 13].

The receptors can also be introduced on the surface via a post-functionalization approach [14], which avoids a part of the synthetic effort to prepare the amphiphilic receptors and is also suitable for more sophisticated recognition moieties, such as aptamers [15].

The work presented in this thesis is related to this branch of research in the König group. We are going to explore the possibility to investigate the concepts so far developed for the vesicular chemosensors using Surface Plasmon Resonance (SPR) and Quartz Crystal Microbalance (QCM) as alternative detection techniques. We are presenting fluorescence microscopy investigations of the vesicular systems in order to have deeper insight in the working mechanism of the vesicular chemosensors. Moreover, we attempt to broaden the research interest towards more biology relevant applications, such as detection of phosphoproteins in standard protein analysis and monitoring of β -lactamases activity.

1.2 REFERENCES

1. Späth, A. and König, B., *Binding of a hemoregulatory tetrapeptide by a bis-guanidinium crown ether*. Tetrahedron, 2010. **66**(32): p. 6019-6025.
2. Grauer, A., Riechers, A., Ritter, S. and König, B., *Synthetic receptors for the differentiation of phosphorylated peptides with nanomolar affinities*. Chemistry-A European Journal, 2008. **14**(29): p. 8922-8927.
3. Bhuyan, M., Katayev, E., Stadlbauer, S., Nonaka, H., Ojida, A., Hamachi, I. and König, B., *Rigid luminescent bis-zinc(II)-bis-cyclen complexes for the detection of phosphate anions and non-covalent protein labeling in aqueous solution*. European Journal of Organic Chemistry, 2011(15): p. 2807-2817.
4. Schmidt, F., Stadlbauer, S. and König, B., *Zinc-cyclen coordination to UTP, TTP or pyrophosphate induces pyrene excimer emission*. Dalton Transactions, 2010. **39**(31): p. 7250-7261.
5. Liu, Q. and Boyd, B.J., *Liposomes in biosensors*. Analyst, 2013. **138**(2): p. 391-409.
6. Allen, T.M. and Cullis, P.R., *Liposomal drug delivery systems: from concept to clinical applications*. Advanced Drug Delivery Reviews, 2013. **65**(1): p. 36-48.
7. Hamada, T. and Yoshikawa, K., *Cell-sized liposomes and droplets: real-world modeling of living cells*. Materials, 2012. **5**(12): p. 2292-2305.
8. Shen, H.H., Lithgow, T. and Martin, L., *Reconstitution of membrane proteins into model membranes: seeking better ways to retain protein activities*. International Journal of Molecular Sciences, 2013. **14**(1): p. 1589-1607.
9. Gruber, B., Stadlbauer, S., Späth, A., Weiss, S., Kalinina, M. and König, B., *Modular chemosensors from self-assembled vesicle membranes with amphiphilic binding sites and reporter dyes*. Angewandte Chemie International Edition, 2010. **49**(39): p. 7125-7128.
10. Gruber, B., Stadlbauer, S., Woinaroschy, K. and König, B., *Luminescent vesicular receptors for the recognition of biologically important phosphate species*. Organic & Biomolecular Chemistry, 2010. **8**(16): p. 3704-3714.

11. Gruber, B., Balk, S., Stadlbauer, S. and König, B., *Dynamic interface imprinting: high-affinity peptide binding sites assembled by analyte-induced recruiting of membrane receptors*. Angewandte Chemie International Edition, 2012. **51**(40): p. 10060-10063.
12. Banerjee, S. and König, B., *Molecular imprinting of luminescent vesicles*. Journal of American Chemical Society, 2013. **135**(8): p. 2967-2970.
13. Balk, S. and König, B., *Thermally induced molecular imprinting of luminescent vesicles*. Journal of Inclusion Phenomena and Macrocyclic Chemistry, 2014. **81**(1-2): p. 135-139.
14. Müller, A. and König, B., *Preparation of luminescent chemosensors by post-functionalization of vesicle surfaces*. Organic & Biomolecular Chemistry, 2015. **13**(6): p. 1690-1699.
15. Müller, A. and König, B., *Vesicular aptasensor for the detection of thrombin*. Chemical Communications, 2014. **50**: p. 12665-12668.

Chapter 2

A bis (zinc-cyclen)-biotin conjugate probe for detection of phosphoproteins in western blot analysis

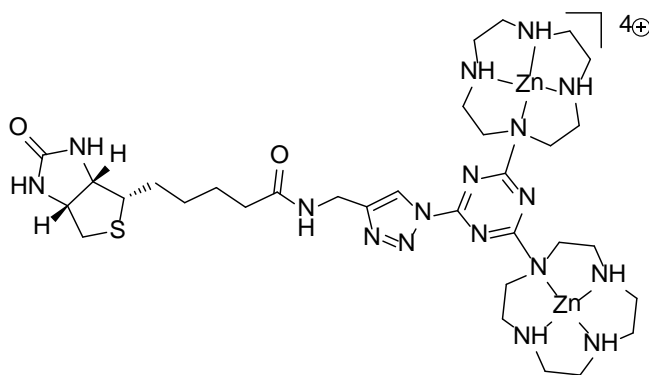
2.1 INTRODUCTION

Phosphorylation and dephosphorylation at specific sites of proteins play a key role in a large number of cellular signal pathways and are involved in the regulation of a wide range of cellular functions [1-3]. The discrimination between phosphorylated and non-phosphorylated proteins in standard analytical techniques is of great importance, both in mechanistic studies [4, 5] and for diagnostic purposes [6, 7]. A wide range of analytical strategies which mainly use mass spectrometry as a key method to investigate phosphorylation in biological systems has been reported in literature [8].

Gel electrophoresis is one of the most common techniques for analyzing protein mixtures. After separation, detection of proteins is typically performed by means of non-selective Coomassie Brilliant Blue (CBB) stain or silver stain. When selectivity is required, the separated proteins are transferred on a suitable membrane and specific detection is performed via immunodetection. For that purpose, several antibodies against phosphorylated proteins have been developed [9] and are currently employed.

Even if immunodetection on blotted proteins is a very well established approach, efforts have been made for developing alternative methods to detect phosphoproteins directly on the SDS gel or on membranes. For example Schulenberg and co-workers [10] as well as König and co-workers [11] established fluorescent probes which selectively bind to phosphorylated proteins in standard protein analysis.

As a contribution to the field, we investigated a potentially selective probe for phosphorylated proteins to be used in western blot analysis. The probe consists of a bis (zinc-cyclen) moiety covalently linked to a biotin derivative. Bis (zinc-cyclen) based sensors have been reported [12, 13] to be able to detect selectively phosphate-containing biomolecules; while biotin, due to its strong affinity to avidins, is a well-known biotechnology tool, which is widely used for purification and detection purposes. In Scheme 2.1, we show the structure of the probe.



Scheme 2.1: Biotin-bis (zinc-cyclen) complex conjugate.

The probe is expected to bind to phosphorylated target species with the bis (zinc-cyclen) moiety and to be detected via interaction of the biotin with Streptavidin-Horseradish Peroxidase (HRP) and enhanced chemiluminescent ECL substrate. In Figure 2.1, we show a schematic representation of the assay.

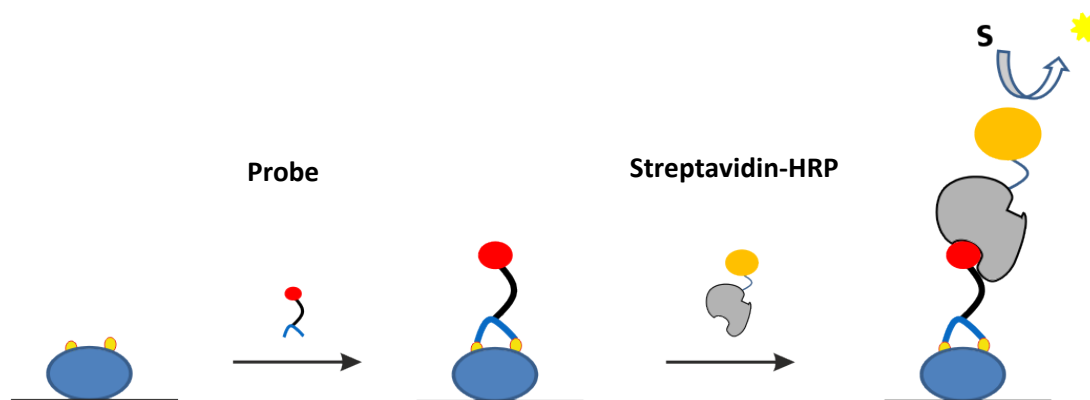


Figure 2.2: Schematic representation of the assay. The probe binds to phosphorylated sites of the immobilized target molecule. The Streptavidin-HRP binds to the biotin moiety and the ECL substrate reaction reveals the presence of the target molecule.

The assay scheme is analogue to a standard immunodetection assay, in which a primary antibody is used instead of the probe.

2.2 RESULTS AND DISCUSSION

We investigated highly phosphorylated α -S1-casein and plasmidic DNA (pDNA) as target analytes. The molecules were immobilized on the membranes via western blot (for the proteins) or dot blot (for the pDNA); the membranes were immersed in a solution of our bivalent probe, washed and then incubated with a Streptavidin-HRP solution. The detection was then performed with ECL substrate.

Several parameters had to be considered for the optimization of the assay, such as incubation and washing times, concentrations of the components in the different steps of the procedures and the choice of a proper blocking agent.

2.2.1 Protein detection with BSA as blocking agent

Figure 2.3 shows the CCD images of three membranes containing α -s1-casein, dephosphorylated α -S1-casein and ovalbumin. Different concentrations of the probe were used.

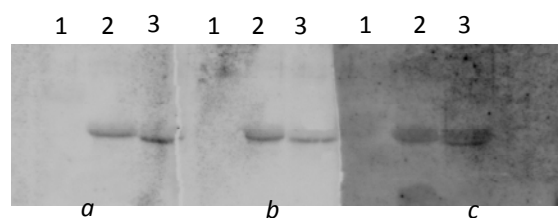


Figure 2.3: Ovalbumin (lane 1), α -s1-casein (2) and dephosphorylated α -s1-casein (3) ($10\ \mu\text{g}$ each) were blotted on membranes a, b c. $10^{-7}\ \text{M}$ (a), $10^{-6}\ \text{M}$ (b), $10^{-4}\ \text{M}$ (c) probe concentrations were employed. Membranes were blocked with BSA for 1 h.

Both α -S1-casein and dephosphorylated α -s1-casein are detected. No signal is observed for ovalbumin. The background signal is significantly larger for $10^{-4}\ \text{M}$ probe concentration.

In Figure 2.4, we show the CCD image of 5 membranes, each containing the same amount of α -s1-casein and treated with a different concentration of the probe.

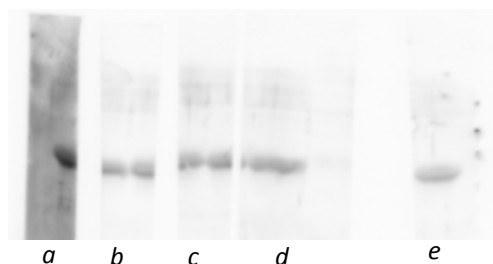


Figure 2.4: 10 μg of α -s1-casein were blotted on each membrane. 10^{-4} M (a), 10^{-9} M (b), 10^{-12} M (c), 10^{-15} M (d) and 0 M (e) probe concentrations were employed. Membranes were blocked with BSA for 1 h.

A band is present in all the membranes. With a probe concentration of 10^{-4} M, the background signal is larger. The influence of the probe concentration for membranes b to e seems to be not significant under these conditions.

2.2.2 pDNA detection

Figure 2.5 shows the CCD images of six membranes, each prepared by blotting a 1:10 dilution series of pDNA. We investigated how different blocking agents influence the ability of the probe to interact with pDNA. The blockings were performed overnight.

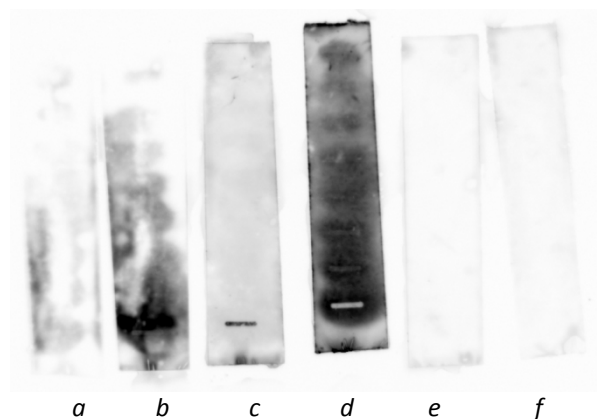


Figure 2.5: Each membrane contains a 1:10 dilution series (from 3 μg to 0.3 pg, from bottom to the top) of plasmidic DNA samples. BSA (a and b), ovalbumin (c and d) and milk powder (e and f) were used as blocking agent. Membranes a, c and e were treated with 10^{-5} M probe solutions, while membrane b, d and f were treated with 0 M probe solution.

When milk powder or BSA are employed as blocking agents, no signal is present. With ovalbumin as blocking agent, a band is visible for 3 μg of pDNA, while lower amounts of pDNA do not give any signal.

The detection of pDNA using ovalbumin as blocking agent and 10^{-5} M probe concentration is reproducible (Figure 2.6).

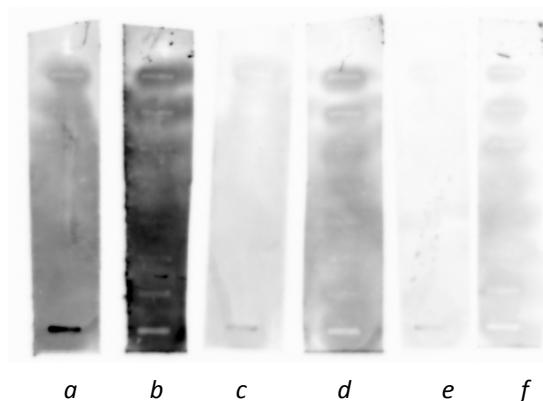


Figure 2.6: Each membrane contains a 1:10 dilution series (from 3 μg to 0.3 μg , from bottom to the top) of pDNA samples. Membranes a, c and e were treated with 10^{-5} M probe solution, while membranes b, d and f were not treated with the probe. Different concentrations of Streptavidin-HRP were used: 0.2 $\mu\text{g}/\text{ml}$ (a and b), 0.1 $\mu\text{g}/\text{ml}$ (c and d) and 0.05 $\mu\text{g}/\text{ml}$ (e and f).

2.2.3 α -s1-Casein detection with overnight ovalbumin blocking

In Figures 2.7 and 2.8, we show the CCD images of three nitrocellulose membranes incubated with different concentrations of the probe. In order to investigate the selectivity of the probe, we loaded on each membrane two non-phosphorylated control proteins (BSA and a non-phosphorylated polyhistidine tagged protein) in addition to α -s1-casein. 1.5 μg (Figure 2.7) and 10 μg (Figure 2.8) of each protein were blotted on the membranes.

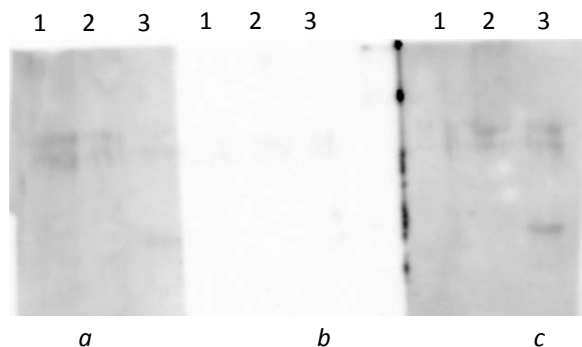


Figure 2.7: 1.5 μ g of a polyhistidine tagged protein (lane 1), BSA (2) and α -s1-casein (3) were blotted on membranes a, b and c. 10⁻⁵ M (a), 0 M (b), 10⁻⁴ M (c) probe concentrations were employed.

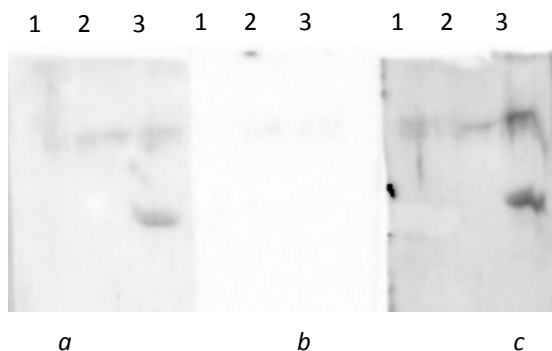


Figure 2.8: 10 μ g of a polyhistidine tagged protein (lane 1), BSA (2) and α -s1-casein (3) were blotted on membranes a, b and c. 10⁻⁵ M (a), 0 M (b) and 10⁻⁴ M (c) probe concentrations were employed.

The membranes which were not treated with the probe show no signal. Figures 2.7a and 2.7c show a weak band corresponding to α -s1-casein, while a well-defined band is observed in Figures 2.8a and 2.8c.

No signal is visible for the polyhistidine tagged protein. The presence of a weak signal at higher molecular weight, which is present in all the lanes, doesn't allow us to determine whether the probe has an appreciable affinity to BSA.

In Figure 2.9, we show the CCD images of two membranes blocked with ovalbumin overnight. The non-phosphorylated polyhistidine tagged control protein, a prestained molecular weight marker and standard (not prestained) molecular weight marker were blotted on the membranes.

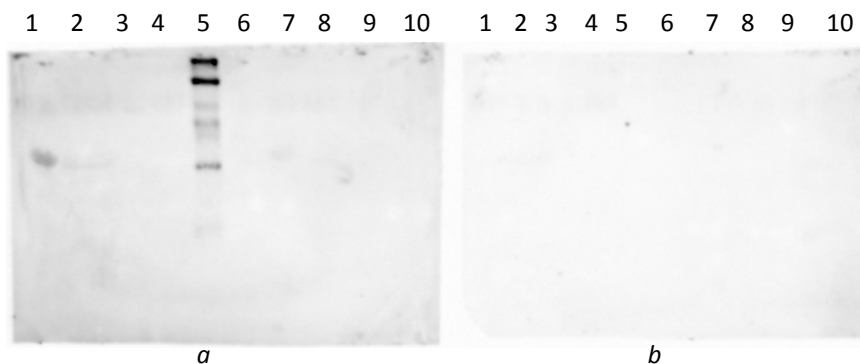


Figure 2.9: α -s1-Casein (8 μ g in lane 1, 1.5 μ g in lane 7), dephosphorylated α -s1-casein (2 and 8), BSA (3 and 9), the polyhistidine tagged protein (4 and 10), prestained molecular weight marker (5), non-prestained molecular weight marker (6), were blotted on membranes a and b. 10^{-5} M (a) and 0 M (b) probe concentrations were employed.

No band was observed for the membrane in Figure 2.9b. In Figure 2.9a, a well-defined band corresponding to α -s1-casein is present in lane 1, while the same protein in lane 7 is barely visible. Almost all proteins of the prestained molecular weight marker (lane 5) show a signal as well. No signal was observed for non-phosphorylated control proteins BSA (lanes 3 and 9) and the polyhistidine tagged protein (lanes 4 and 10). A rather weak signal is observed for dephosphorylated α -s1-casein in lane 2.

As a control experiment to verify the presence of the proteins on the membranes, the same membranes were stained with unspecific ponceau S staining (Figure 2.10).

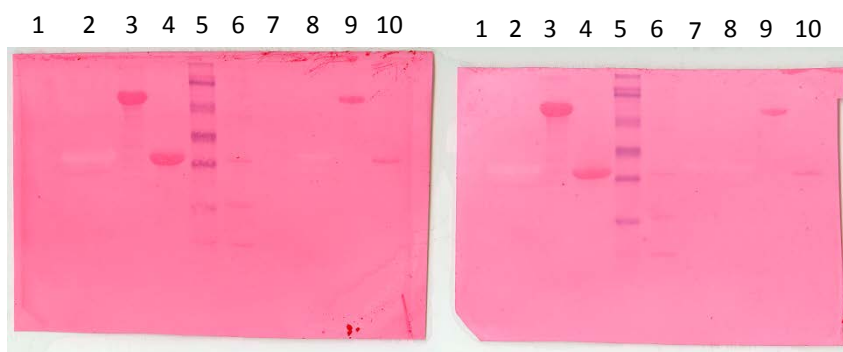


Figure 2.10: Same membranes as in Figure 2.9 stained with ponceau S.

Ponceau S stained membranes have a red background due to the blocking agent. The polyhistidine tagged protein and BSA show a well-defined red band, while α -s1-casein and dephosphorylated α -s1-

casein show no signal or negative signal. The non-prestained molecular weight marker show defined bands as well.

2.3 CONCLUSION

The blocking conditions were a crucial factor to evaluate the efficacy of the probe for phosphorylated protein detection. BSA turned out to be not appropriate: Figure 2.3 shows that detection of α -s1-casein is possible by use of the probe; however, further investigations (Figure 2.4) indicated that the signal observed for casein under those conditions is due to unspecific binding of Streptavidin-HRP to the casein. The main effect of the probe is to increase the background signal when it is used in a significant concentration (10^{-4} M).

The tests with pDNA as analyte allowed the optimization of the blocking conditions in terms of incubation time and blocking agent. Overnight incubation at 4 °C with ovalbumin turned out to be effective for detection of 3 μ g of pDNA with good reproducibility (Figures 2.5 and 2.6). Variation of the concentration of Streptavidin-HRP conjugate didn't show any improvement in the background signal neither in the limit of detection. The optimized detection of pDNA was performed by incubating overnight the membrane at 4°C with ovalbumin, followed by 1 h incubation with a 10^{-5} M solution of probe; after 3x10 min. washing steps, the membrane was soaked for 1 h in a solution of streptavidin-HRP washed 4x15 minutes and finally incubated with ECL substrate.

Under these conditions, the probe showed an appreciable affinity towards α -s1-casein.

Figures 2.9 and 2.10 demonstrate that the probe interacts selectively with α -s1-casein with a sufficient affinity to allow detection of 8 μ g of protein; the probe is not able to bind with the same affinity to dephosphorylated α -s1-casein, BSA and the polyhistidine tagged protein. 1 μ g of α -s1-casein seems to be close to the limit of detection of the method.

The rather poor performances of the assay can be rationalized considering two factors. Firstly, the order of magnitude of the binding constant between bis (zinc-cyclen) receptors and phosphorylated molecules in homogeneous aqueous solution: for similar sensors, the reported affinity is in the μ M range [14], which is significantly weaker than the typical antibody-antigen affinity (characteristic of western blot detection); secondly, the ability of the bis (zinc-cyclen) moiety to weakly bind also to other negatively charged residues in a protein might explain the background signal observed in some experiments. The use of enzymatic amplification isn't sufficient to overcome those limitations and to achieve better performances.

2.4 EXPERIMENTAL SECTION

Materials: BSA was from Roth GmbH, ovalbumin and α -S1-casein were purchased from Sigma-Aldrich, Tris from USB, Acrylamide from Fluka, λ -PPase from New England Biolabs, plasmidic DNA pBR322 DNA from Fermentas life science. The polyhistidine tagged protein was provided by Dr. Bernd Reisinger (Prof. Sterner group, Institute of Biophysics und physical Biochemistry, University of Regensburg). The probe was synthesized by Dr. Mouchumi Bhuyan [15]. If not otherwise specified, MilliQ water was employed.

Dephosphorylation of α -s1-casein: dephosphorylated α -s1-casein was prepared by incubating 40 μ g of α -s1-casein with 400 Units of λ -PPase in Tris-HCl (50 mM), NaCl (100 mM), dithiothreitol (2 mM), $MnCl_2$ (2 mM), EGTA (0.1 mM), 0.01% Brij 35, pH 7.5, at 30 °C for 6 h.

SDS-PAGE: proteins were resolved in minigels under reducing and denaturing Laemmli conditions. Stacking gel consisted of 5% acrylamide (w/v), 125 mM Tris-HCl (pH 6.8), 0.1% SDS (w/v); running gel consisted of 15% acrylamide, 375 mM Tris-HCl (pH 8.8), 0.1% SDS (w/v). Running buffer consisted of 25 mM Tris, 192 mM glycine, SDS 0.1% (w/v). Gels were run with PeqLab 45-1010i apparatus, at 150 V. Proteins samples were heated at 95 °C for 10 minutes in denaturing and reducing Rotiload 1 (Roth GmbH) sample buffer.

Western blot: proteins were transferred from gel to nitrocellulose membrane with BioRad Mini Trans Blot Electrophoretic Transfer Cell apparatus. 25 mM Tris, 192 mM glycine, 0.1% SDS (w/v) buffer was used for blotting. Blots were run at 125 V for 1 h.

Dot blot of pDNA samples: pDNA was immobilized by dot blot on nylon membranes. The dot blot instrument was provided by Dr. Jorge Perez-Fernandez (Prof. Tschochner group, Institute of Biochemistry, Genetics and Microbiology, University of Regensburg).

Standard detection procedure: after protein transfer, membranes were soaked in blocking buffer (40 mM Tris HCl, 300 mM NaCl, 1% (v/v) Tween 20 (pH 7.4), 5% (w/v) blocking agent) for 1 h or overnight at 4 °C. Membranes were then incubated with a solution of probe (different concentrations were employed, reported case by case in the result section of this chapter) in washing buffer (40 mM Tris HCl, 300 mM NaCl, 1% (v/v) Tween 20 (pH 7.4)) for 1 h. After washing, membranes were incubated with 0.2 μ g/ml (in washing buffer) of Streptavidin-HRP for 30 minutes. Unbound Streptavidin-HRP

was washed away by 4 x 15 minutes washing with washing buffer. Detection was performed with ECL substrate (Super Signal West Dura). We used Fujifilm LAS 3000 system for documentation.

Ponceau S staining was performed by incubation of the membranes with 0.1% (w/v) Ponceau S solution in 5% AcOH for 1 h.

2.5 REFERENCES

1. Hunter, T., *Protein kinase and phosphatase Yin and Yang of protein phosphorylation and signaling*. Cell, 1995. **80**: p. 225-236.
2. Hunter, T., *Signaling - 2000 and Beyond*. Cell, 2000. **100**: p. 113-127.
3. Cohen, P., *The origins of protein phosphorylation*. Nature Cell Biology, 2002. **4**: p. E127-E130.
4. Johnson, H. and White, F.M., *Toward quantitative phosphotyrosine profiling in vivo*. Seminar in Cell & Developmental Biology, 2012. **23**(8): p. 854-862.
5. Salomon, A.R., Ficarro, S.B., Brill, L.M., Brinker, A., Phung, Q.T., Ericson, C., Sauer, K., Brock, A., Horn, D.M., Schultz, P.G. and Peters, E.C., *Profiling of tyrosine phosphorylation pathways in human cells using mass spectrometry*. Proceedings of the National Academy of Sciences of USA, 2003. **100**(2): p. 443-448.
6. Bahk, Y.Y., Bari, M. and Youg, J.K., *Biomedical application of phosphoproteomics in neurodegenerative diseases*. Journal of Microbiology and Biotechnology, 2013. **23**(3): p. 279-288.
7. Mandell, J.W., *Phosphorylation state-specific antibodies*. The American Journal of Pathology, 2003. **163**(5): p. 1687-1698.
8. Engholm-Keller, K. and Larsen, M.R., *Technologies and challenges in large-scale phosphoproteomics*. Proteomics, 2013. **13**(6): p. 910-931.
9. Brumbaugh, K., Johnson, W., Liao, W.-C., Lin, M.-S., Houchins, J.P., Cooper, J., Stoesz, S. and Campos-Gonzalez, R., *Overview of the generation, validation, and application of phosphosite-specific antibodies* Signal Transduction Immunohistochemistry: Methods and Protocols, 2011. **717**: p. 3-43.
10. Schulenberg, B., Goodman, T.N., Aggeler, R., Capaldi, R.A. and Patton, W.F., *Characterization of dynamic and steady-state protein phosphorylation using a fluorescent phosphoprotein gel stain and mass spectrometry*. Electrophoresis, 2004. **25**(15): p. 2526-2532.
11. Riechers, A., Schmidt, F., Stadlbauer, S. and König, B., *Detection of protein phosphorylation on SDS-PAGE using probes with a phosphate-sensitive emission response*. Bioconjugate Chemistry, 2009. **20**: p. 804-807.

12. Mizukami, S., Nagano, T., Urano, Y., Odani, A. and Kikuchi, K., *A fluorescent anion sensor that works in neutral aqueous solution for bioanalytical application*. Journal of American Chemical Society, 2002(124): p. 3920-3925.
13. Grauer, A., Riechers, A., Ritter, S. and König, B., *Synthetic receptors for the differentiation of phosphorylated peptides with nanomolar affinities*. Chemistry-A European Journal, 2008. **14**(29): p. 8922-8927.
14. Gruber, B., Stadlbauer, S., Späth, A., Weiss, S., Kalinina, M. and König, B., *Modular chemosensors from self-assembled vesicle membranes with amphiphilic binding sites and reporter dyes*. Angewandte Chemie International Edition, 2010. **49**(39): p. 7125-7128.
15. Bhuyan, M., *Synthesis and exploration of functionalized zinc(II) and terbium(III) complexes as molecular probes*. PhD dissertation, 2012.

Chapter 3

SPR and QCM-D investigations of functionalized supported membranes

3.1 INTRODUCTION

Functionalized amphiphilic vesicles containing metal complex binding sites and reporting dyes have been employed as chemosensors and as models to investigate the dynamics of molecules embedded in phospholipid membranes. The fluidity of the membrane, which depends on the chemical structure of the amphiphile and on the temperature, plays a key role in determining the properties of the functionalized vesicles.

When amphiphilic fluorescent dyes and amphiphilic artificial receptors are co-embedded in the liposomes bilayer, they form mixed patches. Molecules with affinity to the receptor induce a perturbation of such patches, which turns into a change in the fluorescence intensity. The functionalized liposomes can therefore be used as sensors [1, 2].

The mobility of the embedded molecules can be used to induce cooperative effects between different receptors in order to improve the selectivity and the affinity of the vesicular sensors. The recruiting of embedded receptors at the surface of a liquid crystalline membrane by a ditopic analyte has been demonstrated by a FRET assay [3]. The analyte induces a rearrangement of the receptors at the surface, which leads to an enhanced affinity between the analyte and the functionalized vesicles.

The possibility to conveniently rearrange the embedded receptors was employed to develop “molecularly imprinted vesicles” via polymerization of the rearranged receptors. Polymerizable amphiphilic receptors are co-embedded in a liquid crystalline membrane of liposomes and incubated with a ditopic analyte which is able to arrange the receptors. The organized receptors are then polymerized in order to be kept at the right distance. The affinity of the polymerized vesicles for the analyte is higher compared to the non-polymerized ones [4].

The vesicular chemosensors concepts so far developed in the group employed fluorescence as detection technique. Fluorescence has many advantages over other techniques: it can easily provide a high sensitivity and high specificity, and it is usually a fast and easy to use method. The main drawback, at least for some applications, is that most of the molecules we are interested in are not fluorescent, therefore labeling or the inclusion of a fluorescent moiety in sensors design is necessary. As alternative to the fluorescent vesicular chemosensors, we explore herein the possibility to transfer the above mentioned concepts to other techniques, such as Surface Plasmon Resonance (SPR) and Quartz Crystal Microbalance (QCM). The use of SPR and QCM to observe the same phenomena would in principle allow to validate the previous work and to open new perspectives in terms of applications.

SPR was first proposed as analytical technique in the early '90s [5]. Since then, it was employed to investigate a large number of (bio)molecular interactions [6] and it became a standard method in the field of bioanalysis.

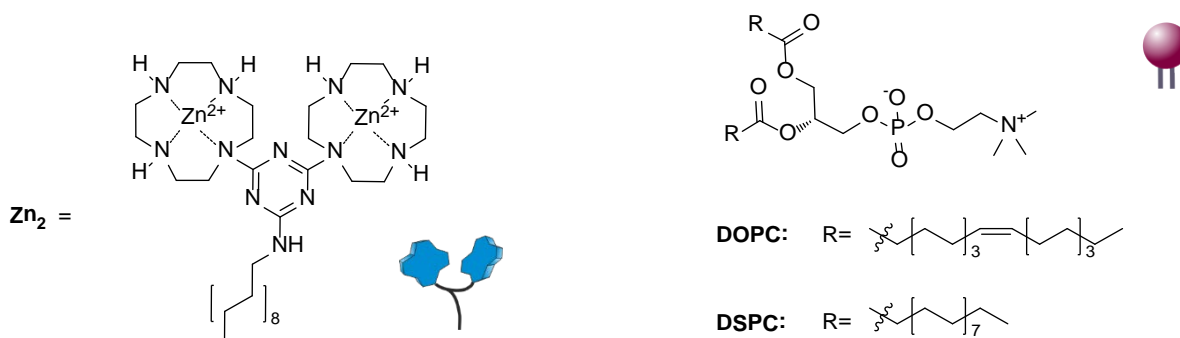
Supported membranes are employed in SPR assays as models of biological membranes to investigate membrane-protein/ligand [7], membrane/protein [8] and membrane/ligand interactions [9]. Functionalized liposomes are utilized in SPR based sensors as signal enhancers thanks to their large dimension, which provokes a large change in the refractive index even at relatively low concentrations [10].

The quartz crystal microbalance (QCM) was applied for the first time to investigate supported membranes in 1989 [11]. Since then, it has been employed as a tool to study the mechanisms of formation of solid supported bilayers [12, 13] as well as the interactions between the membranes and different classes of biomolecules [14].

The study of the arrangement and the dynamics of artificial receptors embedded in supported membranes by means of SPR and/or QCM has not been reported yet.

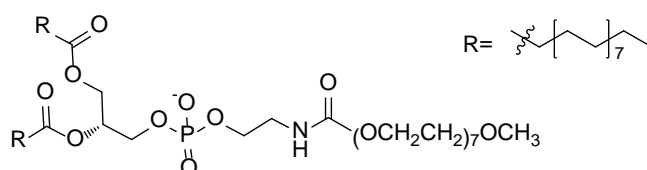
3.1.1 Description of the vesicular systems used

The first step for all the experiments that will be presented in the following paragraphs is the preparation of the functionalized vesicles. The vesicles are prepared by self-assembly of phospholipids and amphiphilic receptors and successive extrusion through a polycarbonate membrane to obtain a uniform size distribution of unilamellar vesicles. The components used for the preparation of the liposomes are the phospholipids 1,2-di-(9Z-octadecenoyl)-*sn*-glycero-3-phosphocholine (**DOPC**) and 1,2-distearoyl-*sn*-glycero-3-phosphocholine (**DSPC**), and a bis (zinc-cyclen) derivative (**Zn₂**). The chemical structures are shown in Scheme 2.1.



Scheme 2.1: Structures of the Zn_2 artificial receptor (left) and of the phospholipids **DSPC** and **DOPC** (right). The counter ions of the Zn_2 receptor are omitted for clarity.

The Zn^{2+} metallorganic complexes are very well known to bind phosphorylated molecules, both in solution [15] and in vesicular chemosensors [1]. We used the Zn_2 derivative as a model receptor, which was widely employed in previous studies on vesicular chemosensors in the group. For a series of experiments, the PEGylated phospholipid 1,2-distearoyl-sn-glycero-3-phosphoethanolamine-N-[methoxy(polyethylene glycol)-350] (ammonium salt) (**DSPE-PEG350**), shown in Scheme 2.2, was used.



Scheme 2.2: Structure of the phospholipid **DSPE-PEG350**.

3.1.2 Different experimental approaches

The investigation of the binding between functionalized vesicles and analytes with SPR or QCM can be done in different ways. A first approach is to immobilize the functionalized vesicles on the surface of the sensor chip and to investigate the binding of the analyte to that surface. In order to do that, we first used a very simple strategy described in [16], which is based on the formation of a self-assembled monolayer (SAM) of 11-mercaptopundecanoic acid (MUA) on the gold surface followed by immobilization of the vesicles. Figure 3.1 shows a schematic representation of such an approach. This

method was used as first choice as it looked straightforward and suitable for using a standardized immobilization strategy in each experiment and varying the analyte.

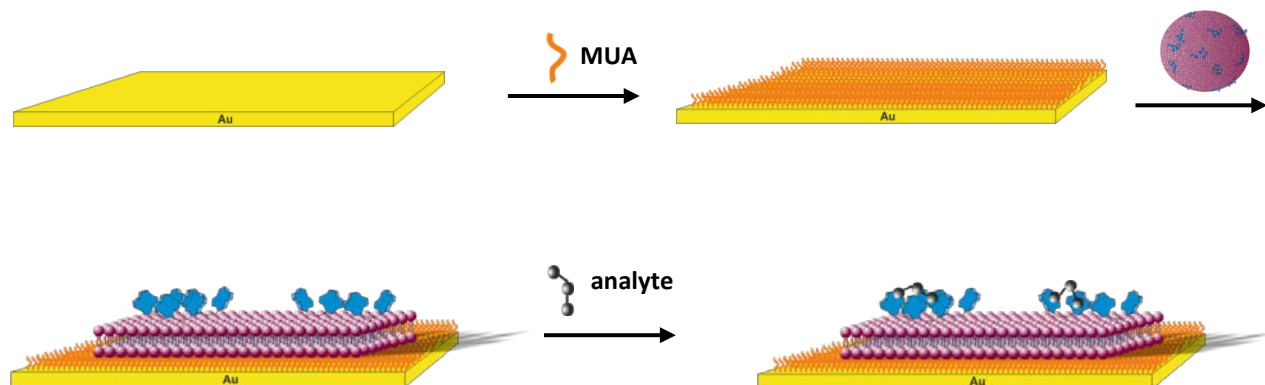


Figure 3.1: Graphical representation of the formation of the functionalized supported membrane on a SPR gold chip and of the binding of an analyte to the same surface.

In order to overcome the poor sensitivity of both SPR and QCM when small analytes are investigated, we explored a second method inspired by the work of Massons and co-workers [17], which consisted in a displacement assay using gold nanoparticles. The approach relies on the saturation of the binding sites on the surface with functionalized nanoparticles and their subsequent displacement by the analyte as illustrated in Figure 3.2.

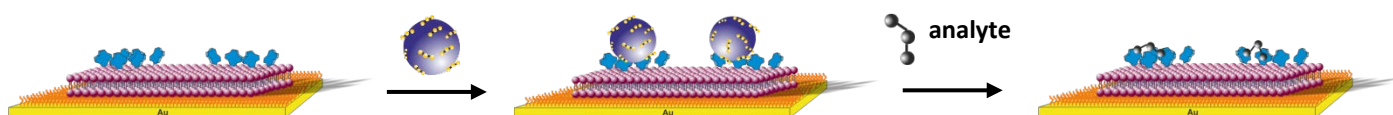


Figure 3.2: Graphical representation of the displacement assay using gold nanoparticles. The gold nanoparticles bind to the functionalized surface and are subsequently displaced by the analyte.

A third approach was based on the immobilization of the analyte on the surface and subsequent binding of the functionalized vesicles to the decorated sensor chip (Figure 3.3). Such an approach was used in a later stage of our investigation, when we were not able to overcome the sensitivity and selectivity problems encountered using the first two assays.

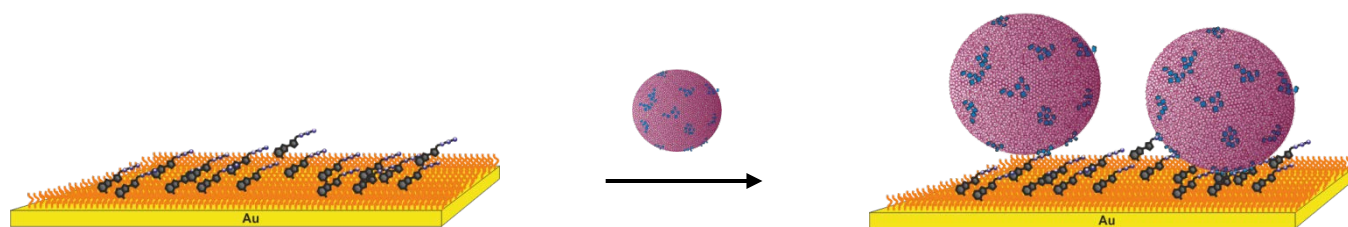


Figure 3.3: Graphical representation of the binding of functionalized liposomes to an analyte modified SPR gold chip.

The binding of the decorated vesicles to the analyte modified surface is expected to give a larger signal compared to the binding of the analyte to the functionalized supported membrane (first approach) and thus to overcome the sensitivity issue typically encountered with small analytes.

3.2 RESULTS AND DISCUSSION

3.2.1 Interaction of analytes with supported membranes monitored by SPR

Formation of supported membranes on SPR gold chips

In Figure 3.4, we show the SPR sensorgrams obtained after injection of Zn_2 doped **DOPC** vesicles on surfaces functionalized with different thiols: (3-mercaptopropyl)trimethoxysilane (MPTMS), 11-mercaptoundecanoic acid (MUA) and 16-mercaptohexadecanoic acid (MHDA).

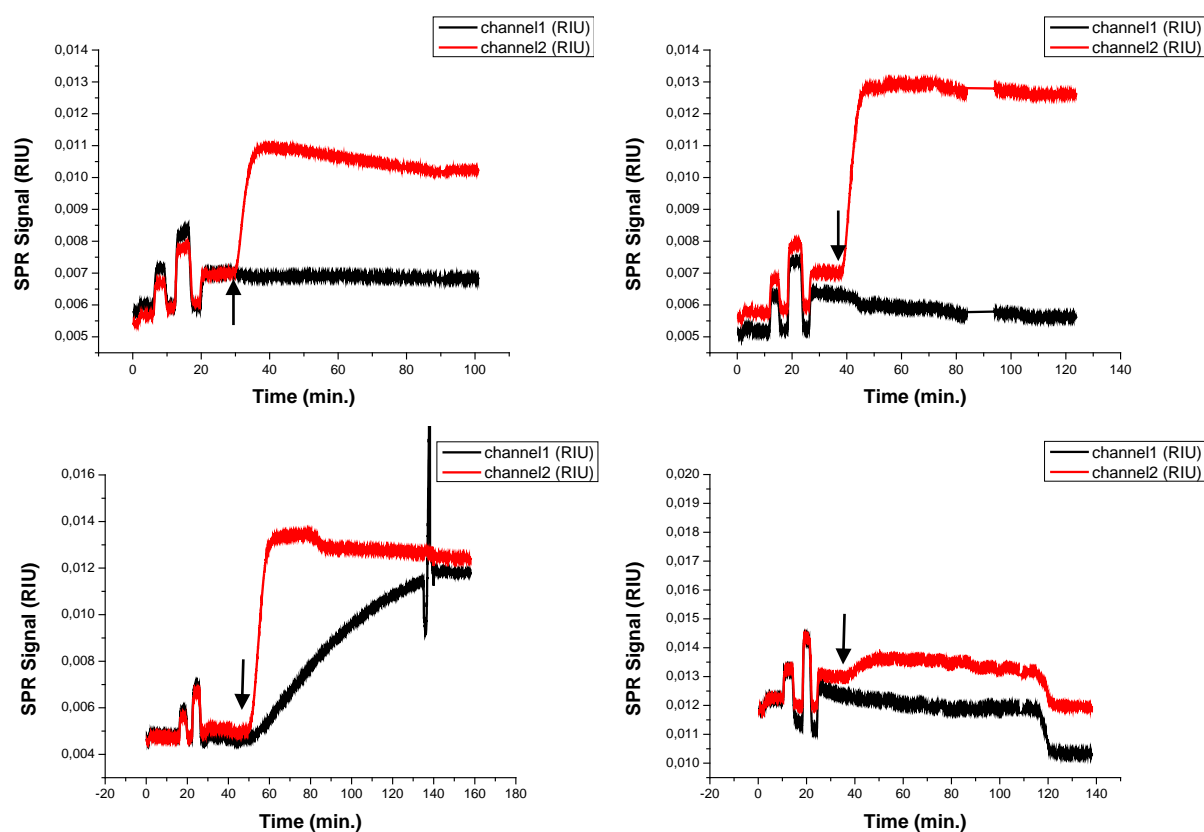


Figure 3.4: SPR sensorgrams obtained after injection of Zn_2 doped **DOPC** vesicles on gold chips functionalized with different thiols: (a) MPTMS, (b) MUA, (c) MHDA and (d) bare gold. In channel 2, Zn_2 doped vesicles were injected, in channel 1 HEPES buffer solution (a, b and d) or non-functionalized **DOPC** vesicles (c) were injected. The arrow indicates the moment at which the vesicle solutions reach the sensor surface.

The sensorgrams were transformed into refractive index units (RIU) by calibration. In all cases, except for bare gold, it is possible to observe an increase of the SPR signal due to the formation of a

supported membrane on the surface. A plateau is reached in a time scale of about 10-15 minutes and the total change of the SPR signal is in the range of 0,004 RIU and 0,007 RIU.

When non-doped **DOPC** vesicles are injected (Figure 3.4c), the signal increases with a slower kinetics and the plateau is reached in about 100 minutes. The total signal change is comparable with the total change for **Zn₂** doped vesicles.

Binding of proteins

In Figures 3.5, 3.6, and 3.7, we show the SPR signals obtained after injection of α -s1-casein, dephosphorylated α -s1-casein and BSA on supported membranes.

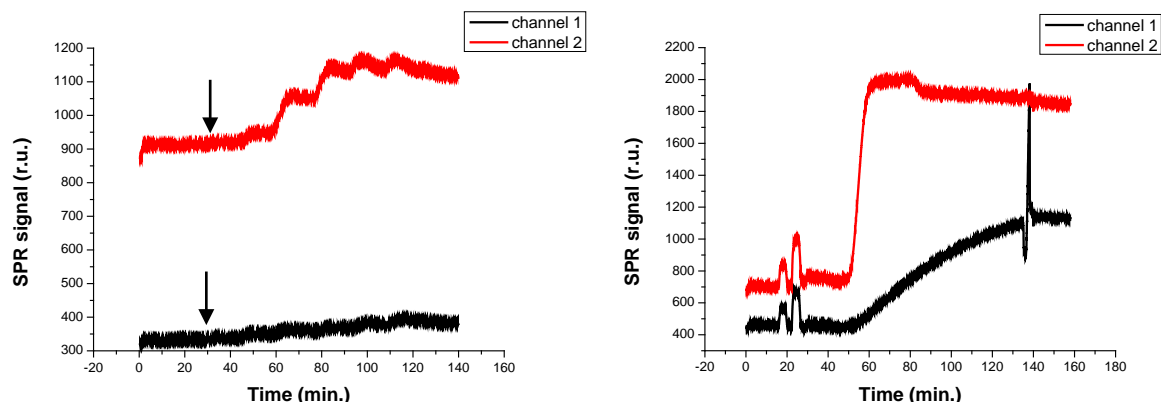


Figure 3.5: SPR sensorgrams obtained after injection of increasing concentrations of α -s1-casein (50 nM, 100 nM, 250 nM, 500 nM, 1 μ M and 2 μ M) on supported **DOPC** (channel 1) and **Zn₂** doped **DOPC** (channel 2) membranes (a); supported membranes formation (b). The arrow indicates the moment at which the solution of the lowest concentration reaches the sensor surface.

The injection of α -s1-casein solutions of different concentrations provokes an increase in the signal of both channels (Figure 3.5). The changes are larger for the surface modified with **Zn₂** doped membranes. Modest changes are observed when α -s1-casein solutions are injected on surfaces which do not contain **Zn₂**.

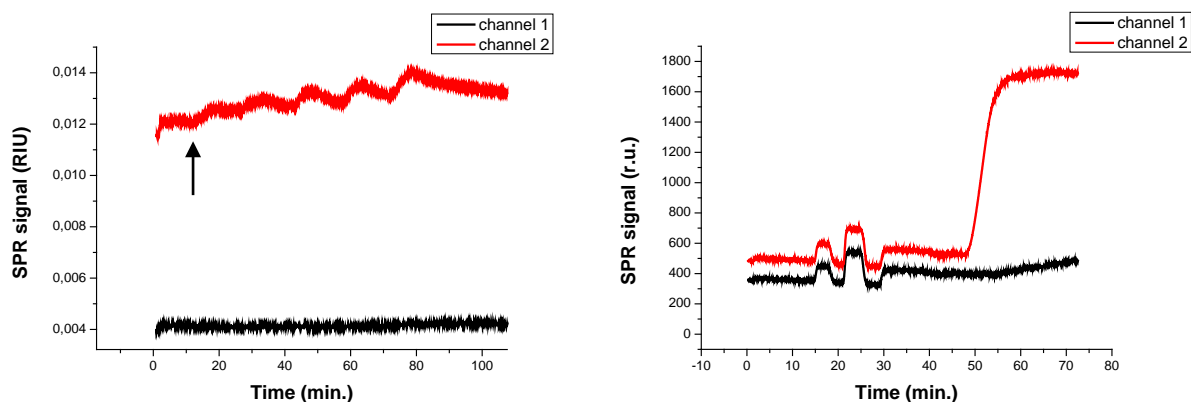


Figure 3.6: SPR sensorgrams obtained after injection of increasing concentrations of BSA (50 nM, 100 nM, 250 nM, 500 nM, 1 μ M and 2 μ M) on supported **DOPC** (channel 1) and **Zn₂** doped **DOPC** (channel 2) membranes (a); supported membrane formation (b). The arrow indicates the moment at which the solution of the lowest concentration reaches the sensor surface.

The Zn_2 doped supported membrane responds to the addition of BSA solutions of different concentrations on Zn_2 doped supported membrane (Figure 3.6a). On the other hand, the injection of the same solutions on the non-functionalized surface doesn't provoke any significant variation of the SPR signal.

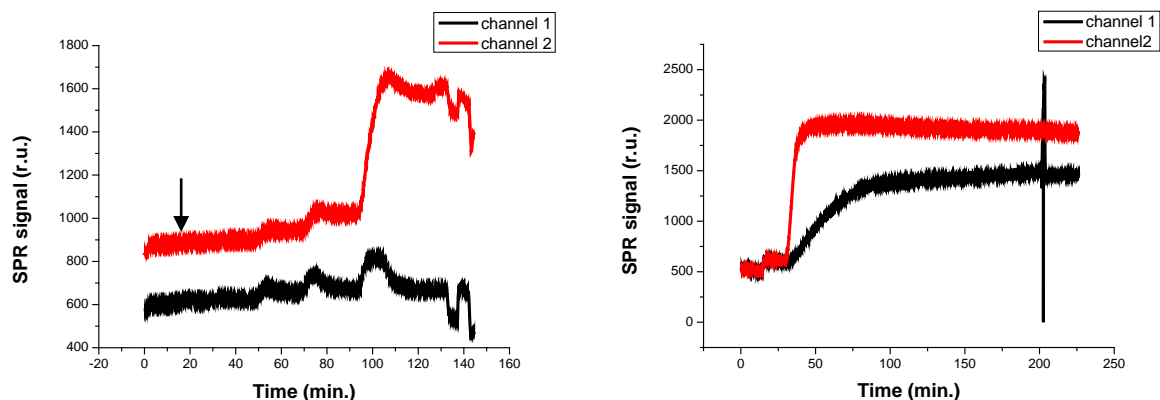


Figure 3.7: SPR sensorgrams obtained after injection of increasing concentrations (50 nM, 100 nM, 250 nM, 500 nM and 1 μM) of dephosphorylated α -s1-casein on supported **DOPC** (channel 1) and Zn_2 doped **DOPC** (channel 2) membranes (a); supported membrane formation (b). The arrow indicates the moment at which the solution of the lowest concentration reaches the surface.

Surprisingly, when the dephosphorylated α -s1-casein reaches the modified surfaces, it causes a rather large variation of the SPR signal (Figure 3.7), which is comparable to the response observed for the phosphorylated α -s1-casein (Figure 3.5). The signal increase is more pronounced for the surface functionalized with Zn_2 doped vesicles. If no receptor is present on the surface, the signal drops to the initial value after rinsing with buffer.

Binding of small analytes

In order to further explore the properties of the functionalized supported membranes, we studied less complex, smaller analytes. We chose the hexapeptide Ac-Gly-pSer-Ala-Ala-Ala-Leu-NH₂ (Figure 3.8) and ATP (Figure 3.9) as target molecules, as they are both known to interact with Zn₂ decorated vesicles [2, 3].

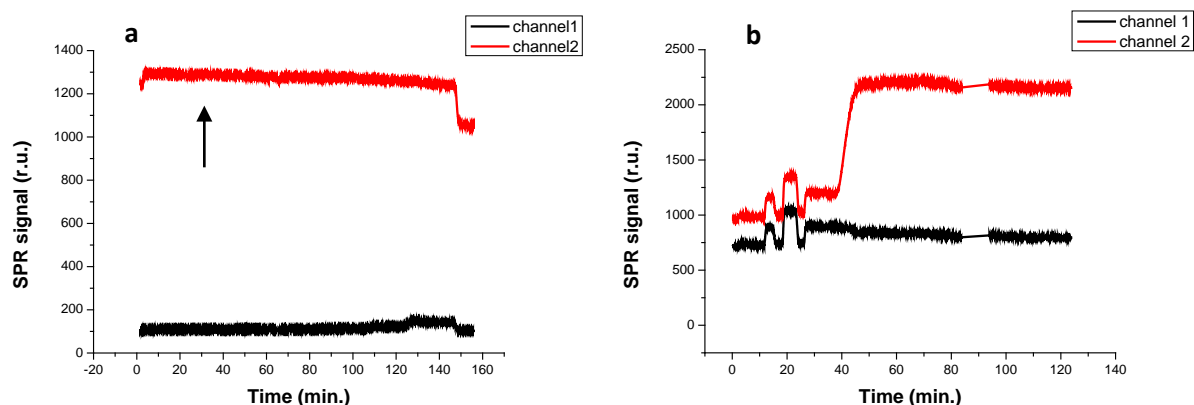


Figure 3.8: SPR sensorgrams obtained after injection of increasing concentrations of Ac-Gly-pSer-Ala-Ala-Ala-Leu-NH₂ (10 μ M, 25 μ M, 50 μ M, 100 μ M, 250 μ M and 500 μ M) on MUA SAM (channel 1) and supported Zn₂ doped DOPC membrane (channel 2) (a); supported membrane formation (b). The arrow indicates the moment at which the solution of the lowest concentration reaches the surface.

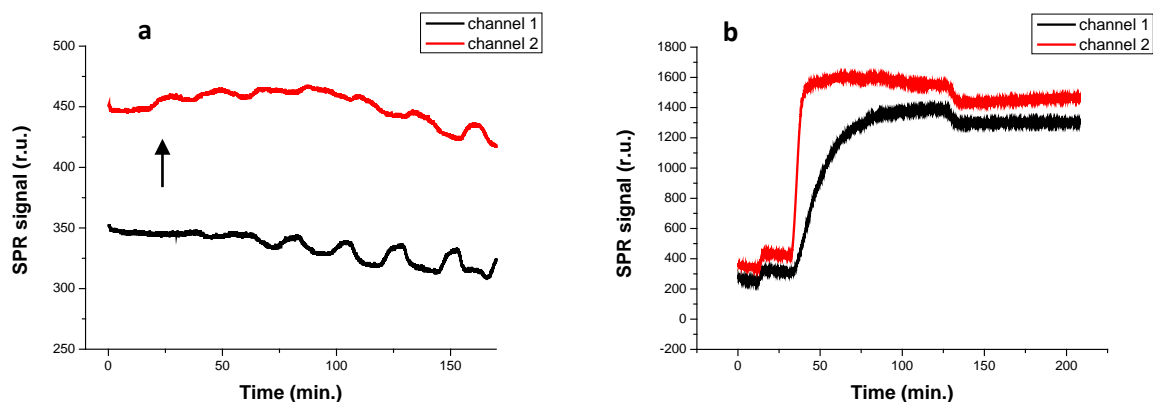


Figure 3.9: SPR sensorgrams obtained after injection of increasing concentrations of ATP (25 μ M, 50 μ M, 100 μ M, 250 μ M, 500 μ M, 1 mM and 2 mM) on supported DOPC (channel 1) and Zn₂ doped DOPC membranes (channel 2) (a); supported membranes formation (b). The arrow indicates the moment at which the solution of the lowest concentration reaches the sensor surface.

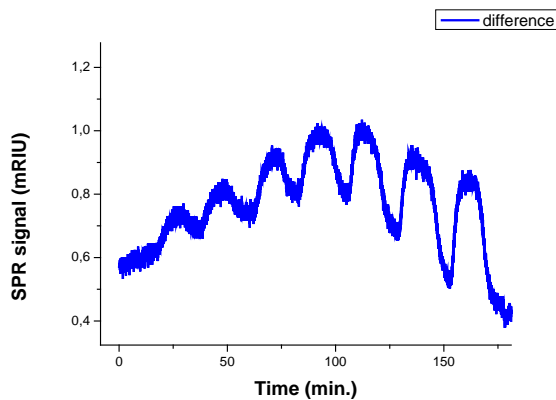
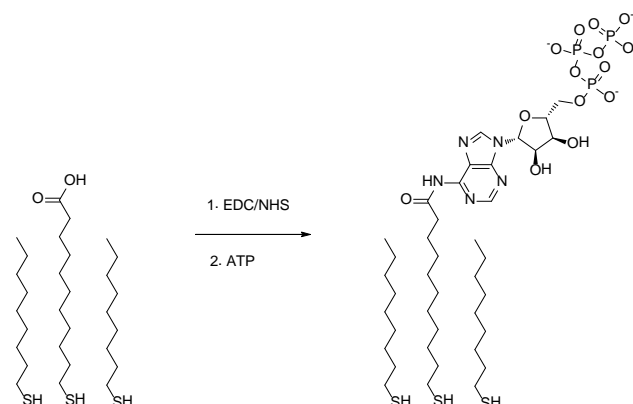


Figure 3.10: Normalized graph obtained as difference between channel 2 and channel 1 of Figure 3.9a.

The injection of the hexapeptide solutions of different concentrations does not provoke any significant changes in the signal for both channels (Figure 3.8). The injection of ATP with increasing concentrations provokes a different change in the SPR signal for the two channels. The curve obtained by subtraction of channel 1 to channel 2 after calibration shows a concentration dependent response (Figure 3.10). The changes are at the very limit of detection and saturation of the signal is reached rather soon.

3.2.2 Interaction of functionalized vesicles with surface immobilized analyte

ATP was immobilized on the SPR surface and the binding of functionalized vesicles was investigated. For that, ATP is coupled via amide coupling to the acidic function of MUA which is immobilized on the gold surface (Scheme 3.3).



Scheme 3.3: Reaction scheme of the attachment of ATP on the functionalized SPR surface via amide coupling.

In Figure 3.11b, we show the sensorgrams obtained after injecting of Zn_2 doped **DOPC** vesicles on an ATP modified surface (channel 2) and a non-ATP-modified surface (channel 1). The sensorgram in Figure 3.11a includes the functionalization step.

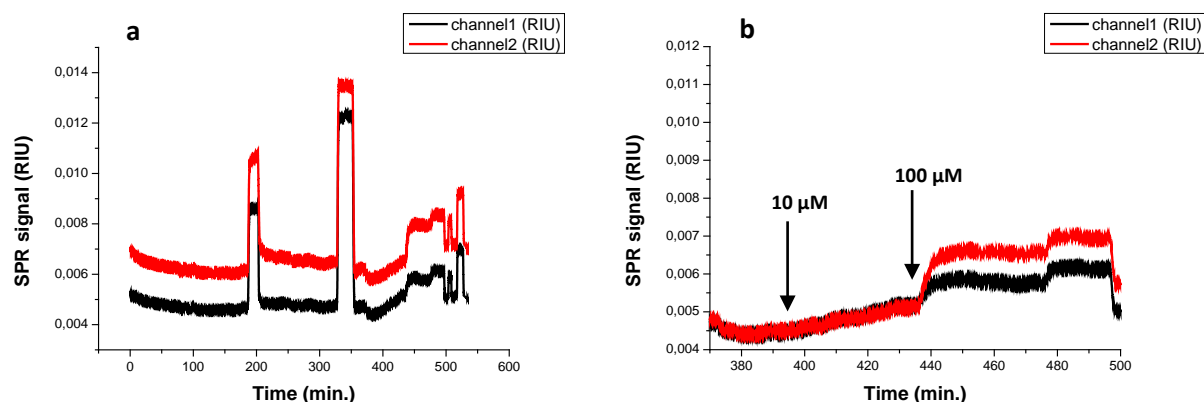


Figure 3.11: SPR sensorgrams obtained after injection of Zn_2 doped **DOPC** vesicles on functionalized surfaces. The surface were first modified with a SAM of 1-heptanethiol and 11-mercaptopundecanoic acid (10:1); subsequently, channel 2 was treated with the procedure for ATP functionalization and channel 1 with the same procedure as channel 2 but leaving out ATP (from 200 to 380 minutes) (a). Zoom of the last part of the same sensorgram (b). The curve for channel 2 is vertically shifted for better comparison.

The two spikes at around 200 and 300 minutes (Figure 3.11a) are provoked by the injections of the EDC/NHS solution and the ethanolamine solution, which are part of the surface functionalization procedure. The two channels give the same change in the signal after injection of vesicles of a total amphiphile concentration of 10 μM . A difference in the signal variation is observed after injection of vesicles of total amphiphile concentration of 100 μM . As expected, the Zn_2 modified vesicles seems to interact more strongly with the surface if the analyte is present.

In order to demonstrate that the observed interaction depends on the presence of the receptor in the liposome composition, we studied the binding of Zn_2 doped and non-doped **DOPC** vesicles to ATP-modified gold surfaces (Figure 3.12).

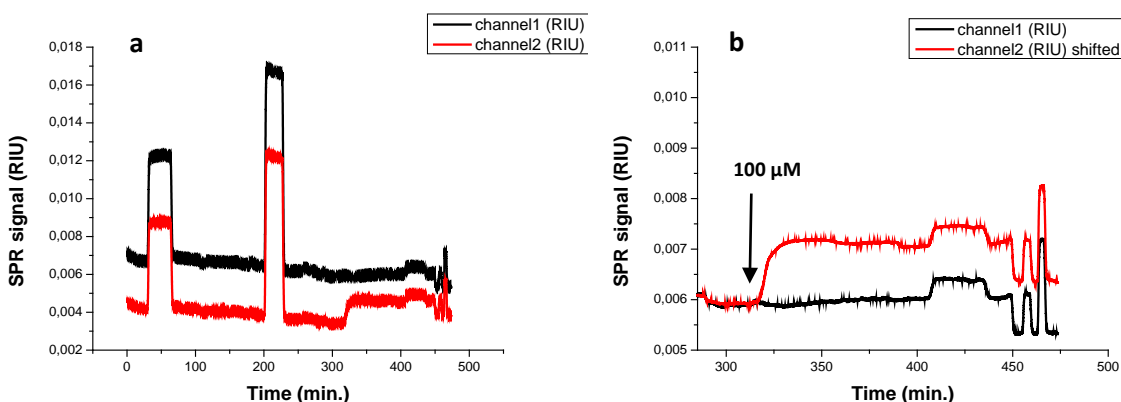


Figure 3.12: SPR sensorgrams obtained for the functionalization of the gold chip (SAM of 1-heptanethiol and 11-mercaptopundecanoic acid, 10:1) with ATP (from 0 to 300 minutes) and after injection of Zn_2 doped **DOPC** vesicles (channel 2) and non-doped **DOPC** vesicles (channel 1) (from 300 to 400 minutes) (a). Zoom of the last part of the same sensorgram (b). The curve for channel 2 is vertically shifted for better comparison.

The sensorgrams in Figure 3.12b clearly show that the affinity of the liposomes to the ATP labeled surface depends on whether or not Zn_2 is included in the composition.

As the sensorgrams in Figure 3.11 show that the Zn_2 doped liposomes interact also with the non ATP modified surface, we decided to further investigate this aspect.

The experiment shown in Figure 3.13 repeats the measures reported in Figures 3.11 and 3.12 and combines them in a single analysis.

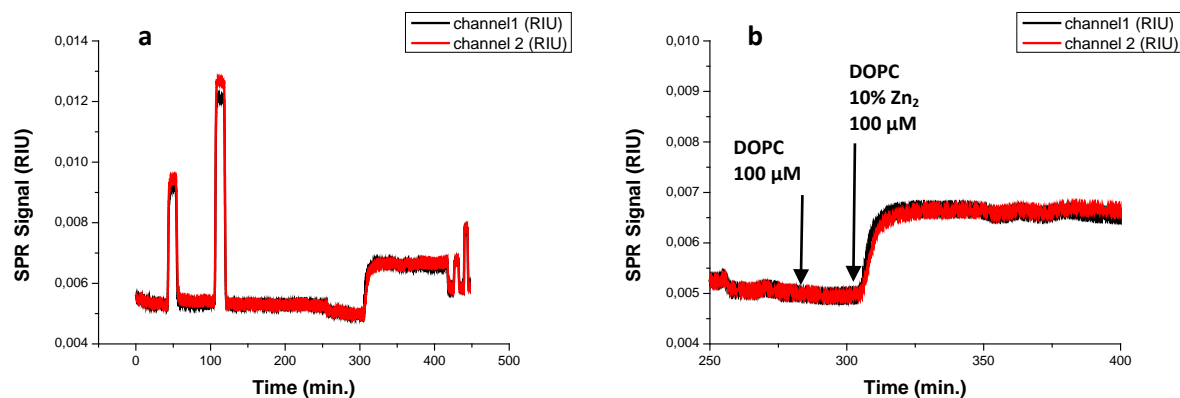


Figure 3.13: SPR sensorgrams obtained after injection of **DOPC** vesicles (280 minutes) and **Zn₂** doped **DOPC** vesicles (300 minutes) of a total amphiphile concentration of 100 μM on functionalized surfaces. The surface were first modified with a SAM of 1-heptanethiol and 11-mercaptopundecanoic acid (10:1); subsequently, channel 2 was treated with the procedure for ATP functionalization and channel 1 with the same procedure as channel 2 but leaving out ATP (from 0 to 250 minutes) (a). Zoom of the last part of the same sensorgrams (b).

No signal change is observed when non doped **DOPC** liposomes reach the surfaces, while a clear increase is detected when the doped ones come in contact with the chip. In contrast to what previously observed (Figure 3.11), the presence of ATP on the surface does not mark a difference in the SPR response.

We further investigated the interaction of the same vesicular systems with gold surfaces functionalized with 1-heptanethiol (Figure 3.14) and with a mixture of 1-heptanethiol and 11-mercaptopundecanoic acid (10:1) (Figure 3.15) in order to examine the contribution of the different components of the SAM to the nonspecific binding observed in the previous experiments, independently from the ATP functionalization.

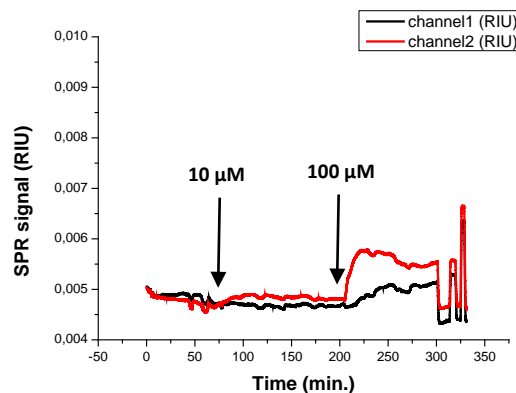


Figure 3.14: SPR sensorgrams obtained after injection of **DOPC** vesicles (channel 1) and **Zn₂** doped **DOPC** vesicles (channel 2) on 1-heptanethiol functionalized gold surface.

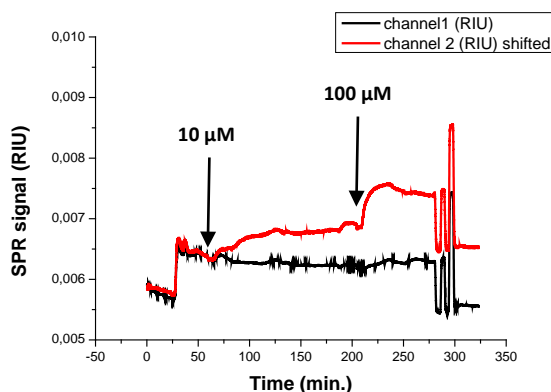


Figure 3.15: SPR sensorgrams obtained after injection of **DOPC** vesicles (channel 1) and **Zn₂** doped **DOPC** vesicles (channel 2) on a 1-heptanethiol and 11-mercaptopundecanoic acid (10:1) functionalized gold surface.

The **DOPC** vesicles interact with the surface in both cases (Figure 3.14 and 3.15) when the total amphiphile concentration of the injected sample is 100 μM . The **Zn₂** doped **DOPC** vesicles interact faster and at lower total amphiphile concentrations than the non-doped ones. The experiments presented in Figures 3.13, 3.14 and 3.15 tell us that the receptor decorated vesicles have stronger affinity compared to the non-decorated ones, towards all the explored surfaces. In particular the interaction doesn't seem to depend on the presence of ATP on the surface (Figure 3.13).

An analogous series of experiments was made with **DSPC** vesicles in order to investigate the effect of the membrane phase (gel instead of liquid crystalline phase) on the interaction of the vesicles with the different surfaces. We first explored the SPR signal response of **Zn₂** decorated **DSPC** vesicular systems when they are injected on a ATP modified surface (Figure 3.16).

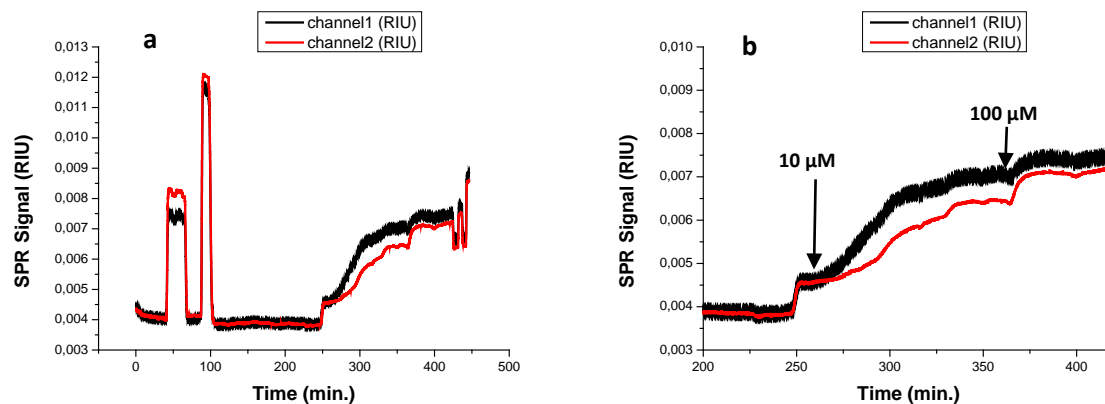


Figure 3.16: SPR sensorgrams after injection of Zn_2 doped **DSPC** vesicle on functionalized sensor chip. The surfaces were first modified with a SAM of 1-heptanethiol and 11-mercaptoundecanoic acid (10:1); subsequently, channel 1 was treated with the procedure for ATP functionalization and channel 2 with the same procedure as channel 1 but leaving out ATP (from 0 to 200 minutes) (a). Zoom of the last part of the same sensorgram (b).

When the liposomes reach the surface, the signal increases in both channels (Figure 3.16b), suggesting that the presence of ATP on the surface has only a minor effect on the affinity of the liposomes to the surface. As for the **DOPC** system, also for the **DSPC** vesicles we investigated the SPR response surfaces functionalized with 1-heptanethiol (Figure 3.17) and with a mixture of 1-heptanethiol and 11-mercaptoundecanoic acid (10:1) (Figure 3.18).

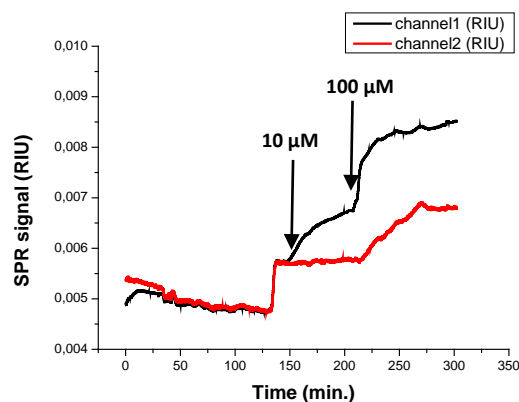


Figure 3.17: SPR sensorgrams obtained after injection of **DSPC** vesicles (channel 1) and Zn_2 doped **DSPC** vesicles (channel 2) on a 1-heptanethiol functionalized gold surface.

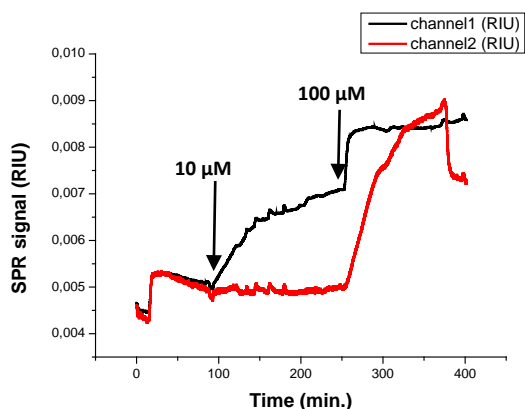


Figure 3.18: SPR sensorgrams obtained after injection of **DSPC** vesicles (channel 2) and **Zn₂** doped **DSPC** vesicles (channel 1) on a 1-heptanethiol / 11-mercaptoundecanoic acid (10:1) functionalized gold surface.

The response of the surfaces upon the injection of **DSPC** vesicles is very similar to the response in case of **DOPC** vesicles. The **DSPC** vesicles interact with all the investigated surfaces. The interaction is different between **Zn₂** doped and non-doped vesicles: the former bind faster and at lower concentrations. No significant difference is observed if the ATP is immobilized on the surface or not. In order to investigate if the non-specific binding of vesicles to surfaces which are not modified with ATP can be suppressed by PEGylation (as reported in [2] for similar systems), we studied the interaction of **Zn₂** doped and non-doped vesicles prepared from a mixture of **DSPC** and **DSPE-PEG350** (1:1) with a 1-heptanethiol / 11-mercaptoundecanoic acid (10:1) functionalized gold surface (Figure 3.19).

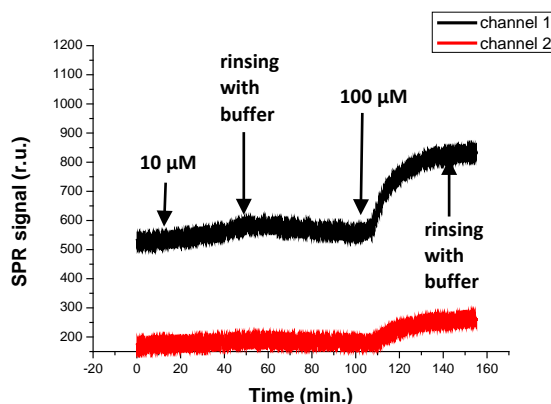


Figure 3.19: SPR sensorgrams obtained after injection of **DSPC** / **DSPE-PEG350** (1:1) vesicles (channel 2) and **Zn₂** doped **DSPC** / **DSPE-PEG350** (1:1) vesicles (channel 1) on a 1-heptanethiol / 11-mercaptoundecanoic acid (10:1) functionalized gold surface.

The PEGylated vesicles (**Zn₂** doped and non-doped) interact with the 1-heptanethiol / 11-mercaptopundecanoic acid (10:1) functionalized surface. A moderate change in the SPR signal is observed after injection of the vesicles at 10 μ M total amphiphile concentration. The signals are constant after rinsing with buffer. After injection of vesicles with a total amphiphile concentration of 100 μ M, a significant increase of the SPR signal is observed. The signals are constant after a further rinsing step with the buffer.

3.2.3 Interaction of gold nanoparticles with supported membranes monitored by SPR

As alternative approach to overcome the sensitivity issues related to the investigation of small analytes via SPR, we monitored the affinity of gold nanoparticles (**AuNPs**) to our supported membranes. The idea is to utilize the nanoparticles to develop a displacement assay: we planned first to bind the gold nanoparticles to the supported membrane and subsequently to displace them with the analyte. In Figure 3.20, we show the interaction of 25 nm diameter **AuNPs** with a supported **Zn₂** doped **DOPC** membrane. After immobilization of the particles, we injected the analyte (**PP_i**) to test the displacement.

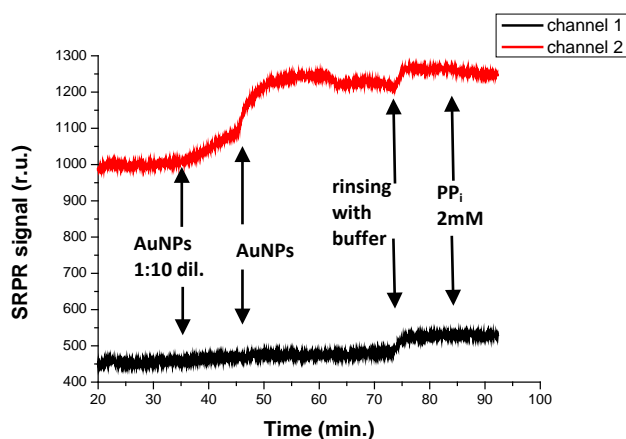


Figure 3.20: SPR sensorgrams obtained after injection of increasing concentrations of **AuNPs** on a MUA SAM (channel 1) and a **Zn₂** doped **DOPC** vesicle (channel 2) functionalized gold surface. 1:10 dil. means that the injected solution was prepared by 1:10 dilution of the **AuNPs** solution received from the supplier with H_2O .

The SPR signal increases as the **AuNPs** reach the membrane functionalized surface (channel 2). The signal is stable after rinsing with buffer and does not change significantly after injection of 2 mM solution of pyrophosphate (**PP_i**).

We studied the effect of introducing a more specific binding unit on the surface of the nanoparticles, performing an analogue analysis using thiolated-ADP functionalized vesicles (Figure 3.22).

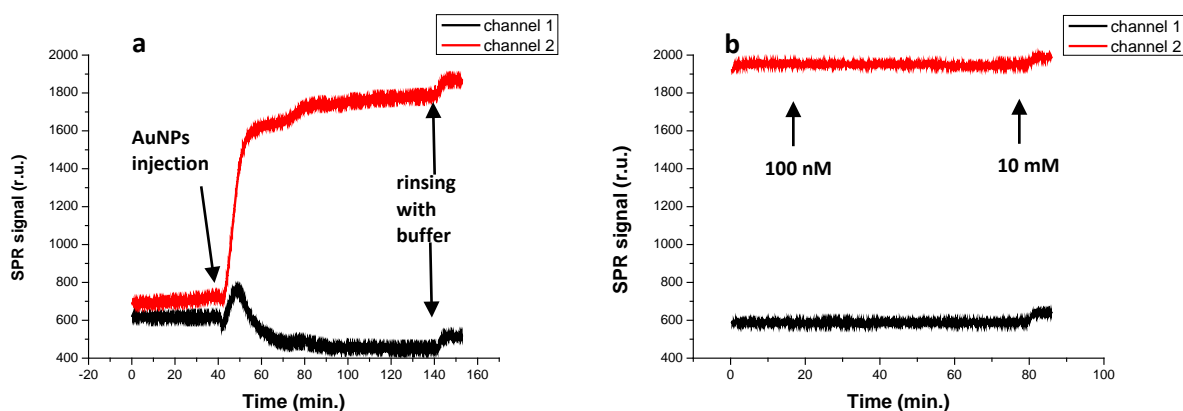


Figure 3.21: SPR sensorgrams obtained after injection of thiolated-ADP functionalized **AuNPs** (channel 2) and non-functionalized **AuNPs** (channel 1) on **Zn₂** doped **DOPC** supported membranes (a). SPR sensorgrams obtained after injection of increasing concentrations of pyrophosphate (100 nM, 1 μM, 10 μM, 100 μM, 1 mM and 10 mM) on the surfaces (b).

The SPR signal increases as the thiolated-ADP functionalized **AuNPs** reach the surface (channel 2). The evolution of the signal after injecting the non-functionalized **AuNPs** is surprising: the signal increases, it reaches a maximum and afterwards it drops to a value lower than the initial.

The injection of pyrophosphate up to 1 mM concentration does not produce a significant change in the SPR signal. An increase of the signal in both channels is observed as the 10 mM solution reaches the surface.

The nanoparticles (coated or non-coated with thiolated-ADP) bind to the **Zn₂** doped supported membrane, but the binding seems to be not reversible, as after injection of buffer or of pyrophosphate solutions, the signal doesn't change, as would be expected if the **AuNPs** were displaced (Figure 3.20 and 3.21b).

3.2.4 Affinity of selected peptides to supported functionalized membrane monitored by quartz crystal microbalance

As the previously discussed SPR studies did not allowed to characterize the binding of small analytes to the modified supported membranes, we investigated QCM as alternative method. As first step we induced the formation of a Zn_2 doped **DOPC** bilayer on gold coated crystal functionalized with a MUA self-assembled monolayer. After the injection of the vesicle solution, a rinsing step with H_2O is necessary in order to form the bilayer (Figure 3.22).

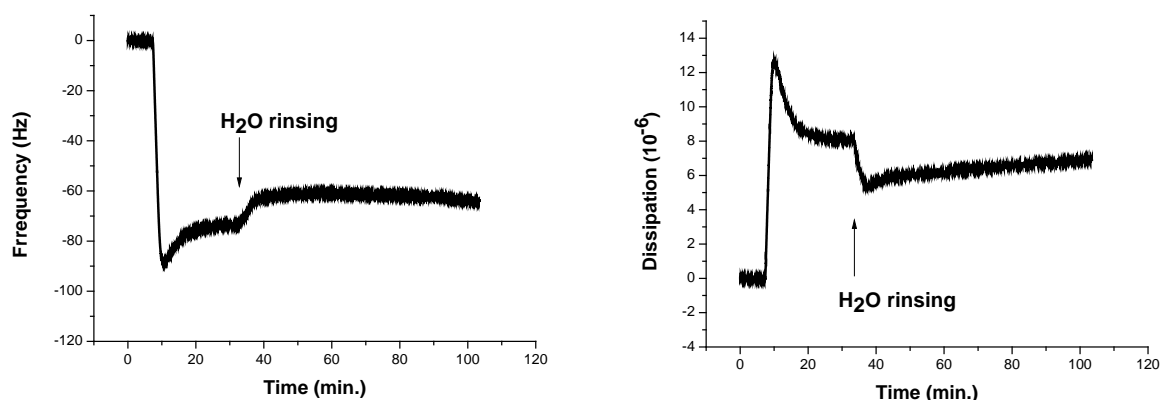


Figure 3.22: Change of the QCM resonant frequency and dissipation with time after injection of Zn_2 doped **DOPC** vesicles at a 0.2 mM total amphiphile concentration followed by a rinsing step with H_2O .

As the vesicles reach the surface, the frequency value drops, it reaches a minimum and it stabilizes. After rinsing with water the frequency rises and reaches and becomes constant. The dissipation evolution in time follows a symmetric behavior.

According previous work done by Kasemo [12] the variation of frequency and dissipation after injection of the liposomes observed in Figure 3.22 indicates the formation of the bilayer on the surface.

At a later stage we investigated the affinity to the functionalized membrane of two different peptides: Ac-Gly-pSer-Ala-Ala-Ala-Leu-NH₂ (**peptide I**) and Ac-Gly-pSer-Ala-Ala-His-Leu-NH₂ (**peptide II**). Both peptides are known to have affinity to Zn_2 decorated vesicular sensors [3]. Moreover, for **DOPC** based liposomes, **peptide II**, which contains a histidine as additional binding site, had demonstrated a significantly stronger affinity, thanks to the cooperative effects of the embedded receptors.

We therefore examined **peptide I** (Figure 3.23) and **peptide II** (Figure 3.24) with the aim to verify if the same phenomenon was visible with the QCM technique as well.

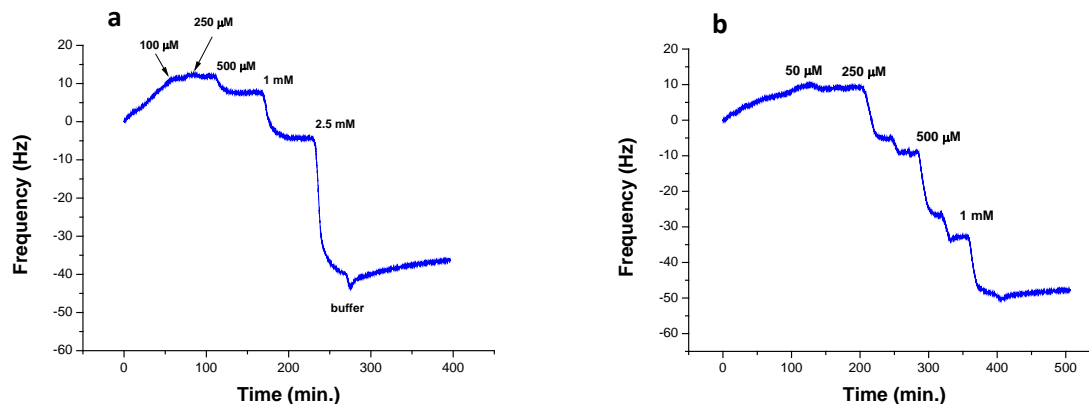


Figure 3.23: Binding curves for the **peptide I** obtained after consecutive injections of increasing concentrations of peptide. The graphs a and b refer to two different experiments.

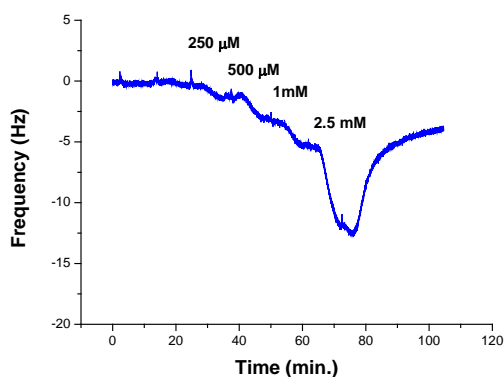


Figure 3.24: Binding curve for the **peptide II** obtained after consecutive injections of increasing concentrations of peptide.

For **peptide I** the frequency signal starts to increase when the solutions of 500 μM (3.23a) and 250 μM (3.23b) reach the surfaces and it further increases with higher concentrations. For **peptide II** (Figure 3.24) the signal significantly increases only upon addition of a 2.5 mM solution.

High concentrations are needed in order to observe a significant change in the frequency upon addition of the peptides to the functionalized crystal. The low response observed for the bivalent **peptide II** suggests that the saturation is reached already at the low concentrations.

3.3 CONCLUSION

The preparation of Zn_2 doped and non-doped supported membranes on the SPR sensor chip is reproducible and can be performed with different types of SAM. For all the different systems which were investigated, we were able to observe an increase in the SPR signal which ends with a plateau. The functionalized SPR surfaces are stable enough to allow the study of the binding of different analytes.

The three proteins which were investigated showed a different response depending on whether Zn_2 is present or not. The presence of Zn_2 gives larger signal changes for all the three cases. Interestingly for BSA, the change in the signal for the non Zn_2 doped surface is very weak (almost zero), while for α -s1-casein and dephosphorylated α -s1-casein, it is significant.

The interaction of BSA with the Zn_2 functionalized surface looks weaker than the interaction of α -s1-casein and dephosphorylated α -s1-casein. The interaction of phosphorylated and dephosphorylated casein looks very similar.

The low selectivity of the interaction is surprising as with the fluorescent chemosensors, it has been observed that the Zn_2 functionalized vesicles are able to bind casein more strongly than dephosphorylated casein. The poor selectivity could be related to the particular experimental conditions imposed by the technique itself (concentrations used, heterogeneous system and high amount of receptor molecules). The binding studies with the “smaller” analytes gave very modest results. The peptide did not induce a response at all. For ATP the responses for the Zn_2 functionalized and the non-functionalized membrane were different (Figure 3.9), but not easily reproducible. Therefore, it was not possible to achieve some quantitative results.

The employment of **AuNPs** to develop a displacement assay exhibited some limitations. The nanoparticle binds to the supported membrane, but cannot be displaced by the analyte.

The analysis of the interaction of the vesicular systems with the ATP-modified gold surfaces presented some difficulties as well. The Zn_2 doped vesicles bind faster and at lower concentrations than the non-doped vesicles, independently from the presence of the analyte on the sensor surface.

One possible explanation could be related to the stability of the vesicles and to the properties at the interphase between the double layer and the solution. The QCM experiments were performed only for Zn_2 doped vesicles. A signal change was observed for both peptides, but only when solutions of

relatively high concentrations were injected on the surface, as the mass variation caused by the binding of the peptides was too small for lower concentrations.

3.4 EXPERIMENTAL SECTION

Materials: N-hydroxysuccinimide (NHS) was purchased from Fluka, 1-ethyl-3-(3-dimethylaminopropyl)carbodiimide (EDC) was purchased from Novabiochem, DOPC, DSPC and DSPE-PEG350 were purchased from Avanti Polar Lipids, the bis-(zinc-cyclen) receptor (**Zn₂**) was synthesized by Andreas Müller according to the procedure described in [18], absolute ethanol, 11-mercaptopundecanoic acid (MUA), 1-heptanethiol, 16-mercaptophexadecanoic acid (MHDA), (3-mercaptopropyl)trimethoxysilane (MPTMS), ATP, α -s1-casein, dephosphorylated α -s1-casein, 4-(2-hydroxyethyl)-1-piperazineethanesulfonic acid (HEPES), 2-(N-morpholino)ethanesulfonic acid (MES) and gold nanoparticles of 20 nm in diameter in stabilized citrate buffer (concentration = 6.54×10^{11} particles/ml) were purchased from Sigma-Aldrich, BSA was purchased from Roth GmbH, H₂O was purified by using a Millipore MilliQ Gradient A10 system, the peptides Ac-Gly-pSer-Ala-Ala-Ala-Leu-NH₂ and Ac-Gly-pSer-Ala-Ala-His-Leu-NH₂ were purchased from GL Biochem (Shanghai) Ltd, polycarbonate membranes for extrusion were purchased from AVESTIN.

SPR instrumentation: all the sensorgrams were recorded on a 2 channels Biosuplar 400T (Analytical μ -Systems, Mivitec GmbH). The gold chips were purchased from the same company.

QCM-D instrumentation: all the QCM-D experiments were performed with Q-Sense E1 system (Q-Sense, Biolin Scientific). Gold coated AT-cut quartz crystals were purchased from the same company. The instrument records frequency and dissipation of the fundamental oscillation and of 3rd, 5th, 7th, 11th and 13th harmonics. Data of the 7th harmonic are shown. The QCM-D experiments were performed in the laboratories of Prof. K. Haupt at the Université de Technologie de Compiègne (France).

Vesicles preparation: in a small glass vessel, the proper volumes of solutions of **DOPC** (2 mM in CHCl₃) and **Zn₂** (1 mM in EtOH) were added. The solvents were removed under vacuum for 15 minutes and HEPES buffer solution (25 mM, pH = 7.4) was added. The suspension obtained was mixed at 900 rpm at room temperature for 15 minutes to obtain a turbid solution and subsequently extruded through a 100 nm pore size polycarbonate membrane to obtain small unilamellar vesicles solution.

For **DSPC** and **DSPC / DSPE-PEG350** 1:1 vesicles, we adopted the same procedure, except that the incubation step before extrusion and the extrusion were performed at 75 °C.

SAM formation on gold surfaces: after rinsing three times with absolute EtOH, the SPR gold chips were immersed in a solution 1 mM of thiol in EtOH for 40 hours to obtain a self-assembled monolayer. The gold slides were then rinsed two times with EtOH and mounted on the SPR instrument.

ATP coupling: the coupling was performed as described in [19]. Gold surfaces functionalized with 1-heptanethiol / 11-mercaptoundecanoic acid (10:1) were used. The carboxylic acid functions were activated by injecting 1 ml of 50 mM NHS, 100 mM EDC in 50 mM MES buffer, pH = 5.5. After rinsing with 50 mM MES buffer, pH = 5.5, 2 ml of 50 μ M ATP solution in 50 mM MES buffer, pH = 6.5, was injected. The surface was then rinsed with 2 ml 50 mM MES buffer, pH = 6.5, and subsequently, the unreacted sites were quenched by injecting ethanolamine 1 mM in 50 mM MES buffer, pH = 8.5. The surface was then rinsed with 50 mM MES buffer, pH = 5.5, and finally with 25 mM HEPES buffer, pH = 7.4.

SPR measurements: the samples were injected at a flow rate of 55 μ l min⁻¹. In order to prepare the supported membranes, the vesicle suspensions were injected on the MUA functionalized gold surfaces at a total amphiphile concentration of 1 mM for non-doped vesicles and of 100 μ M for **Zn₂** doped vesicles.

For the binding studies on supported membranes: after 5 minutes of analyte samples injection, a 25 mM HEPES buffer solution, pH = 7.4 was injected for 10 minutes, the cycle analyte-buffer was repeated for all concentrations. In the experiment shown in Figures 3.7, the injections times were longer than 5 minutes.

For the binding studies of vesicles to functionalized surfaces, the vesicle solutions were injected on the surfaces until a stable signal was reached.

All analyte solutions were prepared in HEPES buffer (25 mM, pH = 7.4).

Thiolated-ADP preparation: thiolated ADP was prepared by reaction of ADP with 10 equivalents of 2-iminothiolane (Traut's reagent) in 25 mM HEPES buffer solution, pH = 7.4, for 1 hour and used without further purification.

AuNPs functionalization with ADP: the gold nanoparticles were incubated for 40 h under stirring in a 1 μ M thiolated-ADP solution.

QCM-D measurements: before use, the crystals were cleaned for 10 minutes with UV/ozone cleaner and afterwards immersed in a 5:1:1 solution of milliQ H₂O : H₂O₂ (30%) : NH₃ (28%) at 75°C for 10 minutes. After 4 times rinsing with milliQ H₂O and 1 time rinsing with EtOH, the crystals were immersed in a 2 mM MUA solution in EtOH overnight.

Vesicles samples were injected at a flow rate of 200 $\mu\text{l min}^{-1}$.

For the experiment shown in Figure 3.23a: for each concentration, 500 μl were injected at 50 $\mu\text{l/min}$, after a stable signal was reached, 25 mM HEPES buffer (pH = 7.4) was injected.

For the experiments shown in Figures 3.25b and 3.26: for each concentration, 500 μl of the solution were injected at 50 $\mu\text{l/min}$. After a stable signal was reached, the solution of the next concentration was injected.

3.5 REFERENCES

1. Gruber, B., Stadlbauer, S., Späth, A., Weiss, S., Kalinina, M. and König, B., *Modular chemosensors from self-assembled vesicle membranes with amphiphilic binding sites and reporter dyes*. *Angewandte Chemie International Edition*, 2010. **49**(39): p. 7125-7128.
2. Gruber, B., Stadlbauer, S., Woinaroschy, K. and König, B., *Luminescent vesicular receptors for the recognition of biologically important phosphate species*. *Organic & Biomolecular Chemistry*, 2010. **8**(16): p. 3704-3714.
3. Gruber, B., Balk, S., Stadlbauer, S. and König, B., *Dynamic interface imprinting: high-affinity peptide binding sites assembled by analyte-induced recruiting of membrane receptors*. *Angewandte Chemie International Edition*, 2012. **51**(40): p. 10060-10063.
4. Banerjee, S. and König, B., *Molecular imprinting of luminescent vesicles*. *Journal of the American Chemical Society*, 2013. **135**(8): p. 2967-2970.
5. Jonsson, U., Fagerstam, L., Ivarsson, B., Johnsson, B., Karlsson, R., Lundh, K., Lofas, S., Persson, B., Roos, H., Ronnberg, I., Sjolander, S., Stenberg, E., Stahlberg, R., Urbaniczky, C., Ostlin, H. and Malmqvist, M., *Real-time biospecific interaction analysis using surface-plasmon resonance and a sensor chip technology*. *Biotechniques*, 1991. **11**(5): p. 620-627.
6. Homola, J., *Present and future of surface plasmon resonance biosensors*. *Analytical and Bioanalytical Chemistry*, 2003. **377**(3): p. 528-539.
7. Patching, S.G., *Surface plasmon resonance spectroscopy for characterisation of membrane protein-ligand interactions and its potential for drug discovery*. *Biochimica et Biophysica Acta*, 2014. **1838**(1 Pt A): p. 43-55.
8. Besenicar, M., Macek, P., Lakey, J.H. and Anderluh, G., *Surface plasmon resonance in protein-membrane interactions*. *Chemistry and Physics of Lipids*, 2006. **141**(1-2): p. 169-178.
9. Mozsolits, H., Thomas, W.G. and Aguilar, M.I., *Surface plasmon resonance spectroscopy in the study of membrane-mediated cell signalling*. *Journal of Peptide Science*, 2003. **9**(2): p. 77-89.
10. Wink, T., van Zuilen, S.J., Bult, A. and van Bennekom, W.P., *Liposome-mediated enhancement of the sensitivity in immunoassays of proteins and peptides in surface plasmon resonance spectrometry*. *Analytical Chemistry*, 1998. **70**: p. 827-832.

11. Okahata, Y. and Ebato, H., *Application of a quartz-crystal microbalance for detection of phase transitions in liquid crystals and lipid multibilayers*. Analytical Chemistry, 1989 **61**: p. 2185-2188.
12. Keller, C.A. and Kasemo, B., *Surface specific kinetics of lipid vesicle adsorption measured with a QCM microbalance*. Biophysical Journal, 1998. **75**: p. 1397–1402.
13. Richter, R.P., Bérat, R. and Brisson, A.R., *Formation of solid-supported lipid bilayers: An integrated view*. Langmuir, 2006. **22**: p. 3497-3505.
14. Becker, B. and Cooper, M.A., *A survey of the 2006-2009 quartz crystal microbalance biosensor literature*. Journal of Molecular Recognition, 2011. **24**(5): p. 754-787.
15. Aoki, S., Zulkefeli, M., Shiro, M., Kohsako, M., K., T. and Kimura, E., *A luminescence sensor of inositol 1,4,5-triphosphate and its model compound by Ruthenium-templated assembly of a bis(Zn²⁺-cyclen) complex having a 2,2'-bipyridyl linker (cyclen = 1,4,7,10-tetraazacyclododecane)*. Journal of the American Chemical Society, 2005. **127**: p. 9129-9139.
16. Ishizuka-Katsura, Y., Wazawa, T., Ban, T., Morigaki, K. and Aoyama, S., *Biotin-containing phospholipid vesicle layer formed on self-assembled monolayer of a saccharide-terminated alkyl disulfide for surface plasmon resonance biosensing*. Journal of Bioscience and Bioengineering, 2008. **105**(5): p. 527-535.
17. Zhao, S.S., Bichelberger, M.A., Colin, D.Y., Robitaille, R., Pelletier, J.N. and Masson, J.F., *Monitoring methotrexate in clinical samples from cancer patients during chemotherapy with a LSPR-based competitive sensor*. Analyst, 2012. **137**(20): p. 4742-4750.
18. Turygin, D.S., Subat, M., Raitman, O.A., Arslanov, V.V., König, B. and Kalinina, M.A., *Cooperative self-assembly of adenosine and uridine nucleotides on a 2D synthetic template*. Angewandte Chemie International Edition, 2006. **45**(32): p. 5340-5344.
19. Krazinski, B.E., Radecki, J. and Radecka, H., *Surface plasmon resonance based biosensors for exploring the influence of alkaloids on aggregation of amyloid-beta peptide*. Sensors, 2011. **11**(4): p. 4030-4042.

Chapter 4

Fluorescence microscopy characterization of
vesicular chemosensors

4.1 INTRODUCTION

As previously described [1, 2], lipid vesicles with embedded artificial receptors and an environment sensitive dye are able to give a fluorescence response upon addition of analytes which have an affinity to the embedded receptors. The fluorescence response is believed to be due to a reorganization of the receptor and dye molecules on the surface of the vesicles which is provoked by the interaction with the analyte (Figure 4.1).

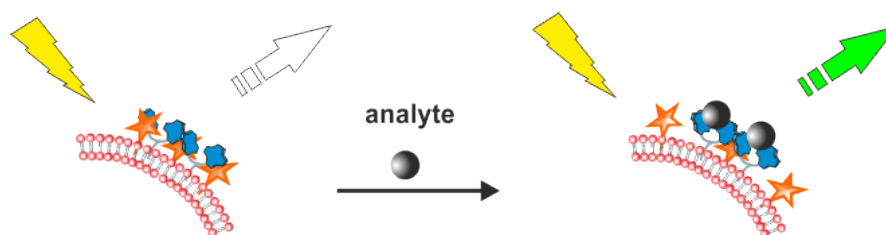


Figure 4.1: Schematic representation of the vesicular chemosensors working principle. Embedded dyes and receptors are organized in patches on the surface of the vesicles. The binding of the analyte molecules to the receptors provokes the reorganization of such patches, which induces a change in the fluorescence.

The mechanistic hypothesis of the sensing principle is supported by the investigation of the vesicular chemosensors doped with different amounts of embedded receptor and dye and by FRET experiments [2, 3].

In order to confirm the mechanistic hypothesis, we were interested in characterizing the organization of the embedded molecules more directly with the aim to visualize the molecules on the surface of the vesicles and possibly to detect changes in their arrangement provoked by the interaction with the analyte.

The investigation of the molecular composition and organization of functionalized lipid membranes can be done following different approaches. Supported membranes, typically bilayers anchored to a solid support (e.g. mica), are widely employed models. Different methods have been proposed in order to characterize such supported membranes. X-ray scattering and fluorescence microscopy, for example, have been reported as tools to investigate domains of synthetically designed lipids in supported lipid films in the field of cell recognition mechanistic studies [4]. AFM and TIRF microscopy have been used by Oreopoulos and co-workers [5] to elucidate the mechanism of the structure change of supported lipid membranes provoked by the interaction with antimicrobial peptides. Okazaki and colleagues [6] combined AFM with FRAP to characterize polymerized domains in fluid

supported bilayers. Fluorescence microscopy imaging techniques were employed by Simonsen [7] to investigate the changes in domain features provoked by the action of phospholipases on supported lipids. A comprehensive description of the techniques applied for the visualization of the supported bilayer systems can be found in a recent review published by Gozen and Jeroska [8].

Another approach consists in investigating liposomes in solution phase rather than solid supported membranes [9]. Electron microscopy techniques (such as cryo-TEM or FF-TEM) have been employed to study several features (such as morphology, dimension and surface properties) of liposomes of different dimensions and compositions [10, 11]. AFM has been employed to investigate structural features [12] as well as physical properties of submicron phospholipid vesicles with different composition [13, 14]. Even though fluorescence microscopy is more limited in terms of resolution compared to AFM and TEM techniques, it has been employed to characterize liposomes. It has been utilized for example to determine the encapsulation efficiency [15] of dye molecules in liposomes as well as to develop an alternative method to measure the size distribution and lamellarity of liposomes [16].

AFM, STM (scan tunneling microscopy) and cryo-TEM measurements of vesicular chemosensors were carried out during the last few years in the König group. In general, the visualization of the liposomes surface with a sufficient high resolution was not possible. As an alternative approach, we therefore decided to explore super resolved fluorescence microscopy (SRFM). SRFM is a relatively recent advancement in the field of fluorescence microscopy. The diffraction limit determines the resolution of standard fluorescence microscopy, which is generally around 200 nm in the lateral dimension and 500 nm in the axial dimension. Starting from the early 1990's, new microscopy techniques which are able to go beyond that limit became available [17]. One of the most recently developed super resolution techniques is the stochastic optical reconstruction microscopy STORM, which is based on the temporal localization of single fluorescent emitters [18]. Fluorescent emitters that can be switched to a stable dark state in a reversible manner are used; the data are recorded as a sequential acquisition of different subsets of the total number of fluorescent emitters. For each acquisition, only a very limited number of optically resolved emitters are activated and their position is determined with high accuracy. The imaging is performed several times (from hundreds to thousands of times, depending on the requirements of the experiment) and for each acquisition, a different subset of emitters is stochastically excited. The super resolved image is obtained as a superimposition of the single acquisitions. According to [17],

10 nm

and an axial resolution of about 50 nm. Figure 4.2 shows a schematic representation of the working principle of the technique.

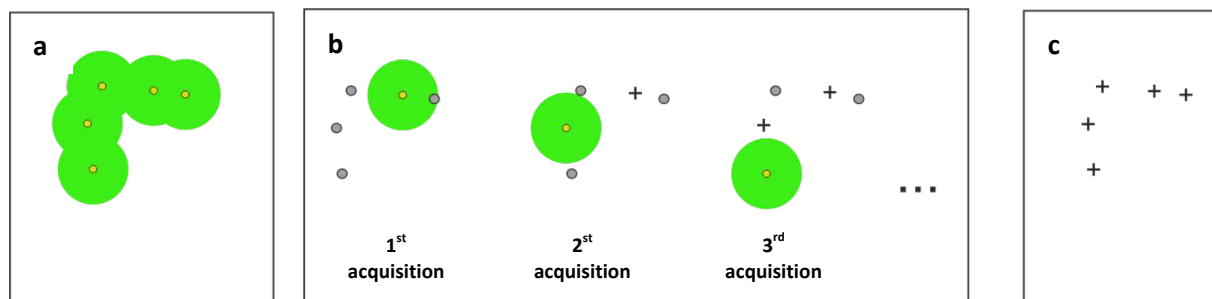
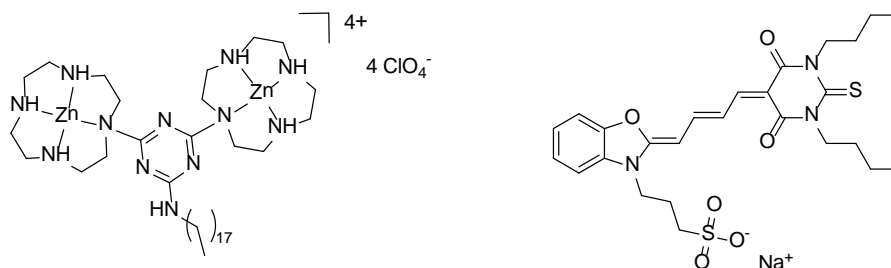


Figure 4.2: Schematic representation of the STORM approach: (a) the fluorophores in the sample are too close to be resolved; (b) stochastic activation and localization of a small subset of fluorophores repeated for several times; (c) image reconstruction by combination of individual localizations.

There are several types of fluorescent probes which are suitable for STORM, such as certain artificial dye pairs, artificial dyes, fluorescent proteins and quantum dots. The artificial dye merocyanine 540 (**MC540**) (structure in Scheme 4.1) was chosen as a probe, as it is a simple solvatochromic dye which can be easily embedded in vesicular chemosensors and it is suitable for STORM [19].

We first planned to investigate **MC540** as a reporting dye in the vesicular chemosensors assay: the fluorescence response of the dye upon analyte addition is a requirement for the visualization of the proposed sensing mechanism by STORM. At a later stage to examine the sensors with STORM in order to characterize the reorganization of the embedded molecules at the surface of the vesicles.

The vesicular sensors were prepared by doping **DSPC** vesicles with **MC540** as reporter moiety and a bis (zinc-cyclen) derivative (**Zn₂**) as artificial receptor (Scheme 4.1).



Scheme 4.1: Structures of bis-(zinc cyclen) receptor (**Zn₂**) and merocyanine 540 (**MC540**).

The **Zn₂** receptor has been already reported in vesicular chemosensors for the detection of phosphorylated compounds [1, 2], we therefore decided to use it in our composition as well.

4.2 RESULTS AND DISCUSSION

The results are presented in two sections. The first one shows the binding properties of **Zn₂** and **MC540** doped **DSPC** vesicles, whereas the second presents the fluorescence microscopy characterization of such systems.

4.2.1 MC540 as reporting dye in vesicular chemosensors

In this section, fluorescence emission titrations of functionalized **DSPC** vesicles (1%mol **MC540** and 10% **Zn₂**) (**VTZ1**) with different ligands are presented. The emission intensities at 584 nm were corrected for dilution and fitting was made with non-linear curve fitting function of Origin using the one site binding model function. In Figure 4.3, we show the fluorescence spectra of a vesicle solution after addition of increasing equivalents of pyrophosphate.

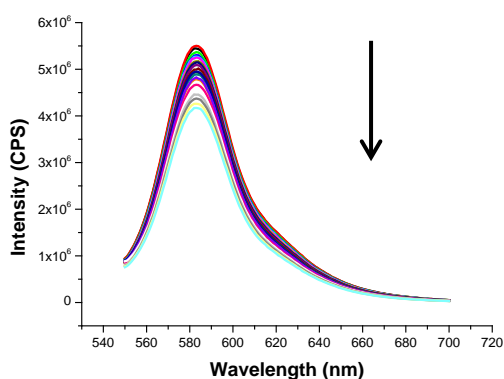


Figure 4.3: Fluorescence spectra of **VTZ1** solution after addition of increasing equivalents (from 0.05 to 6) of pyrophosphate. The addition of analyte provokes a decrease of the fluorescence intensity.

The addition of analyte provokes a decrease of the fluorescence intensity. The system responds to the addition of other anions as well, such as sulfate, acetate, formate and chloride.

Figure 4.4 shows the plots of fluorescence intensity maximum response as function of the total concentration of different analytes.

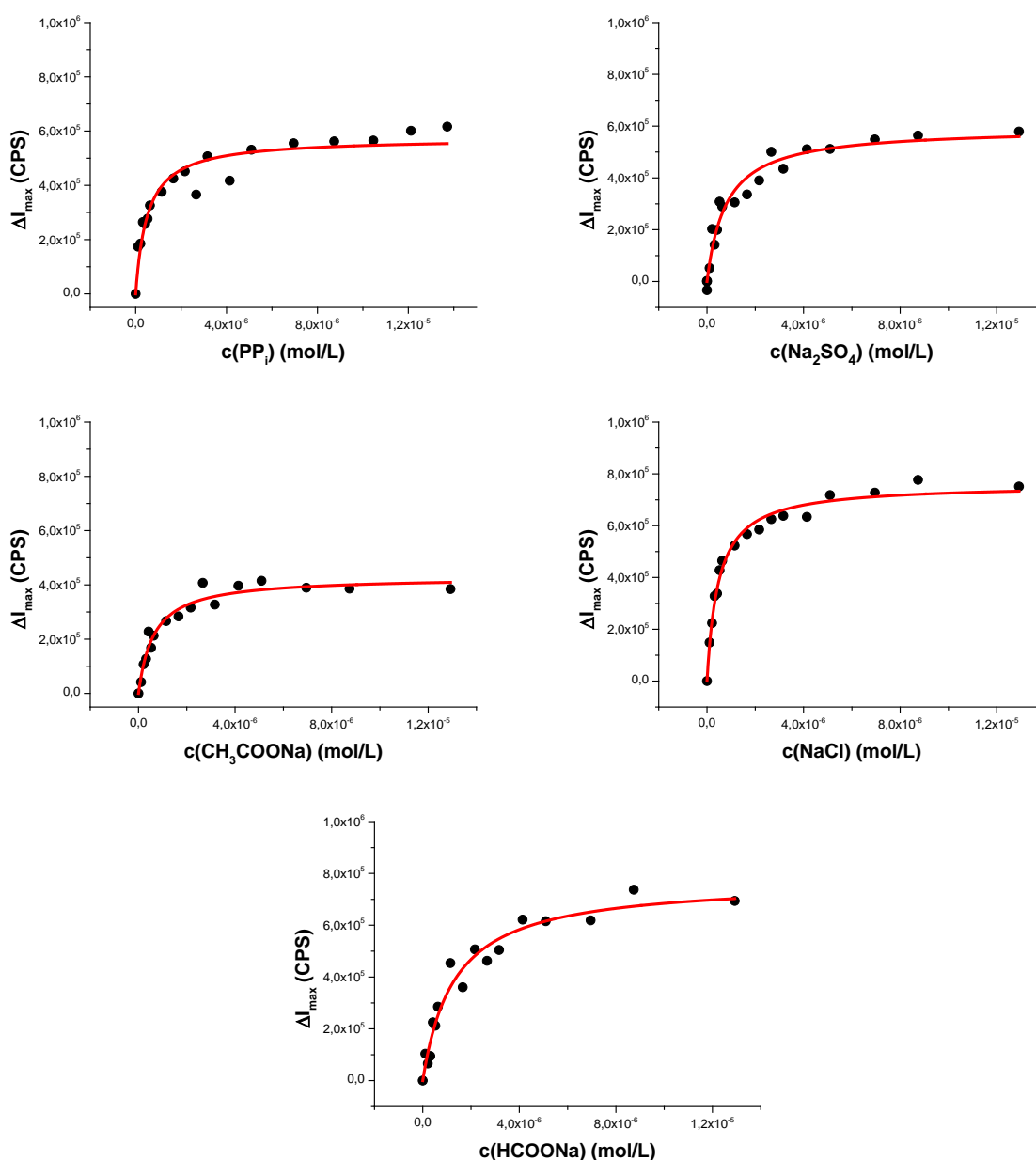


Figure 4.4: Fluorescence emission titrations of VTZ1 with different analytes. The maxima of the fluorescence intensity are plotted against the total concentration of the analyte. The fitting curves are represented in red.

As shown in Figure 4.5, the addition of cyanide and bromide do not provoke any meaningful response.

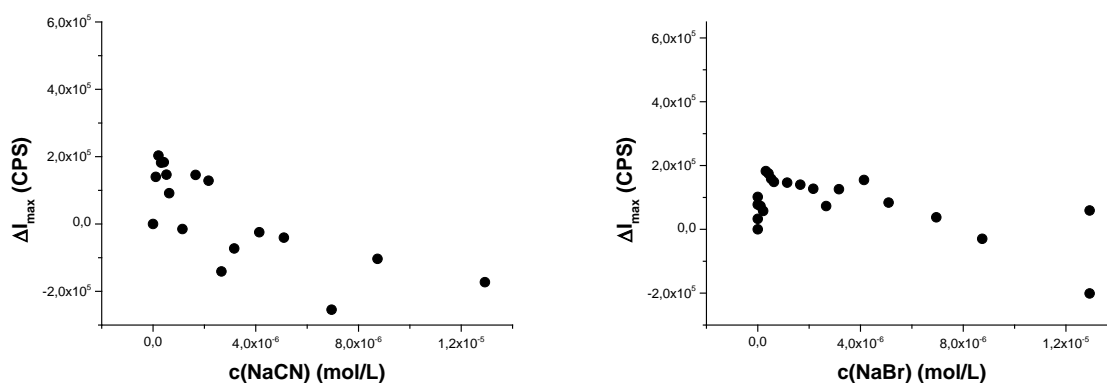


Figure 4.5: Fluorescence emission titrations of **VTZ1** with cyanide and bromide.

A maximum 15% relative change of fluorescence intensity is observed. The binding constants determined for the different analytes are very similar. The values of log K are listed in Table 4.1.

Entry	Analyte	Log K
1	PP_i	6.1
2	Na_2SO_4	6.0
3	CH_3COONa	6.1
4	HCOONa	5.8
5	NaCl	6.2
6	NaBr	-
7	NaCN	-

Table 4.1: log K values for the binding of different analytes to **VTZ1**.

As the **MC540** and **Zn₂** modified vesicular system responds to the addition of different analytes, we preceded with the fluorescence microscopy study of the system.

4.2.2 STORM and TIRFM characterization of vesicular chemosensors

MC540 (9%) and **Zn₂** (1%) doped **DSPC** vesicles were prepared by extrusion and subsequently analyzed with the STORM technique (Figure 4.6).

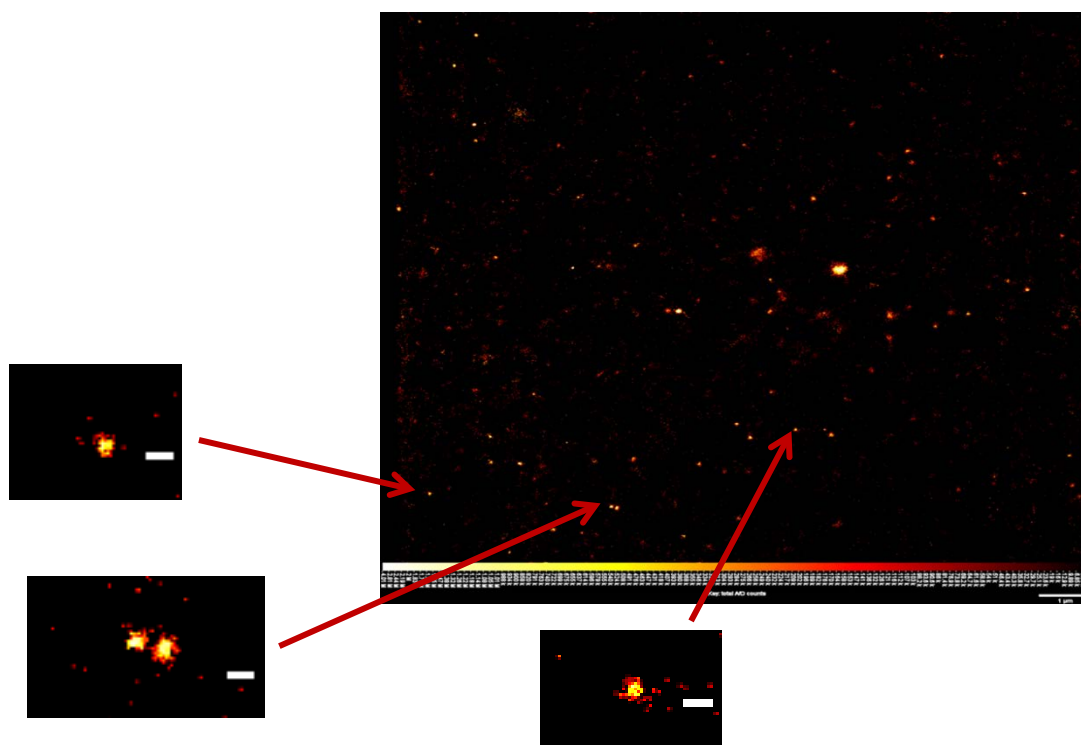


Figure 4.6: STORM images of functionalized vesicles. The three small pictures are enlargements of the areas indicated by the arrows. Scale bars correspond to 100 nm.

The image shows several bright dots (white to light yellow with high intensity, dark red to black with low intensity) with a median diameter of 88 ± 44 nm, which correspond to the vesicles. The limited dimension of the vesicles doesn't allow a detailed characterization of the membrane. We therefore decided to prepare and investigate larger vesicles with the same composition.

We prepared **DSPC/DOPC** (1/1) and **DOPC** GUVs functionalized with 9% **Zn₂** and 1% **MC540**. The use of different lipid compositions is due to the GUVs preparation method which was not suitable for doped **DSPC** vesicles.

The TIRFM images of a **DSPC/DOPC** (1/1) GUV functionalized with 9% **Zn₂** and 1% **MC540** are represented in pictures of Figure 4.7.

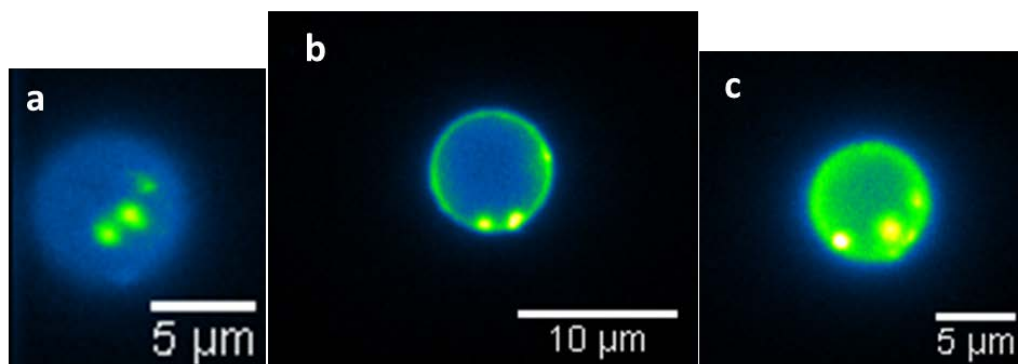


Figure 4.7: TIRFM images of the same **DSPC/DOPC** (1/1) GUV functionalized with 9% **Zn₂** and 1% **MC540** recorded at different times (ca. 5 seconds interval between the pictures).

The vesicle has a diameter between 5 and 10 μm and shows 3 or 4 brighter dots, which correspond to areas on the surface with a higher concentration of dye. The presence of such bright dots indicates that the dye molecules are non-homogeneously distributed on the surface of the membrane. The distance between the dots changes in time, suggesting that the dyes are able to diffuse on the surface of the vesicle.

In Figure 4.8, we show TIRFM images of different **DOPC** GUVs functionalized with 10% **Zn₂** and 1% **MC540**, recorded before and after addition of 10 equivalents (referred to the concentration of **Zn₂**) of pyrophosphate to the sample.

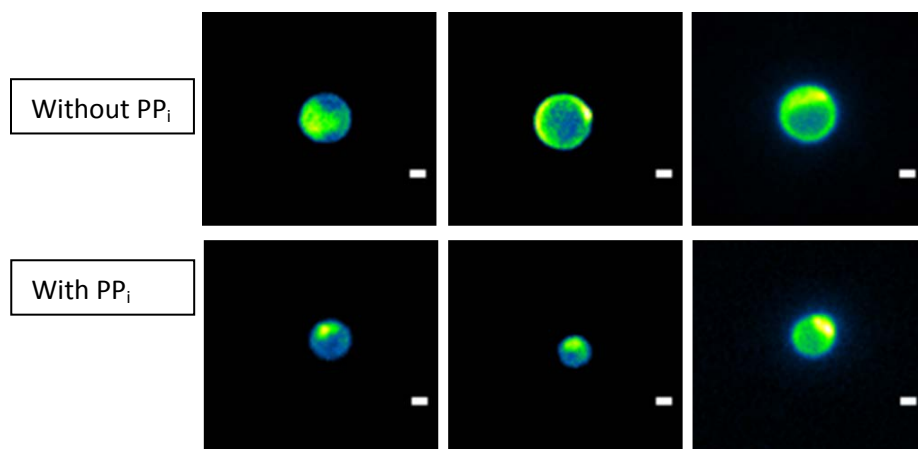


Figure 4.8: TIRFM images of the **DOPC** GUV functionalized with 10% **Zn₂** and 1% **MC540** recorded before (upper row) and after (lower row) the addition of 10 equivalents of pyrophosphate. Scale bars: 5 μm .

The vesicles have a diameter of about 10 μm . All the images show localized brighter parts, which indicates a non-homogenous distribution of the dyes on the surface of the membranes. No significant difference in the fluorescence properties of the GUVs is induced by the presence of PP_i .

During the TIRFM measures of the Zn_2 modified **DOPC** GUVs, a lipid bilayer spontaneously originated by precipitation and fusion of the vesicles. The images of the bilayer before and after the addition of PP_i are depicted in Figure 4.9.

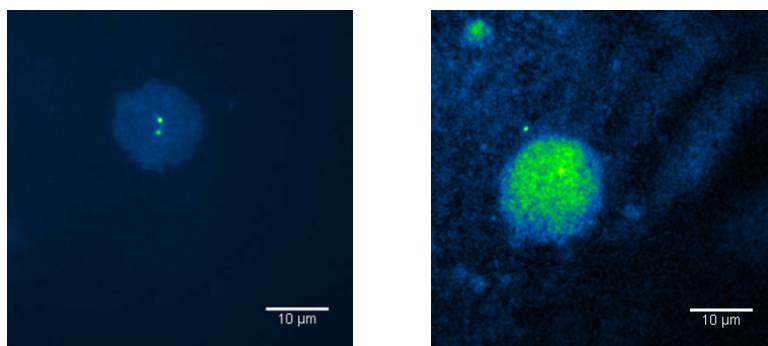


Figure 4.9: TIRFM images of the same **DOPC** bilayer formed by spontaneous sedimentation of **DOPC** GUVs functionalized with 10% Zn_2 and 1% **MC540** recorded before (left) and after (right) addition of 1 equivalent of pyrophosphate.

Before addition of PP_i , two bright dots are present in the center of the bilayer due to a higher concentration of the fluorophore. The two dots are not visible after addition of PP_i to the sample. The **overall higher brightness of the second image is due to different contrast settings of the software.**

4.3 CONCLUSION

The dye **MC540** turned out to be suitable as reporting dye in vesicular chemosensors. The addition of negatively charged analytes provokes a decrease of the fluorescence of a solution of the **Zn₂** and **MC540** functionalized vesicles. The response is surprisingly not selective towards phosphorylated species as reported for vesicular chemosensors doped with the same receptor but different reporting dyes [1, 2].

A possible explanation might be related to the sensing mechanism, which could be different to the one hypothesized for the vesicular chemosensors. This explanation is suggested by the fact that **MC540** in homogeneous aqueous solution is reported to be quenched by Na^+ ions [20], so the observed fluorescence response is possibly provoked by the interaction of the analytes directly with the dye without binding to the **Zn₂** receptor. The different behavior of sodium cyanide and bromide is surprising and suggests that the sensing mechanism might involve at certain extent also the anions. A better understanding of the sensing mechanism could be achieved by investigating the response of the system to salts with different cations.

The high resolution STORM approach did not allow to observe the organization of the fluorophores on the surface of the 100 nm functionalized vesicles. The resolution of the technique is not high enough.

The TIRFM images of the GUVs revealed a non-homogeneous distribution of the embedded fluorophores at the surface of the membrane. According to the images reported in Figure 4.7, the **DSPC/DOPC** GUVs showed that the embedded fluorophores are free to diffuse on the surface of the vesicles as the distance of the bright dots changes with time. The TIRFM data for the bilayer (Figure 4.9) also indicates a non-homogeneous distribution of the fluorophores and a difference in the fluorescence properties after addition of pyrophosphate to the sample.

The overall data are not conclusive regarding the proposed working mechanism of the vesicular chemosensors.

4.4 EXPERIMENTAL SECTION

Materials and instruments: DOPC and DSPC were purchased from Avanti Polar Lipids; 4-(2-hydroxyethyl)-1-piperazineethanesulfonic acid (HEPES) and sodium pyrophosphate were purchased from Sigma Aldrich; sodium sulfate, sodium acetate, sodium formate, sodium bromide and sodium cyanide were purchased from Merck, sodium chloride was purchased from VWR; Merocyanine 540 was purchased from Invitrogen; all the chemicals were used without further purification. All solvents were used in p.a. grade. Polycarbonate membranes for the extrusion of the vesicles were purchased by AVESTIN. If not otherwise specified, MilliQ water was employed.

The fluorescence experiments were performed in 25 mM HEPES buffer at pH = 7.4, the spectra were recorded on a Horiba Fluoromax4 spectrophotometer with 1 ml Hellma cuvettes. DLS measurements were performed on a Malvern Zetasizer Nano instrument at 20 °C using disposable polystyrene cuvettes.

The experimental setup for the fluorescence microscopy experiments is described in [21].

Vesicle preparation: in a small glass vessel, the proper volumes of solutions of lipids (1 mM in CHCl₃), **MC540** (1 mM in EtOH), and **Zn₂** (1 mM in EtOH) were added. The solvents were removed under vacuum for 15 minutes and HEPES buffer solution (25 mM, pH = 7.4) was added. The suspension obtained was mixed at 900 rpm at 75 °C for 15 minutes to yield a turbid suspension. The suspension was then extruded through a 100 nm pore size polycarbonate membrane to give a unilamellar vesicle suspension.

For all the samples except for the GUVs the size distribution of the vesicles solutions was determined by DLS before proceeding with any further investigation. All the vesicles showed an average diameter value around 100 nm and a PDI (polydispersity index) around 0.1.

Titration: the vesicle solutions were diluted to a total amphiphile concentration of 50 μM and fluorescence was recorded after addition of increasing equivalents of analytes. $\lambda_{exc} = 540$ nm. The intensities for the plots in the Figures were corrected considering the volume dilution.

Giant unilamellar vesicles (GUVs) preparation: the GUVs were prepared with the electroformation method. 5-10 μl of a 0.1 mM solution of lipids in chloroform were deposited on the platinum wires of

the electroformation chamber and the solvent was evaporated under vacuum for 30 min. The chamber, which was thermostated at 55 °C, was filled with a 300 mM sucrose solution and a 2 V, 10 Hz alternating electric current was applied to this capacitor-like configuration for ca. 2 h.

Sample preparation for TIRFM: the samples in buffer were prepared by dilution of GUVs in buffer resulting in a total amphiphile concentration of 0.5 μ M. The samples were deposited on clean coverslip glass (Labteck, IBIDI, 96 wells with glass bottom). The samples containing pyrophosphate were prepared by adding proper amounts of a pyrophosphate solution in buffer to the vesicle dispersion. For STORM measurements, the vesicles were immobilized on a polyvinyl alcohol matrix.

STORM procedure: blinking of **MC540** was induced by addition of 2-mercaptoethanol a concentration of 10 mM to the vesicle dispersions. After movie acquisition (1000 to 10000 images per movie), the super-resolution image was reconstructed with rapidSTORM software. The images were processed with the software ImageJ.

The STORM imaging was performed in the laboratories of Professor Yves Mély (Laboratoire de Biophotonique et Pharmacologie, Université de Strasbourg). The group has a strong expertise in the characterization of GUVs by different fluorescence microscopy methods [22-24].

4.5 REFERENCES

1. Gruber, B., Stadlbauer, S., Woinaroschy, K. and König, B., *Luminescent vesicular receptors for the recognition of biologically important phosphate species*. Organic and Biomolecular Chemistry, 2010. **8**(16): p. 3704-3714.
2. Gruber, B., Stadlbauer, S., Späth, A., Weiss, S., Kalinina, M. and König, B., *Modular chemosensors from self-assembled vesicle membranes with amphiphilic binding sites and reporter dyes*. Angewandte Chemie International Edition, 2010. **49**(39): p. 7125-7128.
3. Gruber, B., Balk, S., Stadlbauer, S. and König, B., *Dynamic interface imprinting: high-affinity peptide binding sites assembled by analyte-induced recruiting of membrane receptors*. Angewandte Chemie International Edition, 2012. **51**(40): p. 10060-10063.
4. Kaindl, T., Oelke, J., Pasc, A., Kaufmann, S., Konovalov, O.V., Funari, S.S., Engel, U., Wixforth, A. and Tanaka, M., *Regulation of adhesion behavior of murine macrophage using supported lipid membranes displaying tunable mannose domains*. Journal of Physics: Condensed Matter, 2010. **22**(28): p. 285102.
5. Oreopoulos, J., Epand, R.F., Epand, R.M. and Yip, C.M., *Peptide-induced domain formation in supported lipid bilayers: direct evidence by combined atomic force and polarized total internal reflection fluorescence microscopy*. Biophysical Journal, 2010. **98**(5): p. 815-823.
6. Okazaki, T., Inaba, T., Tatsu, Y., Tero, R., Urisu, T. and Morigaki, K., *Polymerized lipid bilayers on a solid substrate: Morphologies and obstruction of lateral diffusion*. Langmuir, 2009. **25**: p. 345-351.
7. Simonsen, A.C., *Activation of phospholipase A2 by ternary model membranes*. Biophysical Journal, 2008. **94**(10): p. 3966-3975.
8. Gozen, I. and Jesorka, A., *Instrumental methods to characterize molecular phospholipid films on solid supports*. Analytical Chemistry, 2012. **84**(2): p. 822-838.
9. Chen, C., Zhu, S., Huang, T., Wang, S. and Yan, X., *Analytical techniques for single-liposome characterization*. Analytical Methods, 2013. **5**(9): p. 2150-2157.
10. Almgren, M., Edwards, K. and Karlsson, G., *Cryo transmission electron microscopy of liposomes and related structures*. Colloids and Surfaces A: Physicochemical and Engineering Aspects, 2000. **174**: p. 3-21.

11. Bibi, S., Kaur, R., Henriksen-Lacey, M., McNeil, S.E., Wilkhu, J., Lattmann, E., Christensen, D., Mohammed, A.R. and Perrie, Y., *Microscopy imaging of liposomes: from coverslips to environmental SEM*. International Journal of Pharmaceutics, 2011. **417**(1-2): p. 138-150.
12. Ruozzi, B., Tosi, G., Tonelli, M., Bondioli, L., Mucci, A., Forni, F. and Vandelli, M.A., *AFM phase imaging of soft-hydrated samples: a versatile tool to complete the chemical-physical study of liposomes*. Journal of Liposome Research, 2009. **19**(1): p. 59-67.
13. Nakano, K., Tozuka, Y., Yamamoto, H., Kawashima, Y. and Takeuchi, H., *A novel method for measuring rigidity of submicron-size liposomes with atomic force microscopy*. International Journal of Pharmaceutics, 2008. **355**(1-2): p. 203-209.
14. Redondo-Morata, L., Giannotti, M.I. and Sanz, F., *Influence of cholesterol on the phase transition of lipid bilayers: a temperature-controlled force spectroscopy study*. Langmuir, 2012. **28**(35): p. 12851-12860.
15. Lohse, B., Bolinger, P.-Y. and Stamou, D., *Encapsulation efficiency measured on single small unilamellar vesicles*. Journal of American Chemical Society, 2008. **130**: p. 14372-14373.
16. Kunding, A.H., Mortensen, M.W., Christensen, S.M. and Stamou, D., *A fluorescence-based technique to construct size distributions from single-object measurements: application to the extrusion of lipid vesicles*. Biophysical Journal, 2008. **95**(3): p. 1176-1188.
17. Yamanaka, M., Smith, N.I. and Fujita, K., *Introduction to super-resolution microscopy*. Microscopy, 2014. **63**(3): p. 177-192.
18. Rust, M.J., Bates, M. and Zhuang, X., *Sub-diffraction-limit imaging by stochastic optical reconstruction microscopy (STORM)*. Nature Methods, 2006. **3**(10): p. 793-795.
19. Kuo, C. and Hochstrasser, R.M., *Super-resolution microscopy of lipid bilayer phases*. Journal of American Chemical Society, 2011. **133**(13): p. 4664-4667.
20. Adenier, A. and Aaron, J.J., *A spectroscopic study of the fluorescence quenching interactions between biomedically important salts and the fluorescent probe merocyanine 540*. Spectrochimica Acta Part A 2002. **58**: p. 543-551.
21. Darwich, Z., Kucherak, O.A., Kreder, R., Richert, L., Vauchelles, R., Mély, Y. and Klymchenko, A.S., *Rational design of fluorescent membrane probes for apoptosis based on 3-hydroxyflavone*. Methods and Applications in Fluorescence, 2013. **1**(2): p. 025002.

22. Klymchenko, A.S., Duportail, G., Demchenko, A.P. and Mely, Y., *Bimodal distribution and fluorescence response of environment-sensitive probes in lipid bilayers*. Biophysical Journal, 2004. **86**: p. 2929-2941.

23. Haluska, C.K., Schroder, A.P., Didier, P., Heissler, D., Duportail, G., Mely, Y. and Marques, C.M., *Combining fluorescence lifetime and polarization microscopy to discriminate phase separated domains in giant unilamellar vesicles*. Biophysical Journal, 2008. **95**(12): p. 5737-5747.

24. Kucherak, O.A., Oncul, S., Darwich, Z., Yushchenko, D.A., Arntz, Y., Didier, P. and Mely, Y., *Switchable Nile Red-based probe for cholesterol and lipid order at the outer leaflet of biomembranes*. Journal of American Chemical Society, 2010. **132**: p. 4907-4916.

Chapter 5

Investigations of functionalized vesicular systems for
monitoring of β -lactamases

5.1 INTRODUCTION

Multidrug resistant bacteria (MDRB) are able to tolerate the exposure to multiple antibiotics. According to the World Health Organization, the lack of drugs which are able to treat infections caused by MDRB is one of the main worldwide health problems. Beside the discovery and the development of new drugs, prevention of transmission of MDRB infections is essential. The rapid detection and surveillance of drug resistance is therefore a key issue, as it is crucial for making decisions about the proper clinical intervention. Typical detection methods include cell culture based screening methods (the most common ones, even if rather time demanding, that means 24-72 hours) and, for some classes of bacteria, PCR based tests [1].

One of the mechanisms of resistance consists in the expression of β -lactamases, enzymes which are able to deactivate antibiotics by opening the characteristic β -lactam ring. Fluorescence assays for β -lactamases detection have already been developed; the most common one employs nitrocefin [2], a chromogenic cephalosporin which turns from yellow to red after hydrolysis. The method is cheap and fast, but it does not reveal for example staphylococcal penicillinases [3].

We decided to explore the use of the vesicular systems established in our group to develop an assay which allows the detection of β -lactamases and possibly to monitor the action of the enzyme. A big advantage of vesicular systems is the modularity, which allows facile tuning. If a general working principle is developed, it would then be relatively easy to extend it to other systems by minor changes.

The starting point is to introduce in the vesicular system an antibiotic derivative and a reporting dye and to observe if the system responds to the presence of a penicillinase. These components might be embedded or encapsulated in the vesicles or present in solution. We investigated three different possible schemes, which are described below.

A first approach relies on the use of dye-encapsulating vesicles, which are very much documented in literature mainly for heterogeneous assays [4]. The dyes are encapsulated in liposomes in a concentration at which their fluorescence is quenched. The liposomes are usually tagged with a recognition element and the assay is designed in such a way that the filled liposomes are immobilized on an analyte functionalized surface. The detection is then performed by adding an agent which is able to lyse the liposomes (e.g. a detergent or a lipase). The dyes are released and dequenched due to their dilution allowing the detection (Figure 5.1).

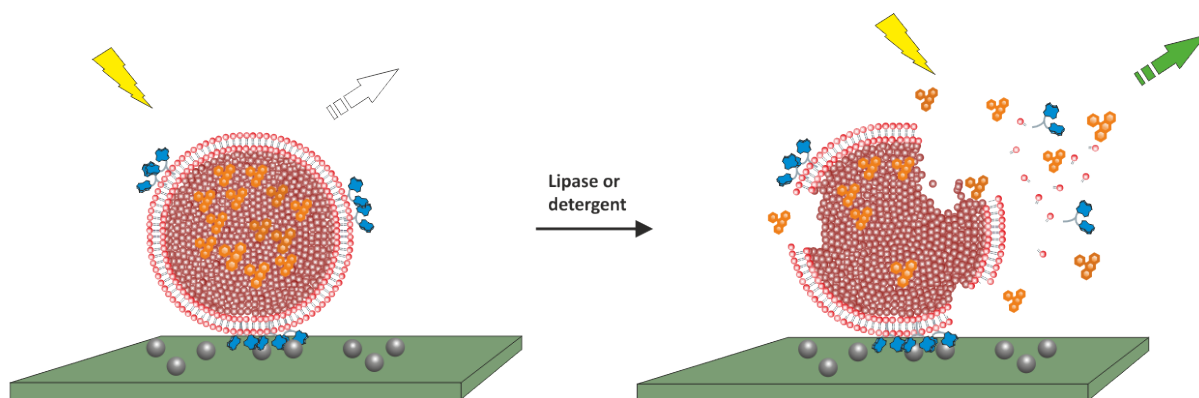


Figure 5.1: Typical dye-encapsulating liposomes based assay. The liposomes filled with dyes selectively recognize the analyte on the surface. After lysis of the liposomes, the dye molecules are diluted and therefore not quenched anymore allowing the detection.

Our intention was to explore an analogous concept in homogenous solution. The plan was to dope the vesicles with an amphiphilic derivative of ampicillin while sulforhodamine B molecules are encapsulated in the liposomes. The reaction of the β -lactamase with the ampicillin derivative is thought to induce the opening of the β -lactam ring, which causes a change in the surface charge of the liposomes, resulting in a destabilization of the vesicles (in our systems, we often observed that embedding negatively charged molecules, e.g. stearic acid, affects the stability of the vesicles). This destabilization should then provoke the release of the encapsulated dyes. Figure 5.2 illustrates the concept:

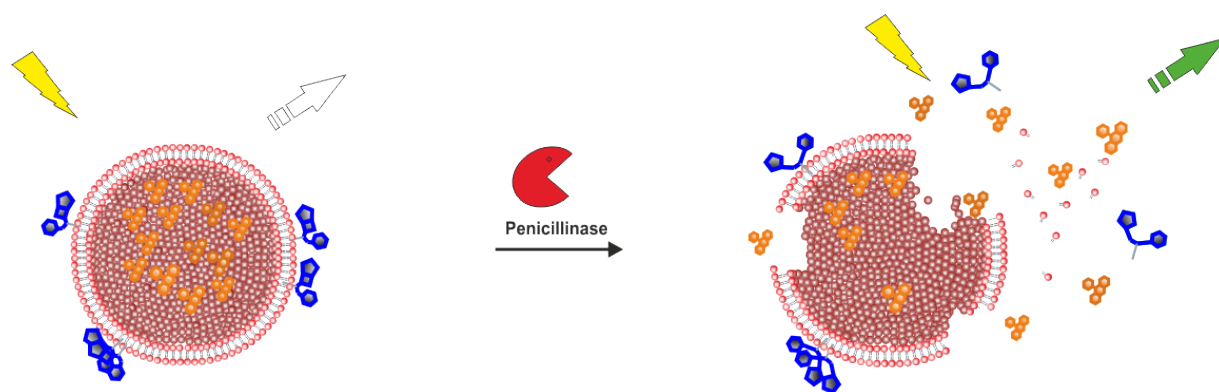


Figure 5.2: Designed dye-encapsulating liposomes based assay for the monitoring of penicillinase activity. In blue, the antibiotic in the β -lactam (left) and in the open (right) forms. In orange, the dye molecules.

A second approach is based on the vesicular chemosensors concept developed in our group [5]. It consists in co-embedding the ampicillin derivative together with a reporting dye in the vesicle membrane. In analogy to what observed with the vesicular chemosensors, the embedded molecules are expected to organize in patches and the fluorophores are supposed to respond to the opening of the β -lactam ring provoked by the reaction with the enzyme.

As third strategy, we used amphiphilic dye doped vesicles (not doped with an ampicillin derivative as before) in a highly concentrated solution of ampicillin. We observed if a response takes place after provoking the opening of the β -lactam ring by adding the enzyme. This very simple approach was suggested by the observation that the dye doped vesicular systems are very sensitive towards charge changes of the surrounding medium.

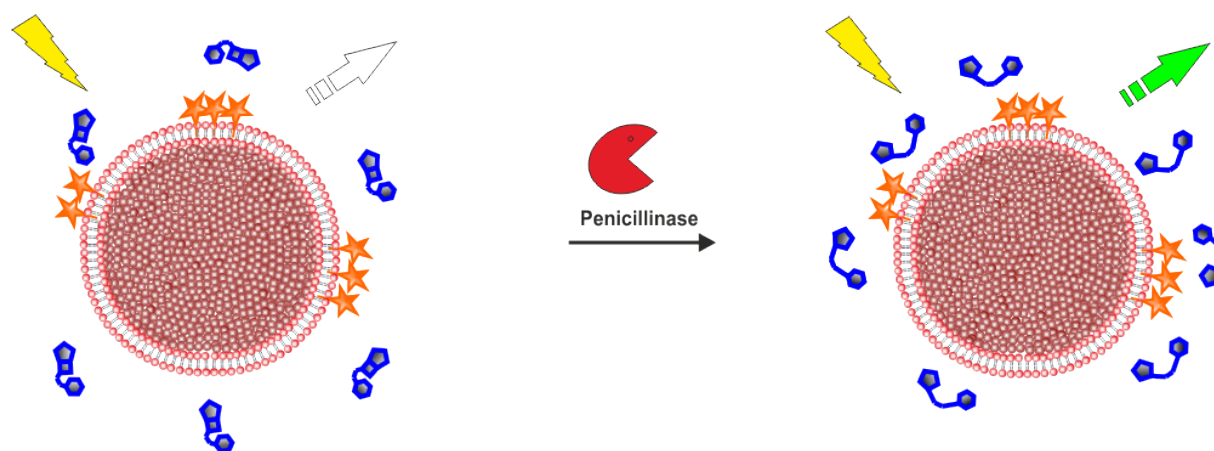
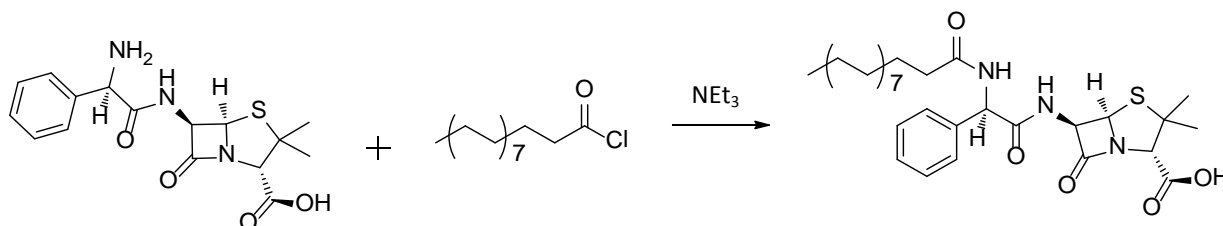


Figure 5.3: Designed dye doped liposomes based assay for the monitoring of penicillinase activity. In blue, the antibiotic in the β -lactam (left) and in the open (right) form. In orange, the amphiphilic co-embedded dyes.

5.2 RESULTS AND DISCUSSION

5.2.1 Synthesis of the amphiphilic ampicillin (Amp-C₁₈) derivative

In order to embed the ampicillin in the vesicular system, we modified the ampicillin by introducing an alkyl chain via a classical coupling with carbonyl chloride, which was freshly prepared by reaction of stearic acid with thionyl chloride, as shown in Scheme 5.1.



Scheme 5.1: Preparation of stearic chloride starting from stearic acid (top) and introduction of the alkyl chain to the ampicillin molecule via coupling with stearic chloride (bottom).

Some difficulties arose from the tendency of the β -lactam ring to open at acidic pH; therefore, only slightly acidic conditions were used in the purification steps. The compound was isolated with a 43% yield.

5.2.2 First approach: dye-encapsulating vesicles

As first step, we prepared vesicles filled with the sulforhodamine B (SRB) dye, a highly water soluble fluorophore which was already reported for the preparation of dye-encapsulating vesicles [6]. Encapsulation is performed by preparing the vesicles in buffer containing SRB in a concentration of 100 μ M. The non-encapsulated dyes are then separated from the vesicles by filtration (centrifugal filters, 3000 MWCO). Figure 5.4 shows the size distribution of SRB containing vesicles.

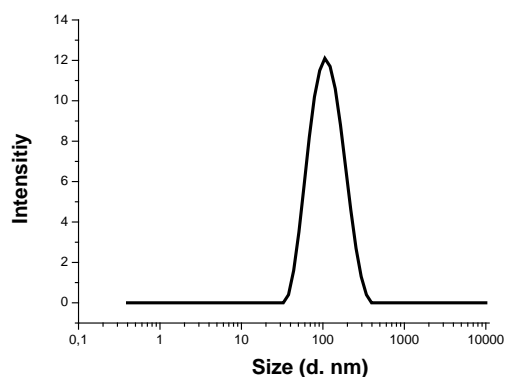


Figure 5.4: Size distribution of SRB-encapsulating **DOPC** vesicles. The average diameter of the sample is 100 nm with a PDI value of 0.17.

After purification, the fluorescence of the vesicles was recorded before and after addition of a lysing agent, the non-ionic surfactant Triton X-100.

The SRB filled vesicles exhibit a weak fluorescence (Figure 5.5, black line). After a lysing agent is added to the solution, the encapsulated molecules are released and the fluorescence increases (Figure 5.5, red line).

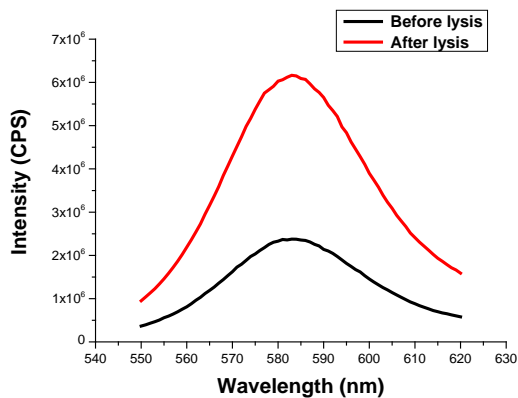


Figure 5.5: Fluorescence spectra of a solution of SRB-encapsulating **DOPC** vesicles before and after lysis of the vesicles.

These studies demonstrated the proof of concept with regard to SRB-encapsulating vesicles and their fluorescence behavior after lysis. With the obtained optimized procedure in hand, we therefore prepared dye-encapsulating vesicles, and the amphiphilic ampicillin derivative (**Amp-C₁₈**) in the vesicles composition.

Figure 5.6 shows the size distribution of **DOPC** and **DSPC** vesicles doped with different amounts of **Amp-C₁₈** (5%, 10%, and 30%).

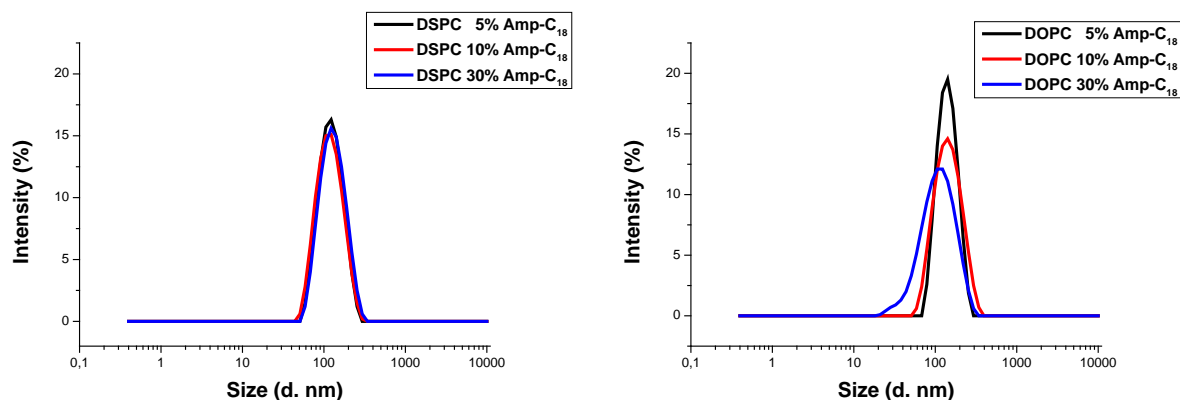


Figure 5.6: DLS spectra of solutions of *DOPC* (right) and *DSPC* (left) vesicles doped with different percentages of *Amp-C₁₈*.

After addition of the 7.2 μ U of penicillinase, the size distribution of the vesicles does not significantly change (Figure 5.7).

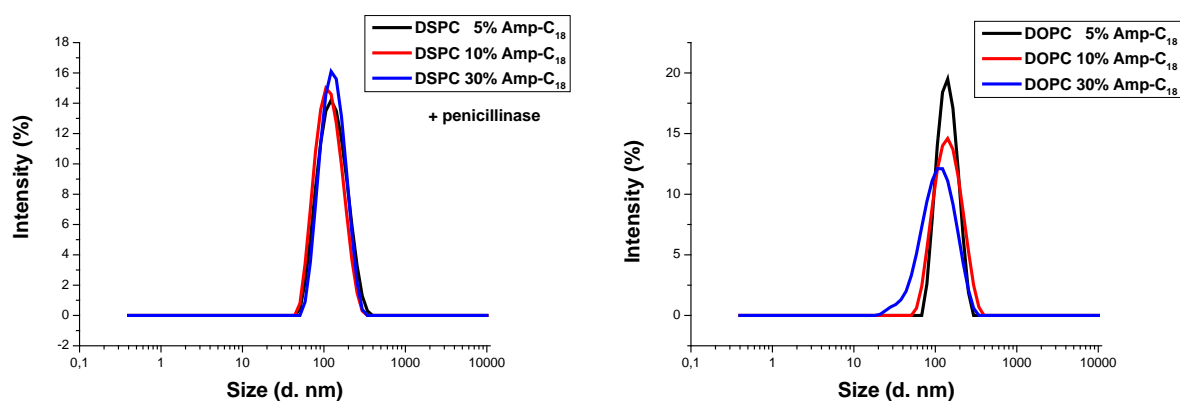


Figure 5.7: DLS spectra of solutions of *DOPC* (right) and *DSPC* (left) vesicles doped with different percentages of *Amp-C₁₈* after addition of penicillinase.

In Table 5.1, the average particles diameter and the polydispersity index (PDI) values for all the different investigated compositions are listed.

<i>Sample</i>	<i>Before penicillinase addition</i>		<i>After penicillinase addition</i>	
	<i>Average diameter (nm)</i>	<i>PDI</i>	<i>Average diameter (nm)</i>	<i>PDI</i>
DSPC 5% Amp-C ₁₈	114.4	0.088	117.8	0.119
DSPC 10% Amp-C ₁₈	110.0	0.109	109.2	0.141
DSPC 20% Amp-C ₁₈	113.7	0.127	112.2	0.110
DSPC 30% Amp-C ₁₈	119.8	0.099	120.9	0.093
DSPC 40% Amp-C ₁₈	113.4	0.150	114.4	0.122
DOPC 5% Amp-C ₁₈	134.2	0.061	136.9	0.072
DOPC 10% Amp-C ₁₈	132.5	0.115	130.3	0.117
DOPC 20% Amp-C ₁₈	123.1	0.108	125.6	0.146
DOPC 30% Amp-C ₁₈	98.13	0.210	98.1	0.170
DOPC 40% Amp-C ₁₈	107.1	0.168	100.7	0.190

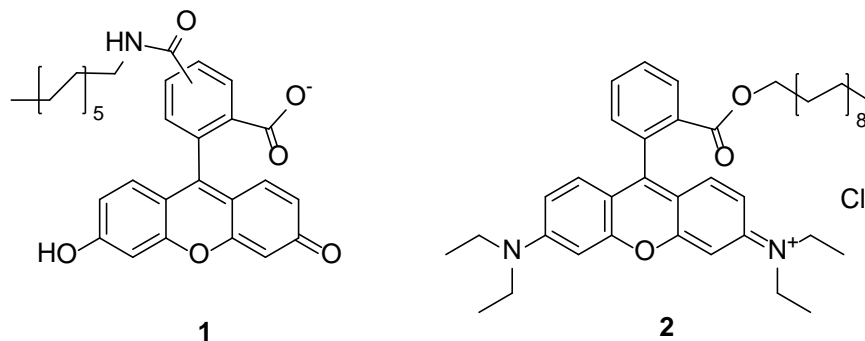
Table 5.1: Average diameter and polydispersity index (PDI) for **DOPC** and **DSPC** vesicles doped with different amounts of **Amp-C₁₈** before and after addition of penicillinase.

No significant changes of the average diameters of the vesicles and of the size distributions are observed. The average diameter is between 100 and 135 nm and PDI values are generally between 0.1 and 0.2. That means that the penicillinase is not able to affect the stability of the vesicles, which would be essential in order to further develop the assay.

We therefore moved to the second approach.

5.2.3 Second approach: amphiphilic dye and Amp-C₁₈ doped vesicular systems

The second approach consisted in co-embedding the **Amp-C₁₈** and a reporting dye. We investigated different compositions: we used **DOPC** and **DSPC** as lipids and added different amounts of two solvatochromic dyes (Scheme 5.2) which were already employed in vesicular chemosensors [ref.], as well as different amounts of **Amp-C₁₈**.



Scheme 5.2: Chemical structures of the amphiphilic dyes used as reporter dyes: amphiphilic carboxyfluorescein **1**, amphiphilic rhodamine B **2**.

Table 5.2, all the different compositions investigated are listed.

Composition	Lipid %	Amp-C ₁₈ %	Amphiphilic dye %
VTZAm 1	DOPC or DSPC, 98	1	1
VTZAm 2	DOPC or DSPC, 90	5	5
VTZAm 3	DOPC or DSPC, 80	10	10
VTZAm 4	DOPC or DSPC, 85	10	5
VTZAm 5	DOPC, 89	10	1
VTZAm 6	DOPC, 80	19	1
VTZAm 7	DOPC, 70	25	5
VTZAm 8	DOPC, 70	29	1

Table 5.2: List of the different vesicle compositions investigated.

In general, it was possible to prepare sufficiently stable vesicles of all the compositions with diameters of around 100 nm and a PDI value of around 0.1.

For most of the compositions, the fluorescence response of the vesicular system upon the addition of penicillinase was not significant. Figures 5.8 and 5.9 exemplarily show the typical fluorescence spectra of different vesicle compositions.

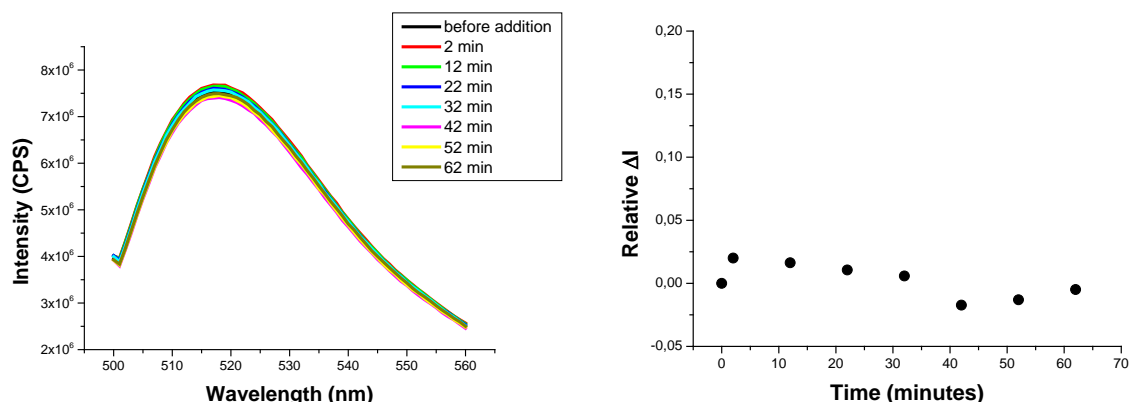


Figure 5.8: On the left: fluorescence spectra of a solution of **DSPC** vesicles doped with **Amp-C₁₈** (19%) and amphiphilic carboxyfluorescein (1%) before and after the addition of 1 U of penicillinase. On the right: a plot of the fluorescence response with time.

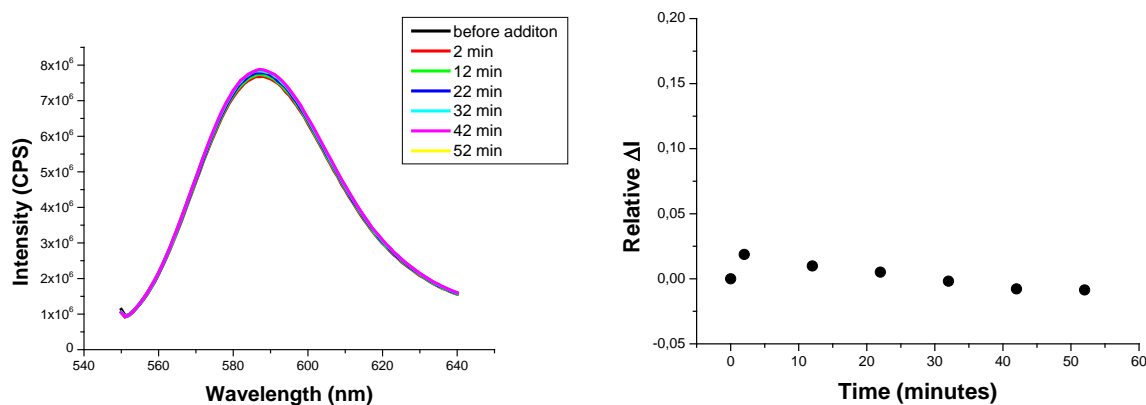


Figure 5.9: On the left: fluorescence spectra of a solution of **DOPC** vesicles doped with **Amp-C₁₈** (10%) and amphiphilic rhodamine B (10%) before and after the addition of 1 U of penicillinase. On the right: a plot of the fluorescence response with time.

The response was more promising for vesicles with a different composition. In Figure 5.10, the response of **DOPC** vesicles doped with 19 % **Amp-C₁₈** and 1% of amphiphilic rhodamine B, is shown.

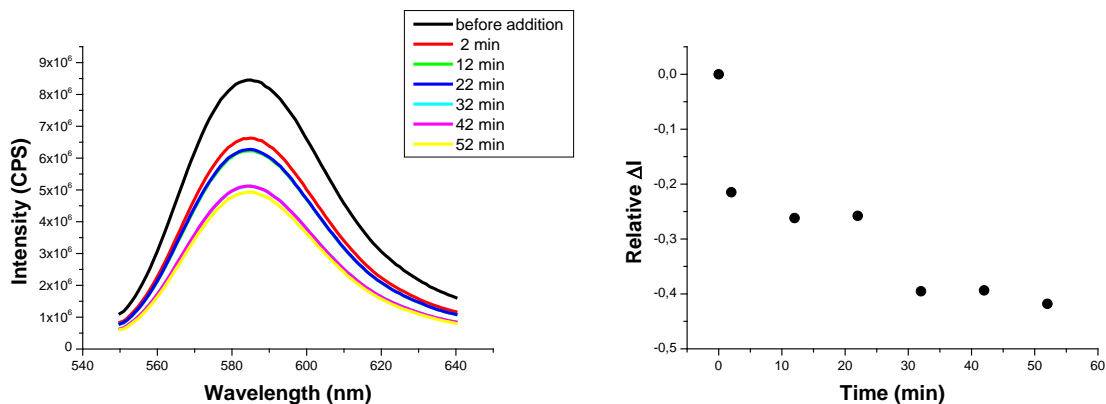


Figure 5.10: On the left: fluorescence spectra of a solution of DOPC vesicles doped with Amp-C₁₈ (19%) and amphiphilic rhodamine B (1%) before and after the addition of 0.8 U of penicillinase. On the right: a plot of the intensity of the emission maximum with time.

The system seems to respond to the addition of the enzyme in a time dependent way. In Figure 5.11, we show the repetition of the experiment.

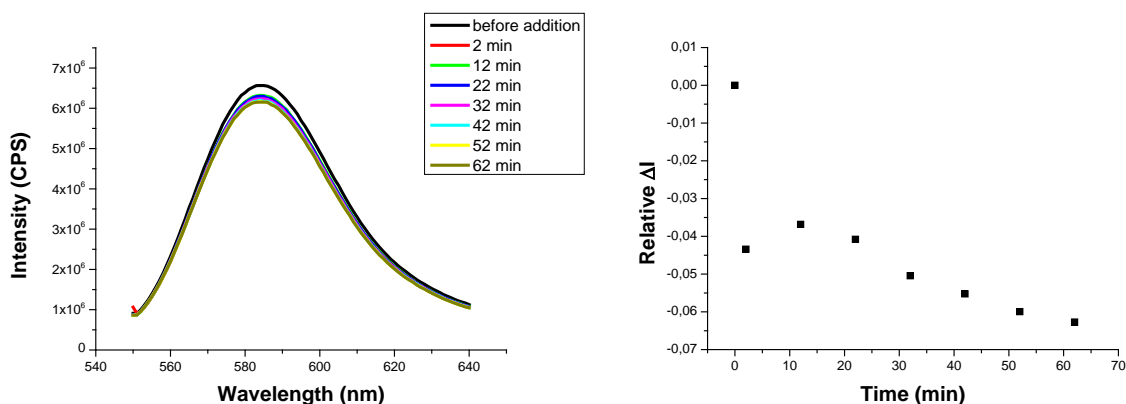


Figure 5.11: On the left: fluorescence spectra of a solution of DOPC vesicles doped with Amp-C₁₈ (19%) and amphiphilic rhodamine B (1%) before and after the addition of penicillinase. On the right: a plot of the intensity of the emission maximum with time.

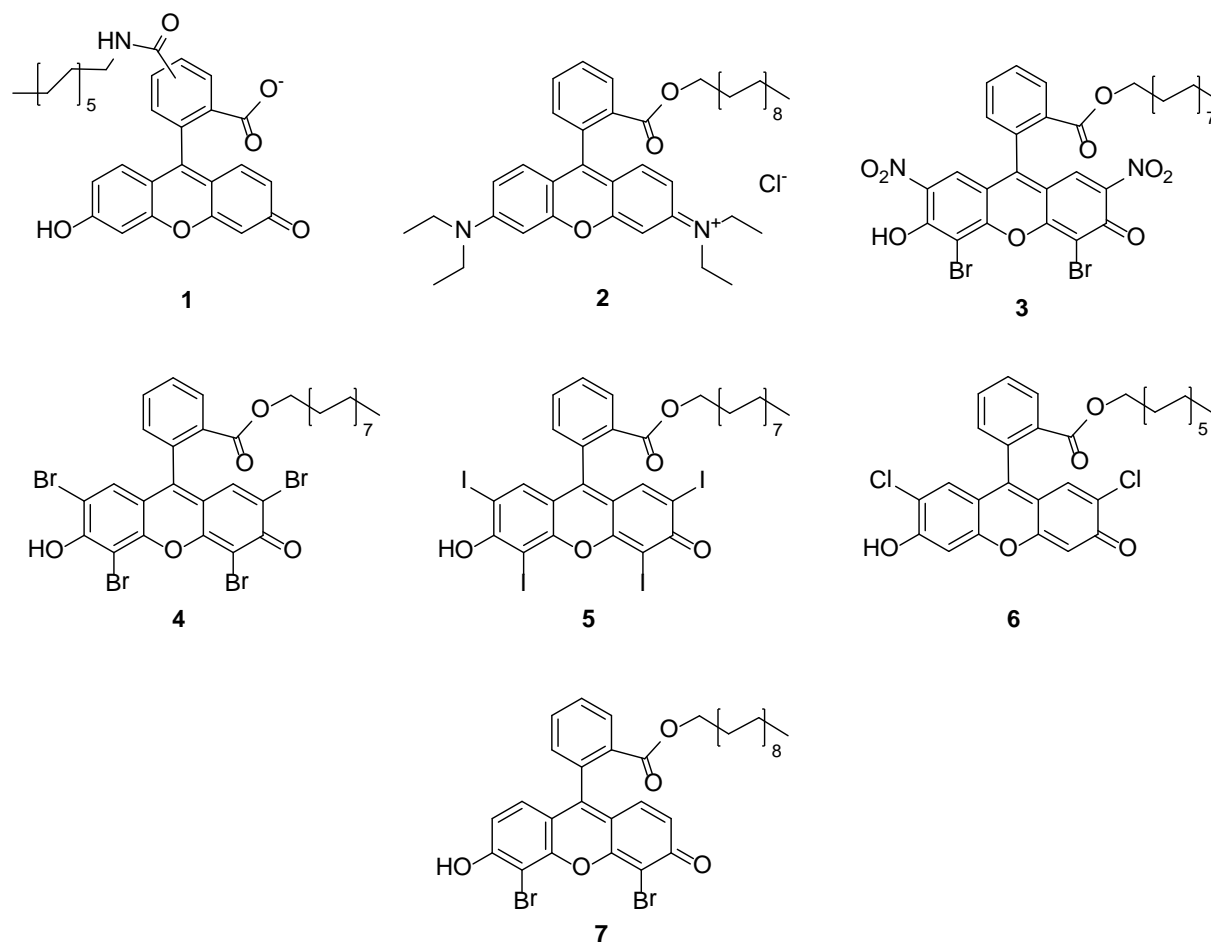
The response of the vesicular system upon the addition of the penicillinase is in this case rather modest. The difference between the first and the second point (2 min after the addition) looks significant, but after that, there is almost no change in the fluorescence.

The remarkable difference between the repeated experiments (Figures 5.10 and 5.11) points out that the reproducibility is not sufficient. All the other compositions listed in Table 5.2 did not significantly respond to the addition of the penicillinase as well.

5.2.4 Third approach: fluorophore embedded in membrane, ampicillin in solution

In a third approach, we investigated amphiphilic dye doped vesicular systems which are not functionalized with the ampicillin derivative. In preliminary studies, as a proof of concept of the possibility to monitor β -lactamase activity, we investigated the response of such systems to the addition of open and closed form (referred to the β -lactam ring) of ampicillin.

The amphiphilic dyes represented in Scheme 5.3 were investigated.



Scheme 5.3: Chemical structures of the amphiphilic dyes investigated. amphiphilic carboxyfluorescein **1**, amphiphilic rhodamine B **2**, amphiphilic eosin B **3**, amphiphilic eosin Y **4**, amphiphilic erythrosine **5**, amphiphilic 2',7'-dichlorofluorescein **6**, amphiphilic 4',5'- dibromofluorescein **7**.

We tested **DOPC** and **DSPC** vesicles doped with 5% of the amphiphilic dyes. We first investigated for all the samples the response after addition of the open and closed form of ampicillin. In Figures 5.12 and 5.13, we exemplarily show the fluorescence changes of samples with dyes **7** and **4**.

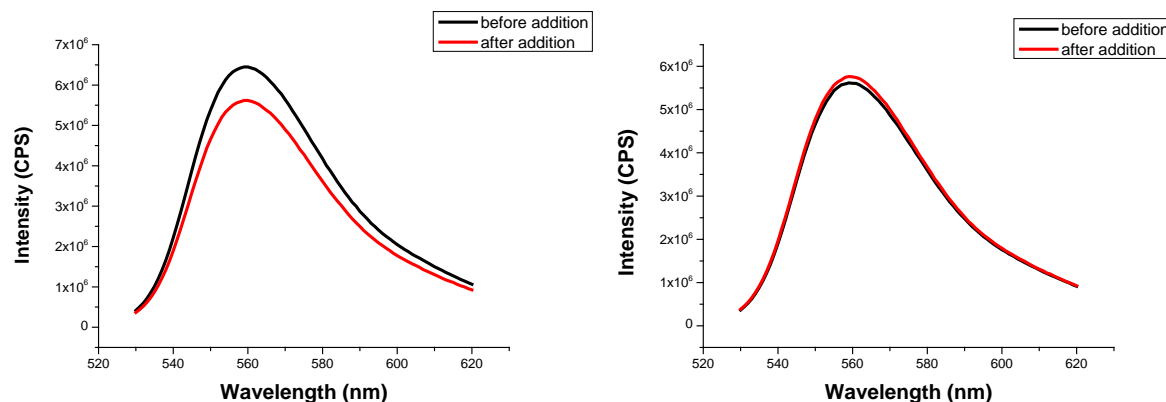


Figure 5.12: Fluorescence spectra of 5% **4** doped **DOPC** vesicles (total amphiphile concentration of 10 μ M) before and after addition of ampicillin (left) and ring opened ampicillin (right) to a total concentration of 0.1 mM.

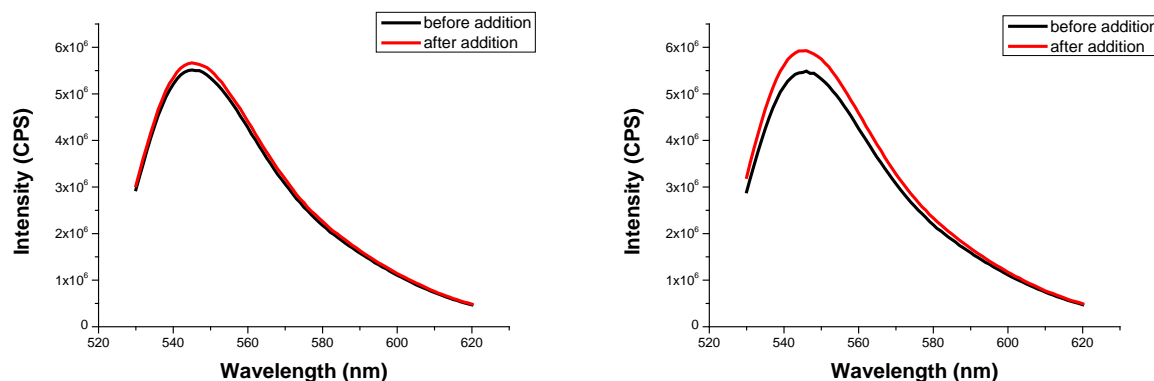


Figure 5.13: Fluorescence spectra of 5% **7** doped **DOPC** vesicles (total amphiphile concentration of 10 μ M) before and after addition of ampicillin (left) and ring opened ampicillin (right) to a total concentration of 0.1 mM.

In both cases, the vesicular system reacts in a different way upon the addition of closed and open ampicillin. The difference is not so large though.

In Figure 5.14, we show the differential fluorescence responses of various vesicular systems upon the addition of the open and closed ampicillin, calculated as $\frac{I - I_0}{I_0}$ where I with as the maximum fluorescence intensity after addition of the substrate and the addition of the open and closed ampicillin, calculated as $\frac{I - I_0}{I_0}$ where I_0 — with as the maximum fluorescence

intensity after addition of the substrate and as the maximum fluorescence intensity before the addition.

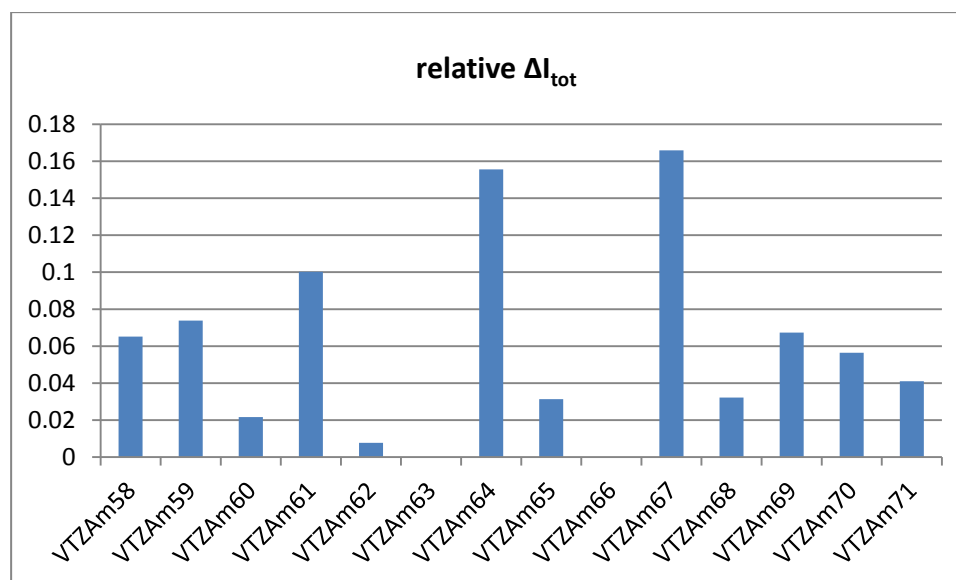


Figure 5.14: Differences between the relative variation of the fluorescence intensity maximum after addition of open and closed ampicillin for all the different compositions investigated. VTZAm63 and VTZAm66 were not investigated due to their instability

Composition	Lipid	Amphiphilic dye (5%)
VTZAm 58	DOPC	1
VTZAm 59	DSPC	1
VTZAm 60	DOPC	7
VTZAm 61	DSPC	7
VTZAm 62	DOPC	3
VTZAm 63	DSPC	3
VTZAm 64	DOPC	4
VTZAm 65	DSPC	4
VTZAm 66	DOPC	5

<i>Composition</i>	<i>Lipid</i>	<i>Amphiphilic dye (5%)</i>
VTZAm 67	DSPC	5
VTZAm 68	DOPC	6
VTZAm 69	DSPC	6
VTZAm 70	DOPC	2
VTZAm 71	DSPC	2

Table 5.3: List of the different vesicle compositions investigated.

It was not possible to prepare stable vesicles with compositions VTZAm63 and VTZAm66 (determined by DLS).

Among all the different compositions, the ones that gave the larger responses were VTZAm64 (**DOPC** doped with amphiphilic eosin Y) and VTZAm67 (**DSPC** doped with amphiphilic erythrosine). The changes are not so pronounced; therefore, we tried to optimize the response by varying the amount of embedded dye. In Figures 5.15 to 5.18, the same experiments with systems containing 1% and 0.1 % of the dyes are shown.

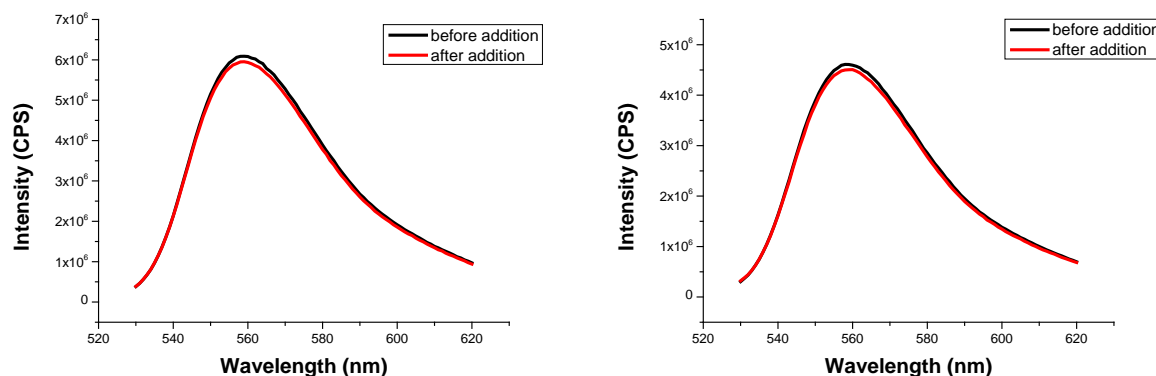


Figure 5.15: Fluorescence spectra of 1% **4** doped **DOPC** vesicles (total amphiphile concentration of 10 μ M) before and after addition of ampicillin (left) and ring opened ampicillin (right) to a total concentration of 0.1 mM.

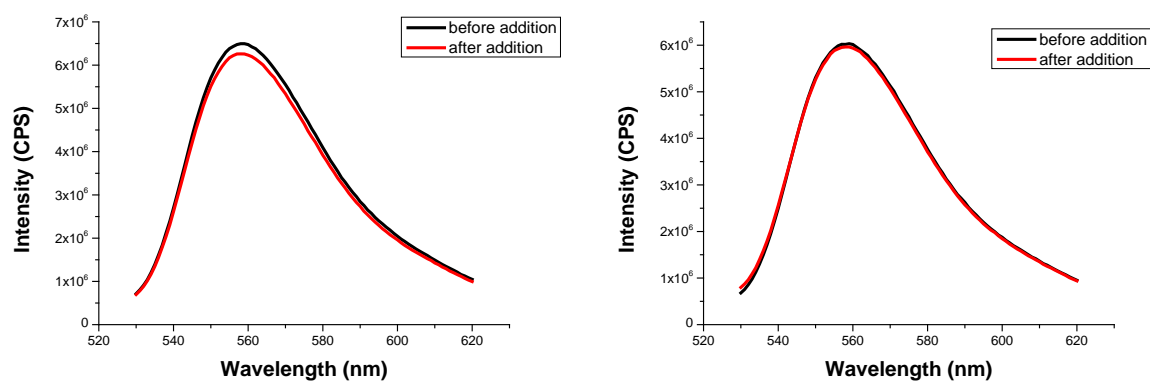


Figure 5.16: Fluorescence spectra of 0.1% 4doped DOPC vesicles (total amphiphile concentration of 10 μ M) before and after addition of ampicillin (left) and ring opened ampicillin (right) to a total concentration of 0.1 mM.

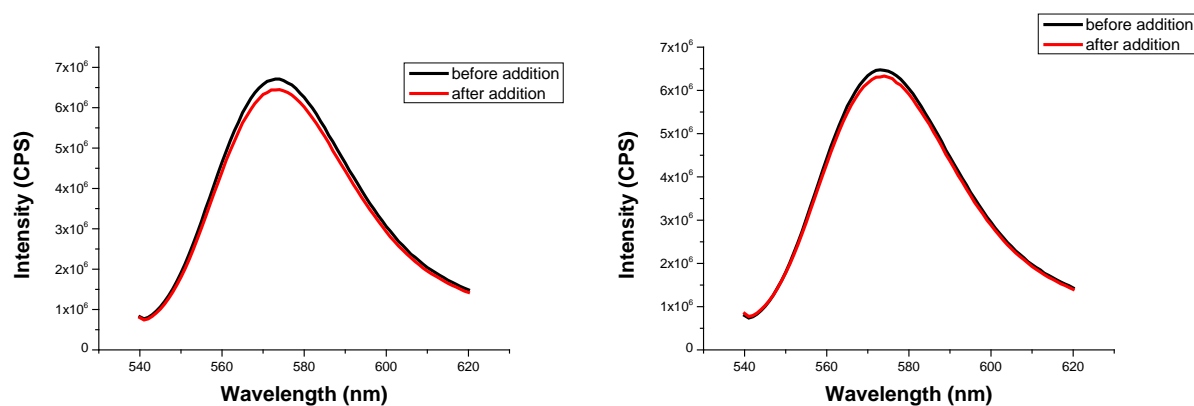


Figure 5.17: Fluorescence spectra of 1% 5 doped DSPC vesicles (total amphiphile concentration of 10 μ M) before and after addition of ampicillin (left) and ring opened ampicillin (right) to a total concentration of 0.1 mM.

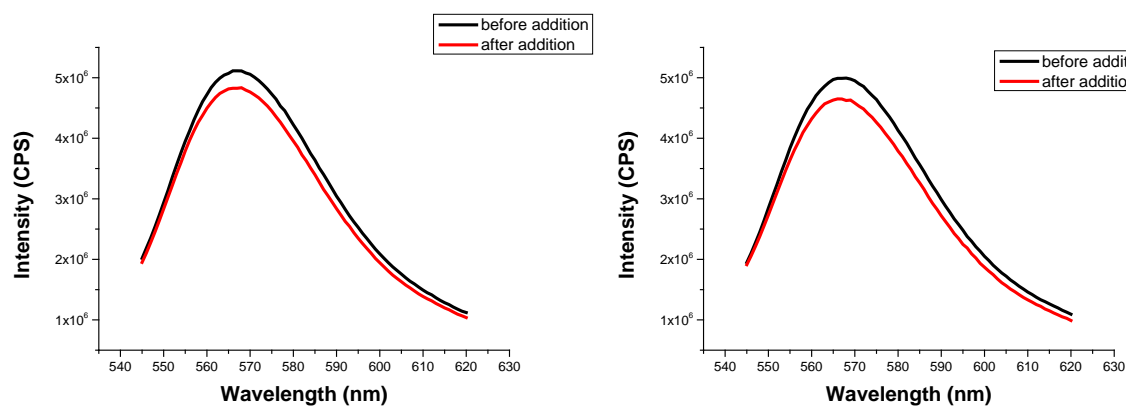


Figure 5.18: Fluorescence spectra of 0.1% 5 doped DSPC vesicles (total amphiphile concentration of 10 μ M) before and after addition of ampicillin (left) and ring opened ampicillin (right) to a total concentration of 0.1 mM.

In all cases, the fluorescence variations upon addition of the two forms of ampicillin are not significant, with $\Delta I_{\text{tot}} = 0$. As varying the amount of the embedded dyes did not improve the system, we used the compositions VTZAm64 and VTZAm67 to test the detection of penicillinase. In Figures 5.20 and 5.21, we show the fluorescence response with time of the vesicular systems in presence of ampicillin in the buffer solution after addition of penicillinase.

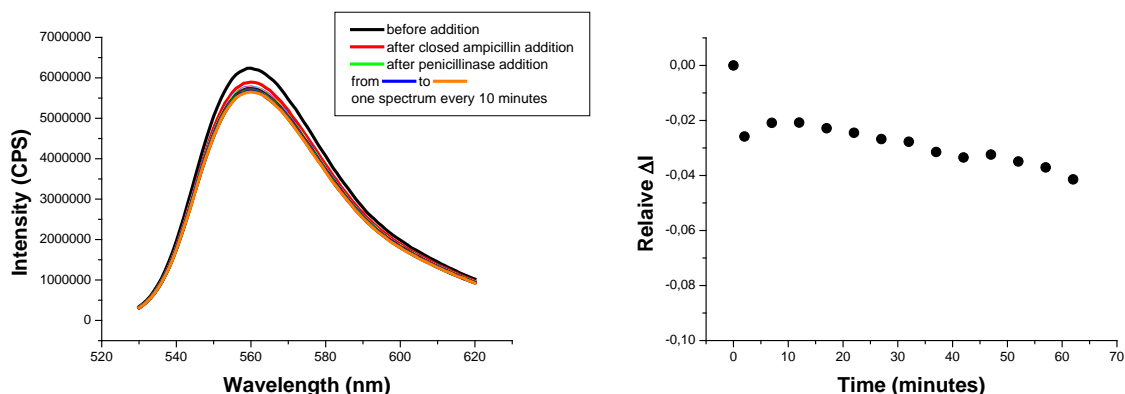


Figure 5.20: On the left: fluorescence spectra of a solution of VTZAm64 vesicles (total amphiphile concentration of 10 μM) in 5mM ampicillin buffer solution after the addition of 0.1 U of penicillinase. Temporal evolution is monitored by recording a spectrum every 10 minutes. On the right: a plot of the fluorescence response with time.

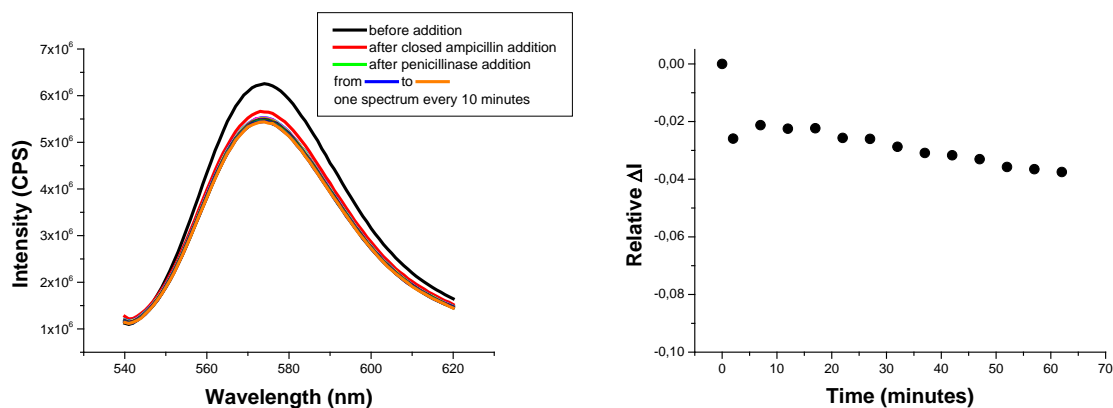


Figure 5.21: On the left: fluorescence spectra of a solution of VTZAm67 vesicles (total amphiphile concentration of 10 μM) in 5mM ampicillin buffer after the addition of 0.1 U of penicillinase. Time evolution was monitored by taking a spectrum every 10 minutes. On the right: a plot of the fluorescence response with time.

The response of the vesicular systems after the addition of the penicillinase is not significant. The fluorescence intensity change with time is very modest and the reproducibility turned out to be insufficient.

As control experiments, we studied the fluorescence of the dyes **4**, **5**, eosin Y (**4** lacking the alkyl chain) and erythrosine (**5** lacking the alkyl chain) the corresponding non-amphiphilic) in homogeneous solution upon the addition of open and closed form of ampicillin (Figures 5.22, 5.23 and 5.24).

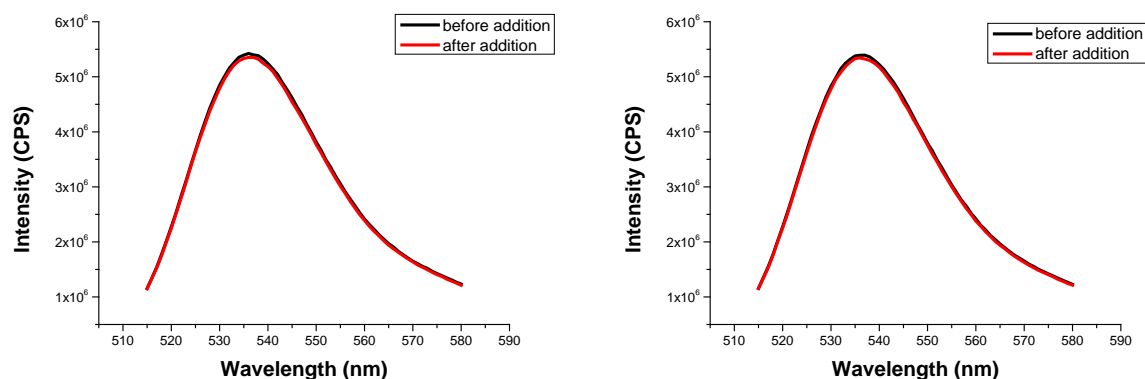


Figure 5.22: Fluorescence spectra of an eosin Y solution before and after addition of ampicillin (left) and ring opened ampicillin (right).

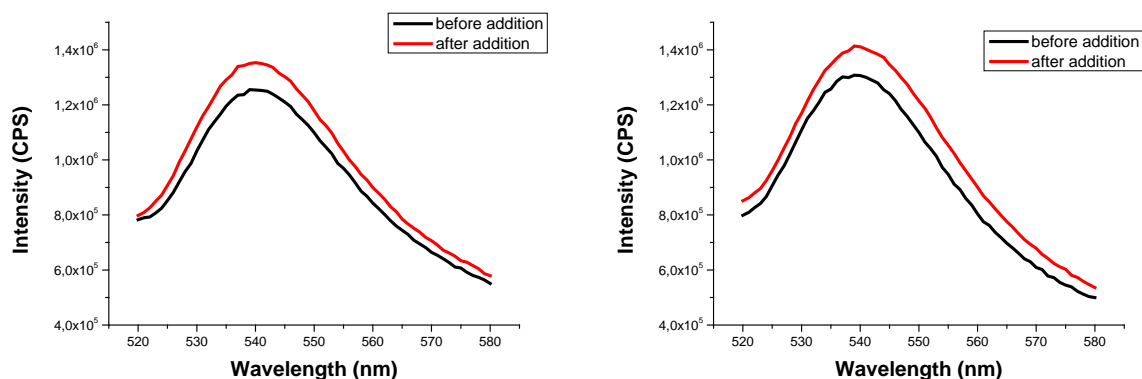


Figure 5.23: Fluorescence spectra of an amphiphilic eosin Y solution before and after addition of ampicillin (left) and ring opened ampicillin (right).

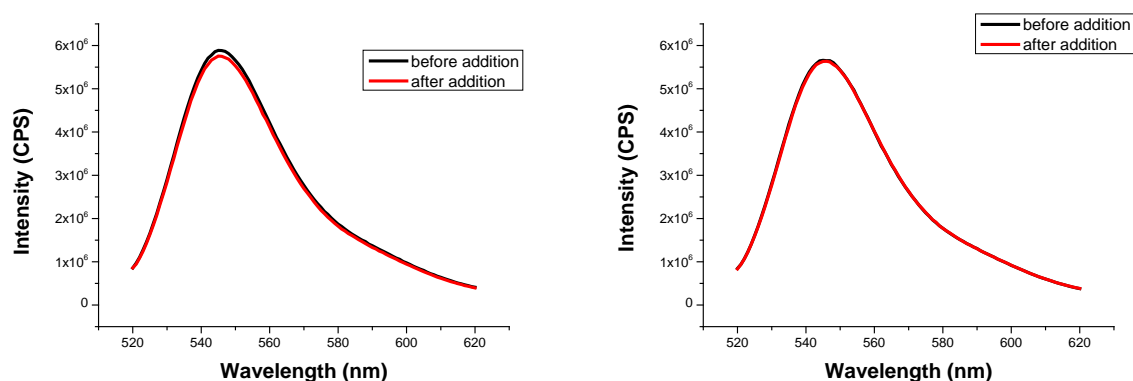


Figure 5.24: Fluorescence spectra of an erythrosine solution before and after addition of ampicillin (left) and ring opened ampicillin (right).

No significant changes are observed for the non-amphiphilic dye solutions after the addition of the two forms of ampicillin.

For the amphiphilic eosin y (Figure 5.23), a significant change is observed after addition of both forms, but there is no difference between the open and closed form. The signal is very weak, most likely because of quenching caused by the aggregation of the amphiphilic molecules.

For amphiphilic erythrosine, no fluorescence was observed.

5.3 CONCLUSION

It was possible to prepare SRB-encapsulating liposomes using the phospholipid **DOPC** in analogy to the procedures employed in our group. The vesicles seemed to be suitable for the assay as after addition of a lysing agent, the fluorescence clearly raised (Figure 5.5).

The **DOPC** and **DSPC** vesicles functionalized with 5%, 10%, 20%, 30% and 40% of **Amp-C₁₈** were prepared and were stable (Figures 5.6 and 5.7, Table 5.1). The addition of penicillinase did not provoke any significant change in the size distribution of the vesicle samples. Such stability of the samples prevented the further development of the assay as the enzyme is not able to trigger any leakage of encapsulated dye molecules. We therefore moved to a different assay scheme.

The approach which was inspired by our vesicular chemosensors shows that the addition of penicillinase does not significantly affect the fluorescence properties of the membrane embedded dyes. The experiment shown in Figure 5.10 looked promising, but further investigations (Figures 5.11 and 5.12) revealed an insufficient reproducibility.

The approach based on the functionalization of the liposomes only with an amphiphilic dye initially seemed to be rather promising. The different vesicle samples were all stable (except of two compositions, Figure 5.14) some of them exhibited a change in the emission properties after addition of open and/or closed form of ampicillin. In particular **4** doped **DOPC** vesicles and **5** doped **DSPC** vesicles gave a different response in presence of open or closed form of ampicillin. The total relative difference of the emission intensity was about 10-15%. It was not possible to obtain a more pronounced response variation by changing the concentration of the embedded amphiphilic dye. The addition of the penicillinase to those vesicles did not show the expected result after the first screening. The cleavage of the ampicillin β -lactam ring in the vesicular solution did not provoke any time dependent changes of the fluorescence properties.

The three different investigated approaches suffer from the same limitations: poor reproducibility and the difficulty to propose a working rational design of the assay. The correct interpretation of the experimental observations is difficult.

The second approach was expected to be more successful as it was inspired by the vesicular chemosensor concept which was successfully applied in our group. Further investigations should be carried out with the general aim to have more insights about the mechanisms of the vesicular chemosensors and to improve the rational design of further assays.

5.4 EXPERIMENTAL SECTION

5.4.1 General

Materials: DOPC, DSPC and were purchased from Avanti Polar Lipids; penicillinase from *Bacillus cereus*, 4-(2-hydroxyethyl)-1-piperazineethanesulfonic acid (HEPES), eosin Y, eosin B, carboxyfluorescein, 2',7'-dichlorofluorescein, sulforhodamine B were purchased from Sigma-Aldrich; erythrosine, 4',5'-dibromofluorescein from Acros; thionyl chloride, stearic acid and triethylamine from Merck; ampicillin Na salt from Serva. All the chemicals were used without further purification. All solvents were used in p.a. grade and dried if necessary.

Polycarbonate membranes for the extrusion of the vesicles were purchased from AVESTIN. If not otherwise specified, MilliQ water was employed.

The fluorescence experiments were performed in 25 mM HEPES buffer at pH = 7.4, the spectra were recorded on a Horiba Fluoromax4 spectrophotometer with 1 ml Hellma cuvettes. DLS measurements were performed on a Malvern Zetasizer Nano instrument at 20 °C using disposable polystyrene cuvettes. NMR spectra were recorded on Bruker Avance 600 (^1H : 600.1 MHz, ^{13}C : 150 MHz, T = 300 K) or on Bruker Avance 300 (^1H : 300.1 MHz, ^{13}C : 75.5 MHz, T = 300 K). The spectra are referenced against the NMR-solvent, chemical shifts δ are reported in ppm and coupling constants J are given in Hz. Resonance multiplicity is abbreviated as: s (singlet), d (doublet), t (triplet), m (multiplet) and b (broad). For the characterization of the compounds (**3**, **4**, **5**, **6**, **7**), carbon NMR signals are reported using DEPT 135 spectra with (+) for primary/tertiary, (–) for secondary and (q) for quaternary carbons. Mass spectra were recorded on Agilent Q-TOF 6540 UHD (ESI-MS, APCI-MS).

Preparation of the open form of ampicillin: 0.4 units of penicillinase were added to a 100 mM solution of ampicillin in HEPES buffer (25 mM, pH = 7.4). The solution was then incubated for 4 h at RT (500 rpm mixing). The sample was lyophilized and mass spectrometry analysis was performed. **ESI-MS:** m/z (%): 368.1277 (100) $[\text{MH}]^+$; calculated $\text{C}_{16}\text{H}_{21}\text{N}_3\text{O}_5\text{S}$ 368.1202.

Preparation of the open form of the Amp-C₁₈: 0.4 units of penicillinase were added to a 1 mM solution of **Amp-C₁₈** in HEPES buffer (25 mM, pH = 7.4). The solution was then incubated for 4 h at RT (500 rpm

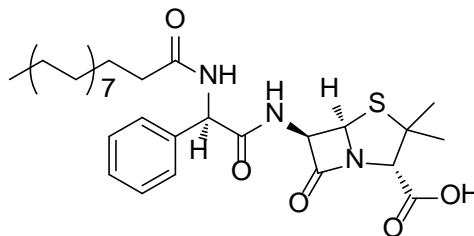
mixing). The sample was lyophilized and mass spectrometry analysis was performed. **ESI-MS:** m/z (%): 634.1277 (100) $[MH]^+$; calculated for $C_{34}H_{55}N_3O_6S$, 634.3812.

Vesicle preparation: in a small glass vessel, the proper volumes of solutions of the lipid (**DOPC** or **DSPC**, 2 mM in $CHCl_3$), **Amp-C₁₈** (1 mM in EtOH) and amphiphilic dye (1 mM) were added. The solvents were removed under vacuum for 15 min and HEPES buffer solution (25 mM, pH = 7.4) was added. The suspension obtained was shortly sonicated in a sonication bath to yield obtain a turbid suspension. The suspension was then extruded through a 100 nm pore size polycarbonate membrane (LiposoFast extruder form AVESTIN) to give a small unilamellar vesicle suspension (RT for **DOPC** vesicles, 60 °C for **DSPC** vesicles).

The SRB-encapsulating vesicles were prepared using buffer containing SRB in a concentration of 100 mM. The vesicles were then separated from the non-encapsulated SRB molecules by filtration with Millipore 3000 MWCO centrifuge filters (6x30 minutes at 4000 rpm).

Before proceeding with any further investigation, the size distribution of the vesicles solution was determined by DLS. All the vesicles showed an average diameter value around 100 nm and a PDI (polydispersity index) value below 0.2 (for most of the samples around 0.1, for few samples around 0.2).

5.4.2 Synthesis



Synthesis of (2S,5R,6R)-3,3-dimethyl-7-oxo-6-((R)-2-phenyl-2-stearamidoacetamido)-4-thia-1-azabicyclo-[3.2.0]heptane-2-carboxylic acid (Amp-C18): 100 mg (0.35 mmol) of stearic acid were dissolved in 5 ml of thionyl chloride and stirred at RT for 2 hours. The excess of thionyl chloride was then removed by vacuum and the crude product was directly used without further purification.

A solution of stearoyl chloride (0.35 mmol) in dry THF (3 ml) under N_2 atmosphere was cooled down to 0 °C. A solution of 0.70 g of Ampicillin Na salt (0.46 mmol) and 200 μ l of triethylamine (1.4 mmol) in dry DMF (2 ml) was added drop wise and the mixture was stirred at 0 °C for 20 minutes. The cooling bath was then removed and the solution was stirred for additional 3 hours. The THF was then removed at the rotary evaporator and DMF at the vacuum pump overnight. The crude product (yellowish solid) was then dissolved in ethyl acetate and the solution was washed with cold (0 °C), slightly acidic aqueous solution of HSO_4^- (pH = 5). The organic phase was dried over $MgSO_4$, filtered and the solvent was removed at the rotary evaporator to give a white solid (43 %). **1H NMR (600 MHz, DMSO- d_6):** δ (ppm) = 0.85 (t, 3H, alkyl chain CH_3), 1.23 (bs, 28H, alkyl chain $(CH_2)_{14}$), 1.41 (s, 3H, penam- CH_3), 1.47 (bs, 2H, $-CH_2CH_2CO-$), 1.53 (s, 3H, penam- CH_3), 2.20 (bm, 2H, $-CH_2CH_2CO-$), 4.20 (s, 1H, penam- $CHCOOH$), 5.39-5.54 ppm (m, 2H, penam- $CHCH-$), 5.72 (d, $J = 8.3$ Hz, 1H, Ph- CH), 7.15-7.55 (m, 5H, aromatic), 8.51 (d, $J = 8.3$ Hz, 1H, NH), 9.12 (d, $J = 7.9$ Hz, 1H, NH). **^{13}C NMR (150 MHz, DMSO- d_6):** (assignments were made with HSQC and HMBC spectra) δ (ppm) = 13.93 (alkyl C), 22.10 (alkyl C), 25.30 (alkyl C), 26.61 (penam-S-C(CH_3) $_2$), 28.68 (alkyl C), 28.72 (alkyl C), 28.81 (alkyl C), 29.06 (alkyl C), 30.42 (penam-S-C(CH_3) $_2$), 31.31 (alkyl C), 34.90 (alkyl C), 55.36 (Ph- $CH-$), 58.13 (penam- $CHCHS-$), 63.73 (penam-S-C(CH_3) $_2$), 67.25 (penam- $CHCHS-$), 70.30 (penam-NCHCOOH), 127.10 (aromatic), 127.44 (aromatic), 127.45 (aromatic), 128.11 (aromatic), 138.33 (aromatic), 168.9 (penam-COOH), 170.23 ($CH_3-(CH_2)_{16}-CO-NH-$), 172.02 (Ph-C(NH)-H-CO-NH-), 173.40 (penam-CO). **ESI-MS:** m/z (%): 616.3776 (100) $[MH]^+$; 638.3592 (49) $[MNa]^+$, calculated $C_{34}H_{53}N_3O_5S$ 616.3706.

5.4.3 Dye-encapsulating vesicles

DLS measurements: 1 ml solutions of a total amphiphile concentration of 100 μ M were used. The DLS spectra were recorded before and after the addition of 7.2 μ U of penicillinase.

Fluorescence measurements: 1 ml of vesicles solutions of a total amphiphile concentration of 10 μ M were used. The fluorescence was recorded before and after the addition of 10 μ l of a 100 mM solution of Triton-X-100. $\lambda_{\text{exc}} = 540$ nm.

5.4.4 Amphiphilic dye and Amp- C_{18} doped vesicular systems

Fluorescence titrations: 1ml solutions of a total amphiphile concentration of 10 μ M were used. The fluorescence was recorded before and after the addition of 10 μ l of a solution of penicillinase (83 U/ml). $\lambda_{\text{exc}} = 495$ nm (amphiphilic carboxyfluorescein embedded vesicles), 540 nm (amphiphilic rhodamine B functionalized vesicles).

5.4.5 Fluorophore embedded in membrane, ampicillin in solution

Synthesis of the amphiphilic dyes: amphiphilic rhodamine B (**2**) was prepared according to [7] and carboxyfluorescein (**1**) according to [5]. Amphiphilic eosin y (**4**) was synthesized by Stefan Troppmann according to [8]. Amphiphilic 4',5'-dibromofluorescein (**7**), eosin B (**3**), erythrosine (**5**) and 2',7'-dichlorofluorescein (**6**) were synthesized by Stefan Troppmann. The amphiphilic 4',5'-dibromofluorescein (**7**) was prepared in analogy to a procedure reported in [9]. 4',5'-dibromofluorescein (0.7 g, 1.3 mmol) was dissolved in 15 ml of DMF and K_2CO_3 (0.5 g, 3.6 mmol) and 1-bromohexadecane (0.4 ml, 1.3 mmol) were added. The solution was stirred at 100 $^{\circ}$ C for 72 h. The reaction mixture was diluted with DCM and washed twice with 1 M HCl. The organic phase was dried over $MgSO_4$, filtered and the solvent was removed. The crude product was purified by column chromatography (SiO_2 , DCM:MeOH 9:1) to give the desired compound (**2**) as red crystals, 275 mg (0.42 mmol), 31%. 1H NMR ($CDCl_3$, 400 MHz): δ (ppm) = 0.84 (t, $J = 6.3$ Hz, 3H), 1.10-1.30 (m, 20H), 3.95 (t, $J = 6.6$ Hz, 2H), 6.92 (m, 4H), 7.28 (dd, $J = 1.5$ Hz, $J = 7.4$ Hz, 1H), 7.71 (m, 2H), 8.25 (m, 1H). ^{13}C

NMR: (CDCl_3 , 75 MHz): δ (ppm) = 14.2 (+), 22.7 (-), 25.9 (-), 28.3 (-), 29.2 (-), 29.4 (-), 29.5 (-), 29.6 (-), 29.6 (-), 29.6 (-), 31.9 (-), 66.0 (-), 101.0 (q), 116.7 (q), 128.9 (+), 130.1 (+), 130.4 (+), 130.6 (+), 131.4 (+), 132.8 (+), 133.6 (q). **ESI-MS:** m/z = 657.1 (MH^+).

Compound 6

Yield: 287 mg (0.50 mmol), 38 %. **$^1\text{H-NMR}$** (MeOD , 400 MHz): δ (ppm) = 0.90 (t, J = 6.7 Hz, 3H), 1.10-1.30 (m, 20H), 3.99 (t, J = 6.2 Hz, 2H), 6.83 (s, 2H), 7.05 (s, 2H), 7.44 (dd, J = 1.4 Hz, J = 7.4 Hz, 1H), 7.85 (m, 2H), 8.31 (dd, J = 1.5 Hz, J = 7.7 Hz, 1H). **ESI-MS:** m/z = 569.2 (MH^+).

Compound 3

Yield: 866 mg (1.08 mmol), 81 %. **$^1\text{H-NMR}$** (CDCl_3 , 400 MHz): δ (ppm) = 0.87 (t, J = 6.7 Hz, 3H), 1.10-1.30 (m, 26H), 1.44 (m, 2H), 4.04 (t, J = 6.6 Hz, 2H), 7.35 (dd, J = 1.4 Hz, J = 7.4 Hz, 2H), 7.43 (s, 2H), 7.78 (m, 2H), 8.32 (dd, J = 1.4 Hz, J = 7.6 Hz, 1H). **$^{13}\text{C-NMR}$** (CDCl_3 , 75 MHz): δ (ppm) = 14.2 (+), 22.7 (-), 25.9 (-), 28.4 (-), 29.3 (-), 29.4 (-), 29.5 (-), 29.6 (-), 29.7 (-), 29.7 (-), 29.7 (-), 31.9 (-), 66.1 (-), 130.3 (q), 130.6 (+), 131.7 (+), 132.8 (q), 133.2 (+), 137.9 (+), 148.1 (q), 165.0 (q). **ESI-MS:** m/z = 803.1 (MH^+).

Compound 5

Yield: 700 mg (0.66 mmol), 50 %. **$^1\text{H-NMR}$** ($\text{DMSO-}d_6$, 400 MHz): δ (ppm) = 0.84 (t, J = 6.7 Hz, 3H), 1.10-1.30 (m, 20H), 3.91 (t, J = 6.1 Hz, 2H), 7.19 (s, 2H), 7.48 (m, 1H), 7.81 (m, 2H), 8.1 (dd, J = 1.2 Hz, J = 7.7 Hz, 2H). **ESI-MS:** m/z = 1060.9 (MH^+).

Fluorescence experiments: 1 ml solutions of a total amphiphile concentration of 10 μM were used. The fluorescence was recorded before and after the addition of 10 μl of a 100 mM solution of open or closed ampicillin. λ_{exc} = 492 nm (for VTZAm58, VTZAm59, VTZAm62, VTZAm63, VTZAm64), 510 nm (VTZAm65), 525 nm (VTZAm60, VTZAm61), 550 nm (VTZAm66, VTZAm67), 520 nm (VTZAm68, VTZAm69) 540 nm (VTZAm70, VTZAm71).

For the enzyme detection experiments, 10 μl of a 100 mM solution of ampicillin were added to the vesicle solution and gently mixed. A fluorescence spectrum was recorded. After that, 10 μl of

penicillinase (83 U/ml) were added and fluorescence spectra after 2, 12, 22, 32, 42 and 52 minutes were recorded.

5.5 REFERENCES

1. Diekema, D.J. and Pfaller, M.A., *Rapid detection of antibiotic-resistant organism carriage for infection prevention*. Clinical Infectious Diseases, 2013. **56**(11): p. 1614-1620.
2. O'Callaghan, C.H., Morris, A., Kirby, S.M. and Shingler, A.H., *Novel method for detection of beta-lactamases by using chromogenic cephalosporin substrate*. Antimicrobial Agents and Chemotherapy, 1972. **1**(4): p. 283-288.
3. Livermore, D.M. and Brown, D.F.J., *Detection of beta-lactamase-mediated resistance*. Journal of Antimicrobial Chemotherapy, 2001. **48**: p. 59–64.
4. Liu, Q. and Boyd, B.J., *Liposomes in biosensors*. Analyst, 2013. **138**(2): p. 391-409.
5. Gruber, B., Stadlbauer, S., Späth, A., Weiss, S., Kalinina, M. and König, B., *Modular chemosensors from self-assembled vesicle membranes with amphiphilic binding sites and reporter dyes*. Angewandte Chemie International Edition, 2010. **49**(39): p. 7125-7128.
6. Edwards, K.A., Curtis, K.L., Sailor, J.L. and Baeumner, A.J., *Universal liposomes: preparation and usage for the detection of mRNA*. Analytical and Bioanalytical Chemistry, 2008. **391**(5): p. 1689-1702.
7. Keller, P.M., Person, S. and Snipe, W., *A fluorescence enhancement assay of cell fusion*. Journal of Cell Science, 1977. **28**: p. 167-177.
8. Kopf, V., *Photosensitizers for aPDT*, 2012, University of Regensburg (GER).
9. Tan, S.S.S., Hauser, P.C., Wang, K., Fluri, K., Seiler, K., Rusterholz, B., Suter, G., Kruettli, M., Spichiger, U.E. and Simon, W., *Reversible optical sensing membrane for the determination of chloride in serum* Analytica Chimica Acta, 1991. **255**: p. 35-44.

SUMMARY

In **chapter 1**, we give a short background on the vesicular chemosensors developed in the König group as introduction to the following chapters.

The **chapter 2** deals with the investigation of a bis (zinc-cyclen)-biotin conjugate as a selective probe for detection of phosphorylated proteins in western blot analysis. The probe was employed in an assay scheme analogue to a standard immunodetection assay, in which the probe was used instead of the primary antibody. A number of different conditions were varied in order to optimize the performances of the assay (such as incubation and washing times, concentrations of the components in the different steps of the procedures, blocking agents). With optimized conditions, phosphorylated α -s1-casein in the μg range was detected with good selectivity towards the non-phosphorylated control proteins.

In **chapter 3**, we attempted to transfer the concepts developed so far in the König group in the field of vesicular chemosensors to the SPR and QCM techniques. The main goals were to characterize, and possibly to use for further applications, the binding of analytes to artificial receptor doped membranes with SPR and/or QCM. Different approaches were investigated, such as the binding of analytes to functionalized membranes which are supported on the sensor surface, the binding of the receptor doped vesicles to analyte functionalized surfaces as well as a displacement assay using gold nanoparticles. All the investigated systems showed a large unspecific interaction between the analytes and the functionalized membranes, which prevented the further development of the project.

Chapter 4 deals with the fluorescence microscopy characterization of vesicular chemosensors. Phospholipid vesicles with embedded artificial bis (zinc-cyclen) receptor together with the dye MC540 were investigated as vesicular chemosensors for different anions and subsequently characterized by high resolution STORM fluorescence microscopy and classic TIRF microscopy. The high resolution approach did not provide information about the spatial organization of the embedded molecules. With TIRFM characterization of giant unilamellar vesicles of the same composition, it was possible to observe a non-homogeneous distribution of the dyes on the surface of the vesicles, which supports the hypothesized working mechanism for the vesicular chemosensors.

Finally, in **chapter 5**, we reported the investigation of vesicular systems for the detection of β -lactamases and the monitoring of their activity. Different approaches were studied investigated: a dye-encapsulating liposome assay, an assay where a reporting dye and an ampicillin derivative are co-

embedded in the vesicular system and a third scheme in which the dye is embedded in the liposomes while the ampicillin remains in solution. All three approaches suffered from an insufficient reproducibility which led to difficulties in the interpretation of the experimental data.

ZUSAMMENFASSUNG

In **Kapitel 1** geben wir als Einleitung zu den folgenden Abschnitten einen kurzen Hintergrund zu auf Vesikeln basierenden Chemosensoren, die in der Arbeitsgruppe König entwickelt wurden.

Kapitel 2 der Dissertation beschreibt die Untersuchung eines Bis-(Zink-Cyclen)-Biotin Konjugats, welches als selektive Sonde zur Detektion von phosphorylierten Proteinen im Rahmen der Western Blot-Analyse eingesetzt wurde. Der Aufbau des Assays entsprach dem der üblichen immunologischen Nachweisverfahren, wobei hierbei die Sonde anstatt eines primären Antikörpers eingesetzt wurde. Eine Reihe unterschiedlicher Bedingungen wurde getestet (wie zum Beispiel die Inkubationszeit, die Dauer der Waschvorgänge, die Konzentrationen der Komponenten in den verschiedenen Ablaufschritten und die Verwendung von Blockierungsmitteln) um die Genauigkeit des Assays zu verbessern. Mit den optimierten Bedingungen wurde phosphoryliertes α -s1-Casein im Mikrogrammbereich mit guter Selektivität gegenüber nichtphosphorylierten Kontrollproteinen nachgewiesen.

Im Rahmen von **Kapitel 3** versuchten wir die in der Arbeitsgruppe König entwickelten Konzepte auf dem Gebiet der Vesikel-basierten Chemosensoren auf SPR- und QCM-Methoden zu übertragen. Die vorrangigen Ziele waren die Charakterisierung von Analytbindungen an mit künstlichen Rezeptoren modifizierten Membranen mittels SPR und/oder QCM sowie falls möglich der Einsatz dieser Techniken für weitere Anwendungen. Verschiedene Ansätze wurden in diesem Zusammenhang erforscht, so zum einen die Bindung von Analyten an funktionalisierten Membranen, die auf die Sensoroberfläche aufgebracht worden waren, zum anderen die Bindung von Rezeptor-modifizierten Vesikeln an Oberflächen, welche mit dem Analyten funktionalisiert worden waren. Überdies wurde ein Verdrängungsassay unter Verwendung von Goldnanopartikeln getestet. Alle untersuchten Systeme zeigten eine große unspezifische Wechselwirkung zwischen den Analyten und den funktionalisierten Membranen, was die weitere Entwicklung des Projekts einschränkte.

Kapitel 4 behandelt die Charakterisierung von Vesikel-basierten Chemosensoren mittels Fluoreszenzmikroskopie. Phospholipidvesikel mit zusammen eingelagertem künstlichen Bis-(Zink-Cyclen)-Rezeptor und Farbstoff MC540 wurden hinsichtlich ihrer Eignung als Chemosensoren für verschiedene Anionen untersucht. Anschließend wurden diese mittels hochauflösender STORM Fluoreszenzmikroskopie und klassischer TIRF Mikroskopie charakterisiert. Unter Verwendung der hochauflösenden Methode konnten keine Informationen über die räumliche Strukturierung der eingebetteten Moleküle erhalten werden. Durch die Charakterisierung von unilamellaren

Riesenvesikeln (GUVs) der gleichen Zusammensetzung mit Hilfe von TIRFM wurde eine nichthomogene Verteilung der Farbstoffe auf der Oberfläche der Vesikel beobachtet, was für das postulierte Funktionsprinzip der vesikulären Chemosensoren spricht.

In **Kapitel 5** berichteten wir schließlich über Studien an Vesikelsystemen zur Detektion von β -Lactamasen und der Verfolgung ihrer Aktivität. Unterschiedliche Vorgehensweisen wurden hierbei getestet: ein Assay basierend auf Farbstoff-einkapselnden Liposomen, ein Format, in dem ein Reporterfarbstoff und ein Ampicillinderivat zusammen in ein Vesikelsystem eingelagert worden waren und ein drittes Verfahren, in dem nur der Farbstoff in die Liposomen eingebettet worden war, während das Ampicillin in Lösung verblieb. Alle drei Ansätze wiesen eine mangelhafte Reproduzierbarkeit auf, was zu Schwierigkeiten bei der Interpretation der experimentellen Daten führte.

LIST OF ABBREVIATIONS

AcOH	Acetic acid
ADP	Adenosine 5'-diphosphate
AFM	Atomic force microscopy
ATP	Adenosine 5'-triphosphate
AuNPs	Gold nanoparticles
Brij 35	Commercial name of a non-ionic polyoxyethylene surfactant
BSA	Bovine serum albumin
CCD	Charge-coupled device
Cryo-TEM	Transmission electron microscopy at cryogenic temperature
Cyclen	1,4,7,10-Tetraazacyclododecane
DCM	Dichloromethane
DLS	Dynamic light scattering
DMF	N,N-Dimethylformamide
DMSO	Dimethyl sulfoxide
DNA	Deoxyribonucleic acid
DOPC	1,2-dioleoyl- <i>sn</i> -glycero-3-phosphocholine
DSPC	1,2-distearoyl- <i>sn</i> -glycero-3-phosphocholine
ECL	Enhanced chemiluminescence
EDC	1-Ethyl-3-(3-dimethylaminopropyl)carbodiimide
EGTA	Ethylene glycol-bis(2-aminoethylether)- <i>N,N,N',N'</i> -tetraacetic acid

LIST OF ABBREVIATIONS

ESI	Electrospray ionization
EtOH	Ethanol
FF-TEM	Freeze fracture transmission electron microscopy
FRAP	Fluorescence recovery after photobleaching
FRET	Förster resonance energy transfer
GUVs	Giant unilamellar vesicles
HEPES	4-(2-Hydroxyethyl)-1-piperazineethanesulfonic acid
HRP	Horseradish peroxidase
MC540	Merocyanine 540
MDRB	Multidrug resistant bacteria
MeOH	Methanol
MES	2-(N-Morpholino)ethanesulfonic acid
MHDA	11-Mercaptohexadecanoic acid
MPTMS	3-(Mercaptopropyl)trimethoxysilane
MS	Mass spectrometry
MUA	11-Mercaptoundecanoic acid
NHS	N-Hydroxysuccinimide
NMR	Nuclear magnetic resonance
PDI	Polydispersity index
pDNA	Plasmidic DNA
PEG	Polyethylene glycol
PEG350-DSPE	1,2-distearoyl- <i>sn</i> -glycero-3-phosphoethanolamine-N-[methoxy(polyethylene glycol)-350] (ammonium salt)

PP _i	Pyrophosphate
QCM	Quartz crystal microbalance
QCM-D	Quartz crystal microbalance with dissipation monitoring
RIU	Refractive index unit
rpm	Rounds per minute
RT	Room temperature
SAM	Self-assembled monolayer
SDS	Sodium dodecyl sulfate
SDS-PAGE	Sodium dodecyl sulfate - polyacrylamide gel electrophoresis
SPR	Surface plasmon resonance
SRB	Sulforhodamine B
SRFM	Super resolution fluorescence microscopy
STM	Scanning tunneling microscopy
STORM	Stochastic optical reconstruction microscopy
TIRFM	Total internal reflection fluorescence microscopy
Tris	Tris(hydroxymethyl)aminomethane
λPPase	Lambda phosphatase

CURRICULUM VITAE

Thomas Zanni

Born on Juli 19 1985 in Feltre (BL) -Italy-

Nationality: Italian

Friedenstraße 16a

93053 Regensburg -D-

+49 1785390927

thozanni@gmail.com

Skype: thomasza1

Education

08/2011- present	PhD thesis Chemistry. Institute of Organic Chemistry, University of Regensburg. Thesis: "Investigation of bioanalytical methodologies for the detection of different analytes" Supervisor: Prof. Dr. Burkhard König.
10/2008 - 03/2011	M. Sc. Chemie (Laurea magistrale). University of Padova (Italy). Thesis: "Expression, purification and NMR study of Trypanosoma brucei Grx3 protein". Supervisor: Dr. Massimo Bellanda (Prof. Mammi group).
09/2005 - 10/2008	B.S. Chemie (Laurea triennale). University of Padova (Italy) Thesis: "TR-EPR study of a helicene-fullerene dyad for photovoltaic applications" Supervisor: Dr. Marco Ruzzi (AK Prof. Brustolon).
2004	Maturità scientifica. Liceo Scientifico "G. Dal Piaz", Feltre (BL) Italy.

International experience

09/2009 - 03/2010	Semester abroad in Madrid (Spain), at the Universidad Complutense de Madrid.
09/2013 - 12/2013	Research collaboration project at the Université Technologique de Compiègne (France), Prof. K. Haupt Group.

Languages

Italian	Mother tongue
English	Fluent
Spanish	Fluent
German	Good knowledge
French	Basic knowledge

Scholarships and memberships

08/2011 - 07/2014	Marie Curie fellowship (Chebana ITN)
10/2006 - 10/2010	ESU scholarship (Veneto regional scholarship)
09/2009 - 03/2010	Erasmus scholarship
since 2012	Member of the German Chemical Society (GDCh)

Conferences and Seminars

09/2014	Chebana (Marie Curie ITN) summerschool Regensburg. Oral presentation: "SPR and QCM-D investigations of functionalized supported membranes"
09/2013	Chebana (Marie Curie ITN) summerschool Biarritz. Oral presentation: " Further investigations of vesicular chemosensors"
02/2013	Chebana (Marie Curie ITN) training week – project management, intellectual property, innovation management (München)
11/2012	TuTech Seminar on Innovation (Hamburg)
09/2012	Chebana (Marie Curie ITN) summerschool Mannheim. Poster presentation: "A bis (zinc-cyclen) – biotin conjugate probe for selective detection of phospho-proteins in western blot analysis"
08/2012	Chebana-UpCore joint seminar. Oral presentation: "A bis (zinc-cyclen) – biotin conjugate probe for selective detection of phospho-proteins in western blot analysis"
08/2012	EuChems Conference Prague. Poster presentation: "Luminescent probes for the detection of proteins in SDS-PAGE analysis"

ACKNOWLEDGEMENTS

I'd like to thank Prof. Dr. Burkhard König for the chance he gave me to come to Germany, study here, work in his group and for supervising my work during the last years.

I am very thankful to Prof. Dr. Joachim Wegener and PD Dr. Sabine Amslinger for being part of the examiner board for my PhD dissertation. I thank Prof. Dr. Olga Garcia Mancheño for being the Chairman in my PhD defense.

I am very thankful to Prof. Dr. Sabine Amslinger and Dita Frisch for the help with the western blot project. To Dr. Thomas Hirsch for helping with the SPR project.

I'd like to thank Prof. Dr. Karsten Haupt and Dr. Claire Rossi, for hosting me in their laboratories in Compiègne.

I'd like to thank Prof. Dr. Yves Mély and Dr. Ludovic Richert, who hosted me in their laboratories in Strasbourg.

I'd like to thank all the members of the Chebana ITN for the interesting scientific meetings and summer- and winterschools. I am grateful to the Research Executive Agency (REA) of the European Union, which granted the Chebana ITN, including my PhD studies (Grant number: PITN-GA-2010-264772).

I'd like to thank all the past and present members of the König group for the general nice working atmosphere (particularly Tascha and Mascha). I am very thankful to Andreas Müller for proofreading the thesis.

Finally I'd like to thank my friends and my family.